

CHARGE syndrome: candidate genes and pathogenesis

Dissertation

for the award of the degree

“Doctor rerum naturalium”

of the Georg-August-Universität Göttingen

**within the doctoral program Genes and Development
of the Georg-August University School of Science (GAUSS)**

submitted by

Yvonne Schulz

from Hamburg, Germany

Göttingen 2014

Thesis Committee

Prof. Dr. med. Dr. h.c. Wolfgang Engel

Department of Human Genetics, Georg-August-University, Göttingen

Prof. Dr. Andreas Wodarz

Department of Microscopical Anatomy and Molecular Cell Biology, University Köln

Medical Center, Köln

Prof. Dr. Ahmed Mansouri

Department of Molecular Cell Biology/Molecular Cell Differentiation, Max Planck

Institute for biophysical Chemistry, Göttingen,

Members of the Examination Board

Referee: Prof. Dr. med. Dr. h.c. Wolfgang Engel

Department of Human Genetics, Georg-August-University, Göttingen

2nd Referee: Prof. Dr. Andreas Wodarz

Department of Microscopical Anatomy and Molecular Cell Biology, University Köln

Medical Center, Köln

Further members of the Examination Board

Prof. Dr. Sigrid Hoyer-Fender

Department of Developmental Biology GZMB, Johann-Friedrich-Blumenbach-

Institute for Zoology and Anthropology, Georg-August-University Göttingen

Prof. Dr. Ernst Wimmer

Department of Developmental Biology GZMB, Johann-Friedrich-Blumenbach-

Institute for Zoology and Anthropology, Georg-August-University Göttingen

Prof. Dr. Steven Johnsen

Clinic for General, Visceral and Pediatric Surgery, University Medical Center,

Göttingen

Date of the oral examination:

Herewith I declare, that I prepared the Dissertation

"CHARGE syndrome: candidate genes and pathogenesis"

on my own and with no other sources and aids than quoted.

Göttingen, August 20th, 2014

Yvonne Schulz

Dedicated to my family

Acknowledgements

I would like to express my sincere gratitude to my doctor father Prof. Dr. med. Dr. h.c. Wolfgang Engel for the opportunity to compile my PhD study in the Institute of Human Genetics. I am overgrateful for the valuable scientific discussions and his encouragement during my PhD study.

I would like to thank the members of my thesis committee Prof. Dr. Andreas Wodarz and Prof. Dr. Ahmed Mansouri for their readiness to invest their time and for the valuable input during our meetings.

I would like to express my deep gratitude to my supervisor PD Dr. Silke Pauli for her unquestioning support, patience and trust and excellent guidance during the entire process of my PhD project. I am thankful for the facilitation to work in such interesting field of research.

Moreover, I thank Prof. Dr. Sigrid Hoyer-Fender, Prof. Dr. Ernst Wimmer and Prof. Dr. Steven Johnsen, who kindly agreed to evaluate my dissertation and participate in examination.

I sincerely thank our collaborators, especially Prof. Dr. Annette Borchers and Dr. Peter Wehner.

I would particularly like to thank the staff of the Goettingen Graduate School for Neurosciences, Biophysics and Molecular Biosciences (GGNB) and my doctoral program “Genes and Development” for the excellent organisation and financial support by the grant of the bridging fund as well as the Deutsche Forschungsgemeinschaft (DFG) for financing my PhD study.

Special thanks go to Johanna Mänz, who always supported my work with great assistance.

Further, I would like to thank the staff of animal keeper for excellent animal care.

I would like to thank my colleagues Johanna Mänz, Luisa Freese, Jessica Nolte, Nadine Mellies, Stefanie Heumüller, Tserendulam Batsukh, Krzysztof Wiecek and all other members of the Human Genetic Institute for their advice and support, friendship and great working atmosphere.

Herewith, I would like to express my heartfelt gratitude to my family, especially to my parents who always supported me with their trust and love. I wish my dad could share this special moment of my life with me...

Thank you to Benjamin Brauer and all my friends who accompanied me through this part of my life journey. Because of you this time became an unforgettable one and will always have a special place in my heart!

Thank you so much!

Table of content

Table of content.....	I
List of figures.....	VI
List of tables.....	VIII
Abbreviations.....	X
Nomenclature.....	XX
Summary.....	XXI
1 Introduction	1
1.1 The chromodomain helicase DNA-binding protein 7	1
1.2 CHD7 exists in large multi-subunit complexes.....	1
1.3 CHARGE syndrome	3
1.4 Neural crest cells - the explorer of the vertebral embryo	4
1.5 NCC development	6
1.6 NCC guidance and signalling factors	7
1.7 <i>Xenopus laevis</i> as a model organism for studying NCC development.....	9
1.8 The mouse as a model organism and its advantages	10
1.9 Aim of the work	11
2 Materials and methods.....	13
2.1 Materials	13
2.1.1 Instruments.....	13
2.1.2 Consumable materials	15
2.1.3 Kits	17
2.1.4 Ready to use buffers and mediums	17
2.1.5 Chemicals.....	18
2.1.6 Buffers and solutions	22
2.1.7 Media and plates	28
2.1.8 Sterilisation	30

2.1.9	Antibiotics	30
2.1.10	Antibodies	30
2.1.11	Morpholinos	31
2.1.12	Oligonucleotides	32
2.1.13	DNA marker	39
2.1.14	Protein marker	39
2.1.15	Vectors	39
2.1.16	Enzymes	40
2.1.17	Polymerases (Kits)	40
2.1.18	Restriction enzymes and Buffers	40
2.1.19	Bacterial strains	40
2.1.20	Cell line	41
2.1.21	Yeast strain	41
2.1.22	Model organisms	41
2.1.23	Software used	41
2.1.24	Internet platforms used	41
2.2	Methods	43
2.2.1	Isolation of nucleic acids	43
2.2.1.1	Isolation of genomic DNA for genotyping of mice	43
2.2.1.2	Isolation of plasmid DNA from bacteria	43
2.2.1.3	RNA isolation from mouse embryos	45
2.2.2	Determination of nucleic acid concentration	46
2.2.3	Reverse transcription	46
2.2.4	Cloning	46
2.2.4.1	Restriction digestion of plasmid DNA	47
2.2.4.2	Ligation of DNA fragments into plasmids	47
2.2.4.3	Transformation	47
2.2.5	Cloning by In-Fusion TM	48

2.2.6	Preparation of glycerin stocks	48
2.2.7	PCR	49
2.2.7.1	Touchdown PCR.....	53
2.2.7.2	Sequencing PCR	54
2.2.8	Quantitative real-time PCR and data analysis.....	55
2.2.9	Purification of DNA	60
2.2.10	Agarose gel electrophoresis	61
2.2.11	Gel extraction	61
2.2.12	Mouse preparation.....	62
2.2.13	Fixation and dehydration of embryos for paraffin embedding	62
2.2.14	Preparation of paraffin sections of mouse embryos	63
2.2.15	Microarray and data analysis	63
2.2.16	Cell biological methods.....	64
2.2.16.1	Culturing of eukaryotic cells.....	64
2.2.16.2	Cryopreservation and revitalisation of eukaryotic cells	64
2.2.16.3	Transfection of eukaryotic cells with plasmids	65
2.2.17	Protein chemical methods	65
2.2.17.1	Protein isolation from HeLa cells	65
2.2.17.2	Measurement of protein concentration	66
2.2.17.3	Co-IP.....	67
2.2.17.4	SDS polyacrylamide gel electrophoresis	68
2.2.17.5	Western blot.....	68
2.2.17.6	Protein detection using antibodies	69
2.2.18	Direct yeast two-hybrid.....	70
2.2.19	Cytological and histological methods	72
2.2.19.1	Immunocytochemistry with eukaryotic cells	72
2.2.19.2	Duolink PLA.....	72
2.2.19.3	Immunohistochemistry (3,3'-Diaminobenzidine (DAB) staining)	74

2.2.20	Mutational analysis	75
2.2.21	Molecular biological methods concerning the model organism <i>Xenopus laevis</i>	76
2.2.21.1	In vitro transcription of sense RNA.....	76
2.2.21.2	Purification of sense RNA	76
2.2.21.3	In vitro transcription of labeled anti-sense RNA.....	77
2.2.21.4	Purification of labeled anti-sense RNA	77
2.2.21.5	Morpholino oligonucleotides.....	78
2.2.21.6	Preparation of <i>Xenopus laevis</i> testis and fertilisation of oocytes..	78
2.2.21.7	Microinjection of <i>Xenopus laevis</i> embryos and culture	78
2.2.21.8	Fixation of injected <i>Xenopus laevis</i> embryos and X-gal staining.	79
2.2.21.9	Whole mount in situ hybridisation.....	79
2.2.22	OVERVIEW	83
3	Results	87
3.1	CHD7 interacts with components of the WAR complex	87
3.2	CHD7 and the members of the WAR complex are co-localised in the nucleus.....	89
3.3	CHD7 shows no direct interaction with WAR complex members	92
3.4	Genome-wide expression analysis demonstrates a misregulation of NCC guidance genes in case of CHD7 loss of function.....	94
3.5	Expression analysis by RT-qPCR confirms the results of the microarray ..	97
3.6	There is no gender specific effect on the expression of <i>Sema3a</i> , <i>Sema3d</i> , <i>Epha3</i> , <i>Trp53bp2</i> , <i>Sox10</i> and <i>Gfra2</i> in <i>Whirligig</i> mouse embryos	99
3.7	CHD7 and SEMA3D show a similar expression pattern in mouse embryos	101
3.8	Results of <i>SEMA3A</i> and <i>SEMA3D</i> mutation screens in patients with CHARGE syndrome.....	103
3.9	Knockdown of <i>Chd7</i> causes alteration in <i>sema3a</i> expression in <i>Xenopus laevis</i>	105

3.10	The Chd7 MO phenotype was successfully rescued by human <i>CHD7</i> RNA	108
3.11	Knockdown of Sema3a and Sema3d causes migration defects of NCCs in <i>Xenopus laevis</i>	111
3.12	Double knockdown of Chd7 and Sema3a or Sema3d has no clear synergistic effect on <i>twist</i> expression in <i>Xenopus laevis</i>	114
4	Discussion	121
4.1	Short summary	121
4.2	CHARGE syndrome shows phenotypical overlap with other syndromes	122
4.3	CHD7 is associated with the WAR complex	122
4.4	CHD7 regulates genes required for proper NCC development	124
4.5	Chd7 regulates <i>sema3a</i> expression and NCC induction and migration in <i>Xenopus laevis</i>	126
4.6	SEMA3A and SEMA3D seem to play a role in the pathogenesis of CHARGE syndrome	127
4.7	Semaphorins might act as modifier in CHARGE syndrome	128
4.8	Future perspective	131
5	References	133
6	Appendix	149
7	Curriculum vitae	153

List of figures

Figure 1: Possible composition of the MLL methyltransferase complex.	3
Figure 2: Schematic overview of induction and delamination of neural crest cells. ...	4
Figure 3: Differentiation of neural crest cells.	6
Figure 4: Results after RT-qPCR/qPCR run.	58
Figure 5: Co-immunoprecipitation experiments with HeLa cells.....	88
Figure 6: Protein localisation after immunocytochemistry performed with HeLa cells.	90
Figure 7: Analysing protein interactions in HeLa cells using the Duolink PLA method.....	91
Figure 8: Results of the direct yeast two-hybrid assay.	93
Figure 9: Schematic representation of the CHD7 constructs for yeast two-hybrid experiments.	94
Figure 10: Heatmap of differentially expressed genes found by microarray.....	96
Figure 11: Results of the gene expression analysis by RT-qPCR.....	98
Figure 12: Repetition of RT-qPCR.	100
Figure 13: CHD7 and SEMA3D expression analysis using paraffin sections of mouse embryos stained with DAB.	102
Figure 14: Results of the <i>SEMA3A</i> mutation screen.	104
Figure 15: Results of the <i>SEMA3D</i> mutation screen.....	105
Figure 16: <i>Sema3a</i> expression analysis by whole mount <i>in situ</i> hybridisation after Chd7 knockdown in <i>Xenopus laevis</i> (neurula stage 20).	106
Figure 17: <i>Sema3a</i> expression after Chd7 knockdown in <i>Xenopus laevis</i> (tailbud stage 27).	107
Figure 18: Rescue of the Chd7 MO phenotype in <i>Xenopus laevis</i> (neurula stage 21).	109
Figure 19: Repetition of the rescue of the Chd7 MO phenotype in <i>Xenopus laevis</i> (neurula stage 20).....	111
Figure 20: <i>Twist</i> expression analysis after knockdown of Chd7, Sema3a or Sema3d in <i>Xenopus laevis</i> (neurula stage 21).....	112
Figure 21: Effect of Chd7, Sema3a or Sema3d knockdown on NCCs (<i>twist</i> expression) in <i>Xenopus laevis</i> (tailbud stage 26).	113
Figure 22: Effect on <i>twist</i> expression after Chd7 knockdown, Chd7/Sema3a and Chd7/Sema3d double knockdown in <i>Xenopus laevis</i>	116

Figure 23: Effect on the NCC marker <i>twist</i> after Chd7 knockdown, Chd7/Sema3a and Chd7/Sema3d double knockdown in <i>Xenopus laevis</i>	119
---	-----

List of tables

Table 1: Function of factors involved in early migration and guidance of neural crest cells.	7
Table 2: Instruments.....	13
Table 3: Consumable materials	15
Table 4: Kits.....	17
Table 5: Ready to use buffers and mediums	18
Table 6: Chemicals.....	19
Table 7: Agarose gel electrophoresis	22
Table 8: Co-immunoprecipitation (Co-IP).....	23
Table 9: DAB staining	23
Table 10: Duolink	24
Table 11: Polymerase chain reaction (PCR)	24
Table 12: RNA isolation	24
Table 13: Western blots	25
Table 14: Whole mount <i>in situ</i> hybridisation.....	26
Table 15: Yeast two-hybrid.....	28
Table 16: Media and plates	28
Table 17: Primary antibodies	31
Table 18: Secondary antibodies	31
Table 19: Morpholinos.....	31
Table 20: Oligonucleotides	32
Table 21: PCR reaction conditions (Immolase TM).....	49
Table 22: PCR program (Immolase TM).....	50
Table 23: PCR reaction conditions (peqGOLD <i>Pwo</i>).....	50
Table 24: PCR program (peqGOLD <i>Pwo</i>).....	51
Table 25: PCR reaction conditions (<i>Pfu</i> Ultra TM High-Fidelity)	52
Table 26: PCR program (<i>Pfu</i> Ultra TM High-Fidelity)	52
Table 27: PCR reaction conditions (Platinum [®] <i>Taq</i>)	53
Table 28: PCR program (Platinum [®] <i>Taq</i>)	53
Table 29: PCR reaction conditions (Touchdown).....	54
Table 30: PCR program (Touchdown).....	54
Table 31: PCR reaction conditions (sequencing).....	55
Table 32: PCR program (sequencing).....	55

Table 33: RT-qPCR/qPCR program	56
Table 34: reaction conditions (RT-qPCR/qPCR).....	57
Table 35: Terms used in Allelic Discrimination Analysis.	57
Table 36: Reagent volumes for different packed cell volume	66
Table 37: Reaction conditions (in vitro transcription of labeled anti-sense RNA)....	77
Table 38: Proteinase K treatment of <i>Xenopus laevis</i> embryos.....	80
Table 39: Microarray gene expression analysis	149

Abbreviations

A	adenine, alanine
aa	amino acid
Aba	aureobasidin A
ad	to, up to
Ade	adenine
ADE2	adenine promotor
<i>ASH2L</i>	<i>ash2 (absent, small, or homeotic)-like</i>
ATP	adenosine triphosphate
b	constant (interception of y-axis), branchial
BAF	Brahma-associated factor
<i>BamHI</i>	<i>Bacillus amyloliquefaciens</i> H I
bp	base pair
BCIP	5-Brom-4-chlor-3-indolylphosphate
BMB	Boehringer Mannheim Blocking Reagent
BRK	Brahma and Kismet
BSA	bovine serum albumin
C	cytosine
c	molar concentration, cochlea
c.	cDNA reference sequence
°C	degree Celsius
CaCl ₂	calcium chloride
cc	cartilage condensation being primordium of vertebral body
cDNA	complementary deoxyribonucleic acid
CHAPS	3-[(3-Cholamidopropyl)dimethylammonio]-1-propanesulfonate
<i>CHD</i>	<i>chromodomain helicase DNA binding protein</i>
<i>CHD7</i>	<i>chromodomain helicase DNA binding protein 7</i>
<i>CHD8</i>	<i>chromodomain helicase DNA binding protein 8</i>
chp	choroid plexus differentiating from roof of fourth ventricle
Cl	chloride
cm	centimetre

cm ²	square centimetre
Co-IP	co-immunoprecipitation
CO MO	control Morpholino
cp	cartilage primordium of body of vertebra
CR	conserved region
Ct	threshold cycle
C-terminus	carboxy-terminus
CTP	cytidine triphosphate
Cy3	cyanine dye 3
DAB	3,3'-Diaminobenzidine
DAPI	4',6-diamidino-2-phenylindole
dATP	deoxyadenosine triphosphate
dCTP	deoxycytidine triphosphate
ddH ₂ O	double distilled water
ddNTPs	dideoxynucleotide triphosphates
DEPC	diethylpyrocarbonate
dGTP	deoxyguanosine triphosphate
DMEM	Dulbecco's Modified Eagle Medium
DMSO	dimethyl sulfoxid
DNA	deoxyribonucleic acid
DNaseI	deoxyribonuclease I
dNTP	deoxynucleotide triphosphate
DO supplement	dropout supplement
DPBS	dulbecco's phosphate buffered saline
DTT	1,4-Dithiothreitol
dTTP	desoxythymidin triphosphate
E	efficiency, embryonic stage
<i>E. coli</i>	<i>Escherichia coli</i>
<i>EcoRI</i>	<i>Escherichia coli</i> . strain R I
e-cup	eppendorf reaction vessel
EDTA	ethylene diamine tetraacetic acid
e.g.	exempli gratia (for example)
EGTA	ethylene glycol tetraacetic acid
EMT	epithelial-to-mesenchymal transition

ENU	N-ethyl-N-nitrosourea
<i>Eph</i>	<i>Ephrin</i>
<i>Epha3</i>	<i>Eph receptor A3</i>
<i>Epha5</i>	<i>Eph receptor A5</i>
<i>Epha7</i>	<i>Eph receptor A7</i>
ESP	Exome Sequencing Project
et al.	et alteri (and others)
EtOH	ethanol
FC	fold change
FCS	fetal calf serum
FDR	false discovery rate
Fig.	figure
FITC	fluorescein isothiocyanate
<i>Foxd3</i>	<i>forkhead box D3</i>
fv	forth ventricle
g	gram, constant of gravitation, ganglia
G	guanine
GenRE	genome research environment
<i>Gfra2</i>	<i>glial cell line derived neurotrophic factor family receptor alpha 2</i>
GnRH	gonadotropin-releasing hormone
G-protein	guaninnucleotide-binding protein
GSF	Forschungszentrum für Umwelt und Gesundheit (Gesellschaft für Strahlenforschung)
GTP	guanosine-5'-triphosphate
H	histidine
h	heart, hour, human, hyoid
HA-Tag	hemagglutinin Epitop marker
hCG	human chorionic gonadotropin
HCl	hydrochloric acid
HeLa	Henrietta Lacks
HEPES	2-[4-(2-hydroxyethyl)piperazin-1-yl] ethanesulfonic acid
Het	heterozygous

hgvs	human genome variation society
His	histidine
HIS3	histidine promotor
H3K4	histone 3 lysine 4
H ₂ O	water
H ₂ O ₂	hydrogen peroxide
Homo	homozygous
<i>HOX</i>	<i>homeobox</i>
<i>HOXA2</i>	<i>homeobox A2</i>
<i>Hprt</i>	<i>Hypoxanthin-phosphoribosyl-transferase</i>
HRP	horseradish peroxidase
<i>Hsc-70</i>	<i>heat shock protein cognate 70</i>
I	isoleucine
IgG	Immunoglobulin G
IP	immunoprecipitation
K	lysine
kb	kilo base pair
KCl	potassium chloride
kDa	kilo Dalton
K ₃ Fe(CN) ₆	potassium ferricyanide
K ₄ Fe(CN) ₆	potassium ferrocyanide
<i>KMT2D</i>	<i>lysine (K)-specific methyltransferase 2D</i>
KNO ₃	potassium nitrate
L	litre, leucine
l	liver
<i>lacZ</i>	<i>beta-D-galactosidase</i>
LB	lysogeny broth
LDS	lithium dodecyl sulfate
Leu	leucine
LEU2	leucine promotor
LiAc	lithium acetate
log	decadic logarithm
–LT	without leucine, tryptophan
–LTHA	without leucine, tryptophan, histidine, adenine

M	molar
m	slope, mandibular
mA	milliampere
MAB	maleic acid buffer
MBS	modified barth solution
MEM	MOPS, EGTA, MgSO ₄ ; Minimum Essential Medium
MEMFA	MEM + Formaldehyde
MES	2-(N-morpholino)ethanesulfonic acid
MetOH	methanol
mg	milligram
MgCl ₂	magnesium chloride
MgSO ₄	magnesium sulphate
mh	midbrain hindbrain boundary
min	minute
MIPS	munich information center for protein sequences
MIQE	Minimum Information for Publication of Quantitative Real-Time PCR Experiments
miRNA	microRNA
ml	millilitre
<i>MLL2</i>	<i>mixed lineage leukemia 2</i>
mM	millimolar
mm	millimetre
MO	Morpholino
mo	medulla oblongata
MOPS	3-morpholinopropane-1-sulfonic acid
mRNA	messenger ribonucleic acid
<i>MscI</i>	<i>Micrococcus I</i>
mv	mesencephalic vesicle
N	normalisation
NaHCO ₃	Sodium bicarbonate
NaH ₂ PO ₄	Sodium dihydrogen phosphate
Na ₂ HPO ₄	Sodium hydrogen phosphate
<i>Nanog</i>	<i>Nanog homeobox</i>

NaOH	Sodium hydroxide
NBT	Nitro blue tetrazolium
NC	negative control
NCBI	National Center for Biotechnology Information
NCC	neural crest cell
<i>NdeI</i>	<i>Neisseria denitrificans</i> I
NEAA	non-essential amino acids
NEB	New England Biolabs
ng	nanogram
<i>NLK</i>	<i>Nemo-Like Kinase</i>
NM	NCBI accession number
nm	nanometre
NP	NCBI Reference Sequence for proteins
<i>NruI</i>	<i>Nocardia rubra</i> I
ns	not specified
N-terminus	Amino-terminus
<i>Oct4</i>	<i>Octamer binding transcription factor 4</i>
OD	optical density
oe	olfactory epithelium
OH	hydroxy
OMIM	Online Mendelian Inheritance in Man
P	proline
p.	protein reference sequence
Pa	pascal (unit of pressure)
<i>Pax2</i>	<i>paired box gene 2</i>
PBAF	polybromo- and BRG1-associated factor containing complex
PBS	phosphate buffered saline
PBST	phosphate buffered saline Tween-20
pCMV	plasmid cytomegalovirus
PCR	polymerase chain reaction
<i>Pdgf</i>	<i>platelet derived growth factor</i>
<i>Pdgfc</i>	<i>platelet derived growth factor C</i>
PEG	polyethylene glycol

pH	potentia hydrogenii
<i>Pitx2</i>	<i>paired-like homeodomain 2</i>
PLA	proximity ligation assay
pmol	picomol
PMSF	Phenylmethanesulfonylfluoride
PolyPhen2	Polymorphism Phenotyping v2 (prediction program)
<i>PPAR_γ</i>	<i>peroxisome proliferator activated receptor gamma</i>
pre-mRNA	premature messenger ribonucleic acid
Ptw	phosphate buffered saline with Tween 20
PVDF	polyvinyliden fluoride
Q	glutamine
q	long arm of chromosome
qPCR	quantitative real-time polymerase chain reaction
R	arginine
R ²	coefficient of determination
<i>RBBP5</i>	<i>retinoblastoma binding protein 5</i>
R ⁿ	normalised reporter fluorescence
RNA	ribonucleic acid
<i>Robo</i>	<i>roundabout</i>
ROX	6-carboxy-x-rhodamine
rpm	revolutions per minute
RT-qPCR	reverse transcription-quantitative real-time polymerase chain reaction
S	serine
s	somites
SANT	Switching-defective protein 3, Adaptor 2, Nuclear receptor corepressor, Transcription factor IIIB
sb	segmental bronchus within accessory lobe of right lung
<i>SdhA</i>	<i>succinate dehydrogenase complex, subunit A</i>

SDS	sodium-dodecyl-sulfate, sequence-detection software
sec	second
<i>Sema3a</i>	<i>sema domain, immunoglobulin domain (Ig), short basic domain, secreted, (semaphorin) 3A</i>
<i>Sema3c</i>	<i>sema domain, immunoglobulin domain (Ig), short basic domain, secreted, (semaphorin) 3C</i>
<i>Sema3d</i>	<i>sema domain, immunoglobulin domain (Ig), short basic domain, secreted, (semaphorin) 3D</i>
<i>Sema3e</i>	<i>sema domain, immunoglobulin domain (Ig), short basic domain, secreted, (semaphorin) 3E</i>
<i>Sema4d</i>	<i>sema domain, immunoglobulin domain (Ig), short basic domain, secreted, (semaphorin) 4D</i>
<i>SET1</i>	<i>histone lysine methyltransferase Set1</i>
<i>SETDB1</i>	<i>SET domain, bifurcated 1</i>
<i>SfiI</i>	<i>Streptomyces fimbriatus I</i>
SIFT	sorts intolerant from tolerant (prediction program)
<i>Slitrk1</i>	<i>SLIT and NTRK-like family, member 1</i>
<i>Slitrk6</i>	<i>SLIT and NTRK-like family, member 6</i>
<i>Slug/snail</i>	<i>Zinc finger protein Slug/ snail family zinc finger</i>
sm	splanchnic mesoderm
S.O.C.	super optimal broth
<i>Sox2</i>	<i>SRY (sex determining region Y)-box 2</i>
<i>Sox9</i>	<i>SRY (sex determining region Y)-box 9</i>
<i>Sox10</i>	<i>SRY (sex determining region Y)-box 10</i>
SSC	saline-sodium citrate
SWI2/SNF2	SWItch/Sucrose NonFermentable
T	thymine, threonine
Tab.	table
<i>Tbp</i>	<i>TATA box binding protein</i>
TBST	Tris-buffered saline and Tween 20
TE	Tris-EDTA
Tris	2-amino-2-hydroxymethyl-propane-1,3-diol

Trp	tryptophan
TRP1	tryptophan promotor
<i>Trp53bp2</i>	<i>transformation related protein 53 binding protein 2</i>
Trx	trithorax
tv	right telencephalic vesicle
<i>twist</i>	<i>basic helix-loop-helix transcription factor twist</i>
U	unit
UTP	uridine-5'-triphosphate
UV	ultraviolet light
V	volt, valine
<i>Vegf</i>	<i>vascular endothelial growth factor</i>
<i>Vegfc</i>	<i>vascular endothelial growth factor C</i>
Vol	volume
VP	vaginal plug
v/v	volume/volume
W	tryptophan
WAR	WDR5, ASH2L, RBBP5
<i>WDR5</i>	<i>WD repeat domain 5</i>
<i>Whi</i>	<i>Whirligig</i>
WMIISH	whole mount <i>in situ</i> hybridisation
WT	wild-type
w/v	weight/volume
x	times concentrated stock
X-Gal	5-bromo-4-chloro-3-indolyl- β -D-galactopyranoside
<i>XhoI</i>	<i>Xanthomonas holcicola</i> I
X-Ray	roentgen radiation
Y2H	yeast two-hybrid
YNB	yeast nitrogen base
I	roman numeral (1)
II	roman numeral (2)
III	roman numeral (3)
α	alpha

β	beta
γ	gamma
%	percent
μg	microgram
μl	microlitre
Δ	delta
∞	infinity
®	registered Trade Mark
™	unregistered Trade Mark
>	greater than
<	less than
~	tilde (informally means approximately)

Nomenclature

In this work mutations were described using the nomenclature according to the human genome variation society (hgvs) (den Dunnen and Antonarakis, 2000; HGVS, 2013). Genes and proteins stated in this work followed the guidelines according to the HUGO Gene Nomenclature Committee (HGNC) for human (Wain et al., 2002), the Mouse Genome Informatics Database (MGI) for mouse (MGI, 2011) and Xenbase Gene Nomenclature Guidelines for *Xenopus laevis* (Xenbase, 2013).

The abbreviation qPCR was used for quantitative real-time PCR and RT-qPCR for reverse transcription-qPCR as proposed by Bustin et al. (2009).

Summary

CHARGE syndrome is a complex malformation syndrome affecting several organ systems like the central nervous system, ear, eye and heart. Heterozygous loss of function mutations in *CHD7*, a conserved chromatin remodelling enzyme, are responsible to cause about two-thirds of CHARGE syndrome cases. CHD7 is present in large multi-subunit complexes regulating gene transcription in a time and cell type specific manner.

In this work, it was shown by co-immunoprecipitation and Duolink proximity ligation assay that CHD7 interacts with the WAR complex members WDR5, ASH2L and RBBP5. Additional direct yeast two-hybrid experiments revealed that CHD7 is most likely associated to this complex via its direct interaction partner CHD8.

The WAR complex is one “core” complex of the methyltransferase KMT2D. Mutations in *KMT2D* are the main cause of Kabuki syndrome, a developmental disorder, showing a remarkable phenotypic overlap to features present in CHARGE syndrome. The results of this work demonstrate a possible link of CHD7 and KMT2D to the same regulatory process of chromatin remodelling and chromatin modification, which might explain the phenotypic overlap of CHARGE syndrome and Kabuki syndrome.

It was proposed that CHARGE syndrome belongs to the neurocristopathies. Recent studies demonstrated that CHD7 is required for the formation of multipotent neural crest cells. However, little is known about CHD7 target genes in the process of neural crest cell development. Within this work a genome-wide microarray analysis was performed with embryos (wild-type (*Chd7*^{+/+}), heterozygous (*Chd7*^{Whi/+}) and homozygous (*Chd7*^{Whi/Whi})) of the *Whirligig* mouse line which carries a nonsense mutation in the *Chd7* gene. 98 genes were identified to be differentially expressed comparing homozygous (*Chd7*^{Whi/Whi}) to wild-type (*Chd7*^{+/+}) embryos. In fact, many of these genes are involved in the development of neural crest cells, for example, the specification of neural crest cells, epithelial-to-mesenchymal-transition and guidance of migrating neural crest cells. In this work it was demonstrated that the regulatory effect of *Chd7* on *Sema3a*, a secreted signalling molecule known to have chemorepulsive properties for axons and to guide migrating neural crest cells, is conserved in mouse and *Xenopus laevis*. Further, a regulatory effect on neural crest cell migration in *Xenopus laevis* was exposed for *Sema3a* and *Sema3d*.

In this work three non-synonymous mutations were identified in *CHD7* negative CHARGE patients within the *SEMA3A* gene and the *SEMA3D* gene, respectively. *SEMA3A* mutations are known to be involved in the pathogenesis of Kallmann syndrome, a genetic disorder, which represents the mild phenotypic end of CHARGE syndrome. It is assumed that *SEMA3A* and *SEMA3D* act as modifiers contributing to a more severe phenotype in CHARGE patients if they are mutated. This would explain the high inter- and intra-familial variability observed in CHARGE syndrome. In general, the results discovered in this work help to better understand the pathogenic mechanism behind CHARGE syndrome.

1 Introduction

1.1 The chromodomain helicase DNA-binding protein 7

CHD7 (Chromodomain helicase DNA-binding protein 7) belongs to the CHD (Chromodomain helicase DNA-binding protein) family of ATP (adenosine triphosphate)-dependent chromatin remodelling enzymes which regulate gene transcription (Kim et al., 2008b). In human the CHD family consists of nine members which share two chromatin domains located at the N-terminus and a SWI2/SNF2-like ATPase/helicase domain (Woodage et al., 1997; Flaus et al., 2006; Flanagan et al., 2007). According to domain and sequence similarities the nine members of the CHD family are divided into three subgroups. CHD7 belongs to subgroup III which is characterised by three conserved regions (CR1-3), a SANT (Switching-defective protein 3, Adaptor 2, Nuclear receptor corepressor, Transcription factor IIIB) domain and two BRK (Brahma and Kismet) domains located at the C-terminal region (J. A. Hall and Georgel, 2007; Marfella and Imbalzano, 2007). *CHD7* is located on chromosome 8 (8q12) and it consists of 38 exons with a genomic size of 188 kb (Vissers et al., 2004). CHD7 is highly conserved in different species, such as mouse, chick, zebrafish, *Xenopus laevis* and others where orthologs were identified (Bosman et al., 2005; Aramaki et al., 2007; Bajpai et al., 2010).

1.2 CHD7 exists in large multi-subunit complexes

It is known that chromatin remodelling enzymes form multi-subunit complexes which regulate gene transcription in a certain way depending on the composition of proteins within these complexes (Mohrmann and Verrijzer, 2005; Trotter and Archer, 2008; Ho et al., 2009b). Schnetz et al. (2010) showed in mouse embryonic stem cells that CHD7 binds OCT4 (octamer binding transcription factor 4), SOX2 (SRY (sex determining region Y)-box 2), NANOG (Nanog homeobox) and the enhancer binding protein P300. Another co-localisation of CHD7 was described by Bajpai et al. (2010), who found CHD7 to be associated with members of the remodelling BAF/PBAF complex (Brahma-associated factor/Polybromo- and BRG1-associated factor containing complex) in human neural crest like cells. Takada et al. (2007)

described the involvement of a complex consisting of CHD7, PPAR γ (peroxisome proliferator activated receptor gamma), NLK (Nemo-Like Kinase) and SETDB1 (SET domain, bifurcated 1) in the process of adipogenesis and osteoblastogenesis in mouse bone marrow mesenchymal progenitor cells. Furthermore, it was shown by our group that CHD7 interacts indirectly and directly with the chromatin remodeler CHD8 (Chromodomain helicase DNA-binding protein 8) (Batsukh et al., 2010). Yates et al. (2010) demonstrated that Chd8 is associated with the WAR complex (WDR5 (WD repeat domain 5), ASH2L (absent, small, or homeotic-like) and RBBP5 (retinoblastoma binding protein 5)). Another factor also associated with the WAR complex is the methyltransferase KMT2D (lysine (K)-specific methyltransferase 2D) (OMIM 602113). An alternative symbol is MLL2 (mixed lineage leukemia 2). KMT2D belongs to the SET1 (histone lysine methyltransferase Set1) family and is responsible for histone 3 lysine 4 (H3K4) di- and trimethylation (Song JJ, 2008). Members of the SET1 family of enzymes are commonly associated with multi-subunit complexes which are important for the activation of the methyltransferase (Miller et al., 2001; Yokoyama et al., 2004; Wysocka et al., 2005; Steward et al., 2006; Ernst and Vakoc, 2012). One “core” complex consists of WDR5, ASH2L and RBBP5 (Steward et al., 2006; Song JJ, 2008; Yates et al., 2010). Yates et al. (2010) described the MLL (mixed lineage leukemia) associated WAR complex as a positive regulator of *HOXA2* (*homeobox A2*) transcription. Furthermore, it is known that WDR5, ASH2L and RBBP5 form a subcomplex in the absence of MLL (Fig. 1) (Dou et al., 2006; Steward et al., 2006; Thompson et al., 2008; Thompson BA, 2008). Yates et al. (2010) demonstrated a direct interaction of CHD8 with each component of the WAR complex that seem to function as a negative regulator of *HOXA2* expression.

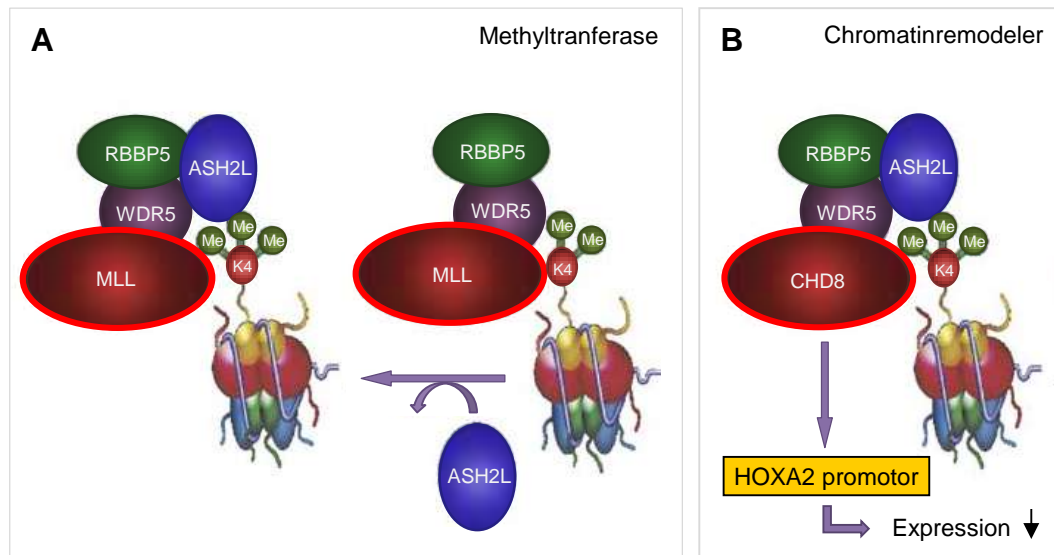


Figure 1: Possible composition of the MLL methyltransferase complex.

(A). MLL is associated via WDR5 with the WAR complex (WDR5, ASH2L and RBBP5). ASH2L is required for trimethylation of H3K4 by the MLL complex. (B) CHD8 seems to bind in the absence of MLL to the WAR complex. This complex might function as a chromatin remodeler which negatively regulates *HOXA2* expression. Figure modified after Steward et al. (2006).

Vissers et al. (2004) identified heterozygous mutations within the *CHD7* gene to be responsible for a malformation syndrome, called CHARGE syndrome.

1.3 CHARGE syndrome

CHARGE syndrome is an autosomal dominant malformation syndrome (OMIM 214800) firstly described in 1979 independently by Hall and Hittner (B. D. Hall, 1979; Hittner et al., 1979). Two years later Pagon et al. (1981) determined the acronym CHARGE association (coloboma, heart defects, atresia choanae, retarded growth and development, genital hypoplasia, ear anomalies/deafness) describing the main features seen in patients and proposed the diagnostic criteria for CHARGE association. Over the years these criteria were refined several times. Blake et al. (1998) defined major (coloboma, atresia of the choanae, cranial nerve disorder and abnormalities of the ear) and minor criteria (heart defects, genital hypoplasia, short stature, developmental delay, tracheoesophageal fistula, orofacial cleft and characteristic facial gestalt) to diagnose CHARGE syndrome. Four major criteria or three major criteria and three out of seven minor criteria must be reported to fulfil the diagnostic criteria of CHARGE syndrome (Blake et al., 1998). An update was defined by Verloes (2005). By identifying *CHD7* mutations as the major cause the

term “CHARGE association” was changed into “CHARGE syndrome” (Vissers et al., 2004; Bergman et al., 2011). Due to the spectrum of malformations, it was hypothesised long time ago that CHARGE syndrome belongs to the neurocristopathies (Siebert et al., 1985; Wright et al., 1986).

1.4 Neural crest cells - the explorer of the vertebral embryo

Neural crest cells (NCCs) are a migratory, multipotent cell population which delaminates from the neural fold or dorsal neural tube (Fig. 2) (Gammill and Bronner-Fraser, 2003). NCCs migrate along specific pathways to populate different niches of the embryo (Rickmann et al., 1985; Kontges and Lumsden, 1996; Morin-Kensicki and Eisen, 1997). Therefore, they are also called the explorers of the vertebral embryo (Gammill and Bronner-Fraser, 2003; Kuriyama and Mayor, 2008).

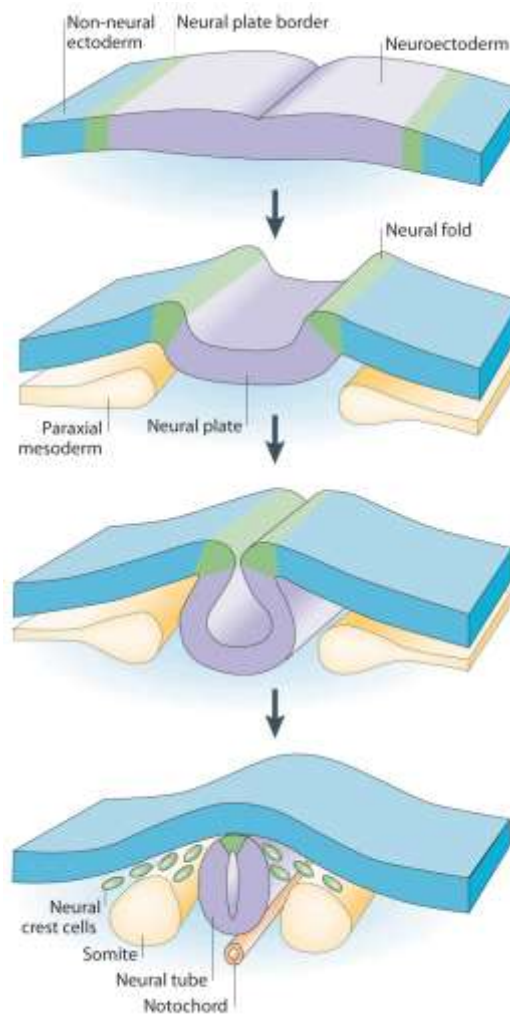


Figure 2: Schematic overview of induction and delamination of neural crest cells.

Introduction

The neural plate border (green) separates the neuroectoderm (purple) from the ectoderm (blue) and is specified by signalling from these two tissues and the underlying mesoderm (yellow). During neurulation the neuroectoderm differentiates into the neural plate due to the elevating neural plate border building neural folds. Further elevation of the neural folds forms the neural tube. The dorsal region of the neural tube where the neural folds joined is now referred to as the neural crest. Neural crest cells delaminate from the dorsal region of the neural tube. Figure taken from Gammill and Bronner-Fraser (2003).

Depending on the localisation within the embryo NCCs give rise to different cell types like neurons, muscle, cartilage or pigment cells (Fig. 3). Therefore, they contribute to the formation of many tissues and organs like heart, skin or the peripheral nervous system (Kuriyama and Mayor, 2008). NCCs are divided into four major groups depending on the region of the longitudinal axis of the embryo where the NCCs delaminate: cranial (cephalic) neural crest, trunk neural crest, vagal and sacral neural crest and cardiac neural crest (Gilbert, 2000).

Cranial NCCs differentiate into different sections of the face like jaw and bones of the middle ear, connective tissue, cartilage, odontoblasts and glia cells (Gilbert, 2000). Depending on the migratory pathway trunk NCCs form melanocytes, dorsal root ganglia, adrenal medulla and sympathetic ganglia (Gilbert, 2000). Vagal and sacral NCCs differentiate into the parasympathic nerves of the gut which allow its peristaltic movements (Gilbert, 2000). The cardiac NCCs form the entire musculoconnective tissue wall of the cardiac outflow tract and contribute to the septum that separates the pulmonary circulation from the aorta (Gilbert, 2000; Kirby and Hutson, 2010). Furthermore, this type of NCCs differentiates into cartilage, connective tissue, neurons and melanocytes (Gilbert, 2000; Kirby and Hutson, 2010).

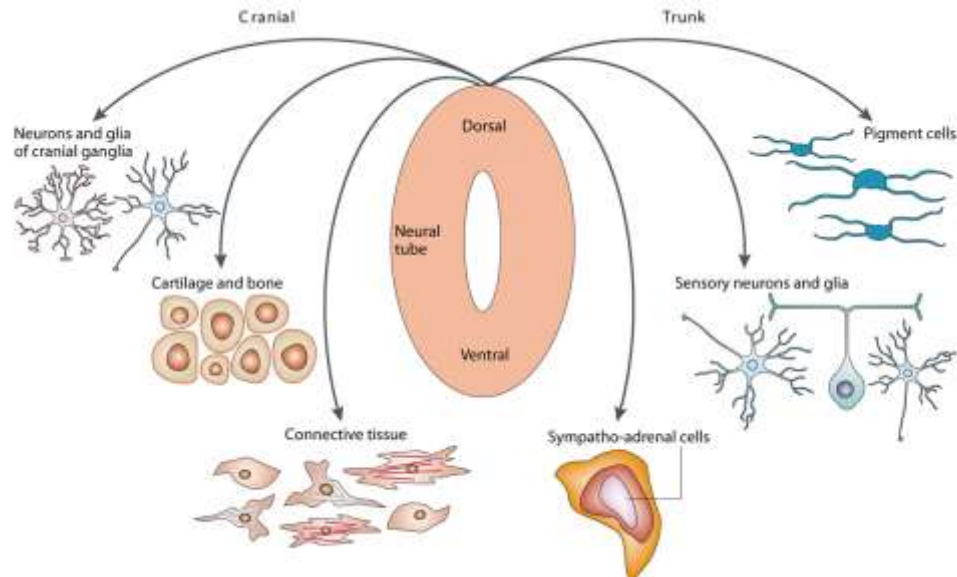


Figure 3: Differentiation of neural crest cells.

Neural crest cells (NCCs) delaminate from the dorsal region of the neural tube and differentiate into multiple cell types. Depending on the region along the longitudinal axis of the embryo different types of NCCs are distinguished which differentiate into different cell types. Cranial NCCs contribute to derivatives of the head region, for instance, neurons and glia of cranial ganglia, cartilage, bones and connective tissue. Trunk NCCs differentiate into melanocytes, sensory neurons and sympathetic ganglia or the adrenal medulla. Figure taken from Knecht and Bronner-Fraser (2002).

1.5 NCC development

The NCC development is a complex process of different events starting with the induction of NCCs at the border of the neural plate by interactions of different signals from the surrounding tissues (Knecht and Bronner-Fraser, 2002; Gammill and Bronner-Fraser, 2003). One of the characteristics of NCCs is their ability to migrate. A process called epithelial-mesenchymal transition (EMT) takes place that enables NCCs to delaminate from the dorsal most region of the neural tube and to migrate along specific pathways until they reach their destination where they differentiate into their predetermined cell types (Gammill and Bronner-Fraser, 2003). During EMT fundamental changes in cell morphology and cell adhesion occur (Kuriyama and Mayor, 2008). The typical apical-basal polarity found in the epithelium of premigratory NCCs is lost due to replacement of tight junctions by gap junctions, allowing the exchange of molecules and ions from one cell to the other (Lampe and Lau, 2000; Kuriyama and Mayor, 2008). A group of transmembrane proteins, namely cadherins, seems to be involved in the early EMT process (Shoval et al., 2007).

Kuriyama and Mayor (2008) assumed that a reduction of type I cadherins in combination with an increase in type II cadherins are linked to NCC EMT. Furthermore, they supposed that matrix metalloproteases which digest the extracellular matrix are required for EMT (Kuriyama and Mayor, 2008).

Once EMT is completed NCCs migrate in clusters along specific pathways to their destination (Kuriyama and Mayor, 2008; Kirby and Hutson, 2010). It has been shown that migrating NCCs are guided by different factors via ligand-receptor signalling (Yazdani and Terman, 2006; Kuriyama and Mayor, 2008).

1.6 NCC guidance and signalling factors

The guidance of migrating NCCs is a complex mechanism which involves different factors that interact with each other to provide the information to NCCs so they know where to go. Table 1 shows an overview about some guidance and signalling factors known to play a role during NCC migration.

Table 1: Function of factors involved in early migration and guidance of neural crest cells.

name	classification and function for NCCs
$\alpha 4\beta 1$ integrin	receptor, controls migration and survival
tenascinC	ECM protein, enables delamination
WNT1	growth factor, initiates migration
TCF	transcription factor, initiates migration
FoxD3	transcription factor, initiates migration
Sox10	transcription factor, initiates migration
semaphorin family	guidance molecule that can attract or repel
neurophilin family	receptor for semaphorins
plexin family	receptor for semaphorins
ephrin family	guidance molecule that can attract or repel
Ephrin family	receptor for ephrins
Slit family	guidance molecule that can attract or repel
Robo family	receptor for Slits
HoxA1/B1	transcription factor, regulates EphA2 expression

Table modified after Kirby and Hutson (2010).

Some factors that play a role in the guidance of NCCs should be further described.

Semaphorins and their receptors neurophilins and plexins

Some of these guidance factors are members of the semaphorin family which are conserved across divergent animal phyla (Yazdani and Terman, 2006). These transmembrane proteins can attract or repel NCCs. In human and mouse 20 semaphorins exist which can be divided into eight classes (Yazdani and Terman, 2006; Kuriyama and Mayor, 2008). Semaphorins primarily act as ligands (Yazdani and Terman, 2006). All of them possess a conserved sema domain of about 500 amino acids that plays a role during binding to their receptors neurophilins and plexins (Yazdani and Terman, 2006). The members of the transmembrane receptor family neurophilin and plexin are expressed in migrating NCCs. Binding of semaphorins to their receptors leads to alteration of the cytoskeleton by reorganising actin filaments and microtubule (Yu and Kolodkin, 1999). Furthermore, semaphorins and its receptors are involved in the correct migratory patterning of NCCs (Eickholt et al., 1999; Brown et al., 2001; Gitler et al., 2004; Lepore et al., 2006; Sato et al., 2006). It has been shown that Sema4D (sema domain, immunoglobulin domain (Ig), short basic domain, secreted, (semaphorin) 4D) either inhibits or enables cell migration and axon outgrowth depending on the member of the plexin receptor family, Sema4D binds to (Yazdani and Terman, 2006). However, the molecular mechanism behind the function of semaphorins is barely understood.

Ephrins and Eph receptors

Ephrins serve as ligands for Eph receptors which belong to the subfamily of receptor tyrosine kinases (Kuriyama and Mayor, 2008). Both, ligands and receptors are membrane-bound proteins, so binding of ephrins to their receptors requires direct cell-cell interaction (Kuriyama and Mayor, 2008). Ephrins are involved in the guidance of axons and in cell migration (Egea and Klein, 2007; Rohani et al., 2011). Until now 13 Eph receptors and eight ephrins are known in mammals (Kuriyama and Mayor, 2008). It has been shown in *Xenopus laevis* that NCCs express Eph receptors while the ligands are expressed in regions of the embryonic tissue where NCCs should either migrate or not migrate (A. Smith et al., 1997). The underlying mechanism by which ephrins mediate their attractive and repulsive effect on NCCs is not clarified.

Slits and Robo receptors

The slit/Robo signalling pathway is involved in different processes, such as guidance of axons and trunk NCCs (Kuriyama and Mayor, 2008; Kirby and Hutson, 2010). In mammals three slit ligands and four Robo receptors have been identified until now (Kuriyama and Mayor, 2008). Like semaphorins and ephrins, slits can act bifunctionally having either a stimulating or repulsing effect on migrating NCCs (De Bellard et al., 2003; Kuriyama and Mayor, 2008).

Most of the described factors (semaphorins, ephrins and slits) were shown to act as negative regulators preventing migrating NCCs from invading the region of their expression (Kuriyama and Mayor, 2008). Further factors involved in the process of NCCs guidance exist. However, the whole machinery behind this guidance process of NCCs is hardly understood.

1.7 *Xenopus laevis* as a model organism for studying NCC development

Since NCCs are a feature of vertebrates, they cannot be studied in traditional model organisms like flies, nematodes or yeast. Historically, NCC development has been studied in amphibian embryos like the African clawed frog *Xenopus laevis* (Collazo et al., 1993). This animal model has the advantage of a relatively fast reproduction cycle and a high number of offspring (Parisis, 2012; Xenbase, n.d.). Furthermore, the breeding can be manipulated by superovulation, so female frogs can lay eggs three to four times a year (Parisis, 2012; Xenbase, n.d.). Amphibian embryos develop externally from the mother animal, so they are easily accessible (Parisis, 2012; Xenbase, n.d.). Oocytes are relatively big with > 1 mm in diameter and can be manipulated (Parisis, 2012; Xenbase, n.d.). One example is the injection of Morpholinos (MO) into the developing oocyte.

MO are synthetic oligonucleotides consisting of about 25 subunits which comprise of a nucleic acid base bound to a morpholine ring and a non-ionic phosphorodiamidate group linkage (GeneTools, n.d.). MO are used as a tool to knockdown gene functions without degrading their target RNA (GeneTools, n.d.). Blocking the translation or modifying pre-mRNA splicing or inhibiting miRNA is the mechanism by which MO knockdown gene expression (GeneTools, n.d.).

Bajpai et al. (2010) performed MO knockdown experiments with *Xenopus laevis* embryos for Chd7, a gene that is conserved in human and *Xenopus*. Downregulation

of *Chd7* revealed features of CHARGE syndrome in *Xenopus laevis* embryos (Bajpai et al., 2010). Furthermore, *Chd7* knockdown experiments demonstrated that the expression of genes involved in early induction of NCCs are not affected while the expression of *sox9* (*SRY (sex determining region Y)-box 9*), *twist* (*basic helix-loop-helix transcription factor twist*) and *slug/snail* (*Zinc finger protein Slug/ snail family zinc finger*) which are involved in NCC specification and early migration processes were downregulated (Bajpai et al., 2010). Therefore, Bajpai et al. (2010) assumed that *Chd7* is involved in the regulation of genes which play a role in the formation of migrating NCCs. However, the question in which way *Chd7* is involved in the EMT process and in the guidance of migrating NCCs was not answered.

1.8 The mouse as a model organism and its advantages

Mouse is a common model organism used for basic research in genetics and human diseases. One of the most striking advantages of the mouse is their similarity to humans in genetics, anatomy and physiology (Simmons, 2008). Over 90 % of the mouse genome resembles the human genome, therefore the mouse afford a good model to study human diseases (Waterston et al., 2002). The mouse genome can be manipulated to induce diseases found in humans either by directly affecting a target gene (knock-out or knock-in) or indirectly by large-scale mutagenesis programmes using chemicals or radiation to induce mutations (Hardouin and Nagy, 2000).

For functional analysis in this work the *CHD7* deficient *Whirligig* mouse line was available that was kindly provided by K. P. Steel (Sanger Centre, Cambridge, United Kingdom) and the Helmholtz Zentrum Munich, Germany. These mice carry a nonsense mutation in exon 11 of the *Chd7* gene generated by large-scale ENU (*N*-ethyl-*N*-nitrosourea) mutagenesis programme (Hrabe de Angelis et al., 2000; Hawker et al., 2005). Homozygous mice (*Chd7^{Whi/Whi}*) die at embryonic stage 10.5 (E10.5) whereas heterozygous mice (*Chd7^{Whi/+}*) resemble many features found in CHARGE patients, such as eye and heart defects, ear anomalies, cleft lip and palate and choanal atresia (Bosman et al., 2005). Therefore, the *Whirligig* mouse line provides a good model to study features of CHARGE syndrome.

1.9 Aim of the work

Chromatin remodelling enzymes exist in large multi-subunit complexes (Schnetz et al., 2010). Are there further CHD7 complex compositions than the ones described in the literature? CHD8 interacts with the WAR complex (Yates et al., 2010). Furthermore, it was demonstrated by our working group that CHD8 interacts with CHD7 (Batsukh et al., 2010). Is CHD7 also associated with the WAR complex? Does CHD7 interact with the members of the WAR complex WDR5, ASH2L and RBBP5? To answer these questions, interaction studies were planned. Co-immunoprecipitation (Co-IP) experiments using HeLa cells should be performed. If CHD7 interacts with components of the WAR complex, where in the cell do the interactions take place? Therefore, Duolink proximity ligation assays (PLA) should be performed. Are the identified interactions direct ones? To clarify this question, direct yeast two-hybrid (Y2H) experiments were planned.

Little is known about the pathogenesis behind CHARGE syndrome. What kinds of genes are regulated by CHD7 and what happens if CHD7 is mutated? To analyse the regulatory effect of CHD7 on other genes, a genome-wide microarray analysis should be performed on whole embryos of the *Whirligig* mouse line. The expression profile of heterozygous (*Chd7*^{Whi/+}) and homozygous (*Chd7*^{Whi/Whi}) animals should be compared to the expression profile of wild-type (*Chd7*^{+/+}) embryos of the same gender. For the confirmation of the microarray data a RT-qPCR (reverse transcription-quantitative real-time polymerase chain reaction) was planned to perform on some of the identified genes. Is there a gender specific effect on the expression of these genes? To validate this question, the RT-qPCR should be repeated for the same genes using RNA of embryos of the *Whirligig* mouse line having the opposite gender than the embryos analysed by the microarray.

Depending on the dataset revealed by the genome-wide microarray analysis, further experiments for certain candidate genes could be performed. An option was the functional analysis of candidate genes in different cell lines, in the mouse model or other animal models, such as *Xenopus laevis*. If required, DNA (deoxyribonucleic acid) samples from CHARGE syndrome patient were available.

Altogether, the aim of this work was to find genes which are regulated by CHD7 and play a role in CHARGE syndrome. Another aim was to identify further interacting partners of CHD7 to help to elucidate the regulatory processes of CHD7. This work

should contribute to better understand the mechanisms behind the pathogenesis of CHARGE syndrome.

2 Materials and methods

2.1 Materials

This section includes all material used to conduct the experiments of this work with further category subdivisions.

2.1.1 Instruments

All instruments used to perform the experiments in this work are listed in table 2.

Table 2: Instruments

device name	company
ABI PRISM [®] 7900HT Sequence Detection System	Applied Biosystems, Darmstadt
advanced primus 96 (PCR cycler)	Peqlab, Erlangen
autoclave	Webeco, Fridolfing
Basic pH Meter PB-11	Sartorius, Goettingen
Synergy [™] Mx	BioTek, Bad Friedrichshall
camera (agarose gel documentation)	Vilbert Lourmat, Eberhardzell
centrifuges: 4 K 15 1-15 K Centrifuge 5415C MicroCentrifuge	Sigma, Hamburg Sigma, Hamburg Eppendorf, Hamburg Roth, Karlsruhe
confocal laser scanning microscope	Olympus, Hamburg
drying oven	Memmert, Schwabach
electrophoresis chamber	Owl Scientific
film processor	AGFA, Cologne
fluorescence microscope BX60	Olympus, Munich
FluorChem [®] Q	Alpha Innotech
forceps HWC 110-10	Hammacher, Solingen
freezer: - 20 °C - 80 °C	Liebherr, Ochsenhausen SANYO, Munich
haemocytometer chamber	Brand, Wertheim
heat sealer	Privileg, Stuttgart

Materials and methods

device name	company
IKA [®] Vibrax-VXR (Shaker)	IKA, Staufen
incubators: bacteria cell culture yeast	Adolf Kuehner AG SANYO, Munich Kranich
magnetic stirrer	IKA, Staufen
micro centrifuge	Roth, Karlsruhe
Microlab Star ^{LET}	Hamilton, Hoechst
micro scissors	Roth, Karlsruhe
microscope	Leitz, Wetzlar
microwave type WR800	Privileg, Stuttgart
Multi 60 well tray lid sterile	Sarstedt, Nuembrecht
NanoDrop TM 8000	Thermo Scientific, Schwerte
Novex [®] Mini Cell (western blot chamber)	Invitrogen, Karlsruhe
pipettes: 1000 µl, 200 µl 100 µl, 20 µl, 10 µl 100 µl 8 canal pipette	Gilson Pipetman Eppendorf, Hamburg Biohit/Satorius, Goettingen
pipette assistant, Accu-jet [®]	Eppendorf, Hamburg
power supply: Apelex PS 304 minipac II Power PAC 3000	Biostep, Jahnsdorf BIO-RAD, Munich
printer: (gel electrophoresis) P91 Doc print TM VX2	Mitsubishi Peqlab, Erlangen
pump (Multifix Typ MC 1000 PEC)	Kranich GmbH
rocking shaker	Heidolph, Schwabach
rotating mixer	Karl Hecht, Sondheim / Rhön
rotator SB2	Stuart, Staffordshire (UK)
scale CP3202 S	Sartorius, Goettingen
scissors: HSB 006-10 HSB 390-10	Hammacher, Solingen Hammacher, Solingen
spectral photometer	Eppendorf, Hamburg
SpeedVac concentrator SVC 100H	Schuetz, Goettingen

device name	company
steriliser	Memmert, Schwabach
sterile laboratory hood	HERAsafe, Schwerte
tank blot	Bio-Rad, Munich
thermomixer 5436	Eppendorf, Hamburg
TissueLyser TL	Qiagen, Hilden
Turboblotter™	Schleicher & Schuell, Dassel
UV table ECX-F20-M	PeqLab, Erlangen
Vortex-Genie® 2	Scientific industries
waterbath	Koettermann, Uetze/Haenigsen
X-ray cassette	Rego X-ray, Augsburg
7900HT Fast Real-Time PCR-System	Applied Biosystems, Darmstadt
3500xL genetic Analyzer	Applied Biosystems, Darmstadt
2720 Thermalcycler	Applied Biosystems, Darmstadt

2.1.2 Consumable materials

Table 3 gives an overview about the consumable materials and the manufacturing companies.

Table 3: Consumable materials

product name	company
ABgene Diamond Ultra 384 well PCR plate	Thermo Scientific, Schwerte
cell culture flasks: 25 cm ² with filter 75 cm ² with filter 75 cm ² without filter	Sarstedt, Nuembrecht Sarstedt, Nuembrecht CellSTAR, Darmstadt
CL-XPosure™ Film (Clear blue X-Ray film)	Thermo Scientific, Schwerte
cover slides, 24x60mm (Menzel-Glaeser)	Thermo Scientific, Schwerte
Cryotube	Greiner Bio-one, Frickenhausen
cuvette	Sarstedt, Nuembrecht
E-Cups (2 ml, 1.5 ml, 750 µl)	Sarstedt, Nuembrecht
Falcon tubes (15 ml, 50 ml)	CellSTAR, Darmstadt

Materials and methods

product name	company
Filter tips (1000 µl, 200 µl, 100 µl, 20 µl, 10 µl)	Kisker, Steinfurt
Folded Filters	Satorius, Goettingen
Glass pipettes	Schuett, Goettingen
Hybond™ CExtra, Nitrocellulose 0.45 µm	Amersham, Freiburg
Hybond™ P, PVDF Transfer Membran 0.45 µm	Amersham, Freiburg
Micro Screwtube 1.5 ml	Sarstedt, Nuembrecht
MultiScreen® Filter Plates	Merck Millipore, Darmstadt
NuPAGE® 4-12 % Bis-Tris Gel	Invitrogen, Karlsruhe
NuPAGE® 3-8 % Tris-Acetate Gel	Invitrogen, Karlsruhe
PCR-Cups	Invitrogen, Karlsruhe
Petri dish (big)	Greiner Bio-one, Frickenhausen
Petri dish (small)	Thermo Scientific, Schwerte
Pipette tips	Eppendorf, Hamburg
QPCR Adhesive Clear Seals	4titude, Berlin
scalpel	Pfm medical, Cologne
Serological pipettes (10 ml, 5 ml, 2 ml)	Sarstedt, Nuembrecht
Serological pipettes (25 ml)	Greiner Bio-one, Frickenhausen
sterile surgical blades	Braun, Tuttlingen
Superfrost® Plus (Menzel-Glaeser)	Thermo Scientific, Schwerte
Transfection tube	Sarstedt, Nuembrecht
Transfer pipettes 3.5 ml	Sarstedt, Nuembrecht
Whatman Paper	Schleicher and Schuell
6-well plate	Sarstedt, Nuembrecht
24 well plate	Sarstedt, Nuembrecht
96-well plate (qPCR)	4titude, Berlin
96-well plate (Bradford)	Thermo Scientific, Schwerte
2-well, 4-well and 8-well slide (BD Falcon™ culture slide)	BD Biosciences, Erembodegem (Belgium)

2.1.3 Kits

The Kits used in this work are listed in table 4.

Table 4: Kits

product name	company
BigDye®	Life Technologies, Darmstadt
Duolink <i>In Situ</i> Detection Reagents Orange	Olink, Uppsala (Sweden)
Duolink <i>In Situ</i> PLA probe anti-Goat PLUS	Olink, Uppsala (Sweden)
Duolink <i>In Situ</i> PLA probe anti-Rabbit MINUS	Olink, Uppsala (Sweden)
DYEnamic ET Terminator Cycle Sequencing Kit (ET-Mix)	GE Healthcare, Munich
Immunoprecipitation Kit (Protein G)	Roche, Penzberg
In-Fusion™ Advantage PCR Cloning Kit	Clontech, Heidelberg
Mini Plasmid Kit	Qiagen, Hilden
mMESSAGE mMACHINE® SP6 Transcription Kit	Life Technologies, Darmstadt
mMESSAGE mMACHINE® T7 Transcription Kit	Life Technologies, Darmstadt
MSB® Spin PCRapace	Invitex, Berlin
NE-PER Nuclear and Cytoplasmic Extraction Reagents	Thermo Scientific, Schwerte
Novocast™ Novostain Universal Detection Kit	Leica Biosystems, Wetzlar
Platinum® SYBR® Green qPCRSuperMix-UDG with ROX	Invitrogen, Karlsruhe
Pure Link® HiPure Plasmid (Midiprep Kit)	Invitrogen, Karlsruhe
QIAquick Gel Extraction Kit	Qiagen, Hilden
RNAspin Mini	GE Healthcare, Munich
RNeasy® mini Kit (250)	Qiagen, Hilden
SuperSignal™ West Pico Chemiluminescent Substrate	Thermo Scientific, Schwerte
Xfect™	Clontech, Heidelberg

2.1.4 Ready to use buffers and mediums

Table 5 includes buffers and mediums which were ready to use as well as the companies selling these products.

Table 5: Ready to use buffers and mediums

product name	company
Aqua-Poly/Mount Coverslipping Medium	Polysciences, Eppelheim
BSA (100 x)	BioLabs, Frankfurt am Main
Developer G153 A+B	AGFA, Cologne
3,3'-Diaminobenzidine (DAB)	Roche, Penzberg
Direct lysis buffer	Peqlab, Erlangen
Dulbecco's Modified Eagle Medium (DMEM)	PAN Biotech, Nuremberg
Dulbecco's Phosphate-Buffered Saline (DPBS)	PAN Biotech, Nuremberg
Fetal bovine serum	PAN Biotech, Nuremberg
MEM NEAA	Gibco, (Life Technologies), Darmstadt
NuPAGE [®] LDS Sample Buffer (4 x)	Invitrogen, Karlsruhe
NuPAGE [®] MES SDS Running Buffer (20 x)	Invitrogen, Karlsruhe
NuPAGE [®] MOPS SDS Running Buffer (20 x)	Invitrogen, Karlsruhe
NuPAGE [®] Tris-Acetate SDS Running Buffer (20 x)	Invitrogen, Karlsruhe
NuPAGE [®] Transfer Buffer (20 x)	Invitrogen, Karlsruhe
OPTI-MEM [®] I + GlutaMax - I	Invitrogen, Karlsruhe
P1 Resuspension buffer	Qiagen, Hilden
P2 Lysis Puffer	Qiagen, Hilden
P3 Neutralisation buffer	Qiagen, Hilden
Rapidfixer	AGFA, Cologne
S.O.C. Medium	Invitrogen, Karlsruhe
TE-Buffer	Invitrogen, Karlsruhe
TrypLE [™] Express	Invitrogen, Karlsruhe

2.1.5 Chemicals

In table 6 all chemicals which were used for the experiments in this work and the corresponding companies selling these products are listed.

Table 6: Chemicals

product name	company
Acetic acid	Merck, Darmstadt
Acetic Anhydrite	Sigma, Hamburg
Acetone	Merck, Darmstadt
Agar-Agar, Kobe I	Roth, Karlsruhe
Agarose	Bio-Budget, Krefeld
Albumin Fraction V (bovine serum albumin (BSA))	Roth, Karlsruhe
Ampicillin	Roth, Karlsruhe
Ampuwa	Fresenius, Bad Homburg
Aprotinin	Sigma-Aldrich, Deisenhofen
β -Mercaptoethanol	Sigma-Aldrich, Deisenhofen
Boehringer Mannheim Blocking Reagent (BMB)	Roche, Penzberg
5-Brom-4-chlor-3-indolylphosphate (BCIP)	Roche, Penzberg
Bromphenolblue	Roth, Karlsruhe
Calcium chloride (CaCl_2)	Roth, Karlsruhe
3-[(3-Cholamidopropyl)dimethylammonio]-1-propanesulfonate (CHAPS)	Sigma-Aldrich, Deisenhofen
Chloroform	J.T. Baker, Griesheim
Coomassie [®] Brilliant Blue R250 Powder	SERVA Electrophoresis, Heidelberg
Desoxy-Nucleotid-Triphosphate (dNTPs) (100 mM)	Invitrogen, Karlsruhe
Diethylpyrocarbonat (DEPC)	Roth, Karlsruhe
Dimethyl sulfoxid (DMSO)	Merck, Darmstadt
Disodium phosphate (Na_2HPO_4)	Roth, Karlsruhe
1,4-Dithiothreitol (DTT)	Invitrogen, Karlsruhe
DO Supplement (-Ade/-His/-Leu/-Trp)	Clontech, Heidelberg
Ethanol	J.T. Baker, Griesheim
Ethidium bromide	AppliChem, Darmstadt
Ethylene diamine tetraacetic acid (EDTA)	AppliChem, Darmstadt
Ethylene glycol tetraacetic acid (EGTA)	AppliChem, Darmstadt

Materials and methods

product name	company
Ficoll 400	Sigma-Aldrich, Deisenhofen
FITC Phalloidin	Sigma-Aldrich, Deisenhofen
Formaldehyde	Invitrogen, Karlsruhe
Formamid	Roth, Karlsruhe
Glycerol	Roth, Karlsruhe
Glycin	Roth, Karlsruhe
G-Protein	Roche, Penzberg
Guanidin hydrochloride	Serva, Heidelberg
Heparin	Roth, Karlsruhe
Hepes	AppliChem, Darmstadt
Hydrochloric acid (HCl)	Merck, Darmstadt
Hydrogen peroxide	Roth, Karlsruhe
2-(4-(2-Hydroxyethyl)-1-piperazinyl)-ethansulfon acid (Hepes)	Sigma, Hamburg
Isopropanol	J.T. Baker, Griesheim
Leupeptin	Sigma, Hamburg
Lipofectamine 2000 Reagent	Invitrogen, Karlsruhe
Magnesium chloride (MgCl ₂)	Bioline, Luckenwalde
Magnesium sulphate (MgSO ₄)	Roth, Karlsruhe
Maleic acid	AppliChem, Darmstadt
Methanol	Roth, Karlsruhe
Milkpowder	Roth, Karlsruhe
Monosodium phosphate (NaH ₂ PO ₄)	Roth, Karlsruhe
Nitro blue tetrazolium (NBT)	Roche, Penzberg
Mineral oil	Sigma, Hamburg
Nitrogen (liquid)	Air Liquide, Kornwestheim
Paraffin	Roth, Karlsruhe
Paraformaldehyde	Roth, Karlsruhe
Pepstatin	Sigma, Hamburg

Materials and methods

product name	company
Peptone	Roth, Karlsruhe
Phenol	Biomol, Hamburg
Phenylmethanesulfonylfluoride (PMSF)	Sigma, Hamburg
Polyvinylpyrrolidone	Sigma, Hamburg
Ponceau S	Sigma, Hamburg
Potassium chloride (KCl)	Roth, Karlsruhe
Potassium ferricyanide ($K_3Fe(CN)_6$)	Sigma, Hamburg
Potassium ferrocyanide ($K_4Fe(CN)_6$)	Sigma, Hamburg
Potassium nitrate (KNO_3)	Merck, Darmstadt,
Proteinase K	Roche, Penzberg
Roti-Nanoquant	Roth, Karlsruhe
Roti Safe	Roth, Karlsruhe
Salmon sperm DNA	Sigma, Hamburg
Sodium azide	Roth, Karlsruhe
Sodium bicarbonate ($NaHCO_3$)	Roth, Karlsruhe
Sodium chloride (NaCl)	AppliChem, Darmstadt
Sodium citrate	Roth, Karlsruhe
Sodium dodecyl sulfate (SDS)	Serva, Heidelberg
Sodium hydroxide solution (NaOH)	Merck, Darmstadt
Torula RNA	Sigma, Hamburg
Triethanolamine	Roth, Karlsruhe
Tris(hydroxymethyl)-aminomethan (TRIS)	AppliChem, Darmstadt
Triton-X-100	Serva, Heidelberg
TRIZOL Reagent	Invitrogen, Karlsruhe
Tween 20	AppliChem, Darmstadt
Vectashield with 4',6-Diamidin-2-phenylindol (DAPI)	Vector, Burlingame (USA)
Yeast extract	Roth, Karlsruhe
X-Gal	Biomol, Hamburg

2.1.6 Buffers and solutions

The following tables show how to prepare the buffers needed for different experiments.

Table 7: Agarose gel electrophoresis

Buffer/solution	Ingredients	
Loading Buffer (50 ml)	50 % (v/v)	Glycerol
	0.1 M	EDTA
	0.02 % (w/v)	Xylencyanol
	0.02 % (w/v)	Bromphenol Blue
	<u>0.02 % (w/v)</u>	SDS
	ad 50 ml ddH ₂ O	
1 x TAE	40 mM	Tris-Acetate (pH 8.5)
	2 mM	0.5 M EDTA
5 x TBE	450 mM	Tris base
	450 mM	boric acid
	20 mM	EDTA
	adjust pH to 8	

Table 8: Co-immunoprecipitation (Co-IP)

Buffer/solution	Ingredients	
Lysis Buffer (25 ml)	5 ml	250 mM Tris-HCl (pH 7.5)
	3.75 ml	1 M NaCl
	2.5 ml	Detergent mix (10 mM Tris-HCl, 10 % Nonidet P40, 5 % sodiumdeoxycholate)
	<u>1 x</u>	Protease inhibitor cocktail tablet
	ad 25 ml ddH ₂ O	
Wash Buffer 2 (50 ml)	10 ml	250 mM Tris-HCl (pH 7.5)
	25 ml	1 M NaCl
	<u>0.5 ml</u>	Detergent mix (10 mM Tris-HCl, 10 % Nonidet P40, 5 % sodiumdeoxycholate)
	ad 50 ml ddH ₂ O	
Wash Buffer 3 (25 ml)	1 ml	250 mM Tris-HCl (pH 7.5)
	<u>0.25 ml</u>	Detergent mix (10 mM Tris-HCl, 10 % Nonidet P40, 5 % sodiumdeoxycholate)
	ad 25 ml ddH ₂ O	

Table 9: DAB staining

Buffer/solution	Ingredients	
Citrate-EDTA Buffer (1 L)	2.1 g	Citric Acid
	0.74 g	EDTA
	adjust pH to 6.2	
	<u>500 µl</u>	Tween 20
	ad 1 L ddH ₂ O	

Table 10: Duolink

Buffer/solution	Ingredients	
Wash buffer A (1 L)	8.8 g	NaCl
	1.2 g	Tris base
	<u>500 µl</u>	Tween 20
	ad 0.8 L ddH ₂ O	
	adjust pH to 7.4	
	ad 1 L ddH ₂ O	
	filter (0.22 µm)	
Wash buffer B (1 L)	5.84 g	NaCl
	<u>24.228 g</u>	Tris
	ad 0.5 L ddH ₂ O	
	adjust pH to 7.5	
	ad 1 L ddH ₂ O	
	filter (0.22 µm)	

Table 11: Polymerase chain reaction (PCR)

Buffer/solution	Ingredients	
dNTPs	10 µl	dATP
	10 µl	dCTP
	10 µl	dGTP
	10 µl	dTTP

Table 12: RNA isolation

Buffer/solution	Ingredients	
DEPC	<u>1 ml</u>	Diethylpyrocarbonate
	ad 1 L ddH ₂ O	
75 % Ethanol/DEPC	75 %	Ethanol
	25 %	DEPC

Table 13: Western blots

Buffer/solution	Ingredients	
Antibody Diluent	2 % in TBST	BSA or milkpouder
Blocking Buffer	5 % in TBST	BSA or milkpouder
Stripping Buffer (1 L, pH 2.2)	1 g 15 g <u>10 ml</u> ad 1 L ddH ₂ O	SDS Glycin Tween 20
TBST (1 L)	10 ml 9 g <u>1 ml</u> ad 1 L ddH ₂ O	Tris-HCl (1 M) NaCl Tween 20
1 x Transfer Buffer (100 ml) (semidry)	5 ml <u>20 ml</u> ad 100 ml ddH ₂ O	NuPAGE Transfer Buffer (20 x) Methanol
1 x Transfer Buffer (1 L) (Wet Blot)	6.05 g 28.52 g 0.1 % <u>20 %</u> ad 1 L ddH ₂ O	Tris Glycin SDS Methanol
Wash Buffer	2 % in TBST	milkpouder

Table 14: Whole mount *in situ* hybridisation

Buffer/solution	Ingredients	
APB (100 ml)	10 ml	Tris (1 M)
	5 ml	MgCl ₂ (1 M)
	2 ml	NaCl (5 M)
	500 µl	Tween 20 (20 %)
	<u>adjust pH 9</u>	
	ad 100 ml ddH ₂ O	
Boehringer Mannheim	<u>10 %</u>	BMB
Blocking Reagent (BMB)	ad MAB	
Denhardts (100 x)	1 g	BSA
	1 g	Ficoll 400
	<u>1 g</u>	Polyvinylpyrrolidone
	ad 50 ml ddH ₂ O	
Hybridisation Buffer	250 ml	Formamide
	125 ml	SSC (20 x)
	50 ml	Torula RNA (10 mg/ml)
	50 mg	Heparin
	5 ml	Denhardts (100 x)
	0.5 ml	Tween 20
	0.5 g	CHAPS
	<u>2.5 ml</u>	EDTA (2 M)
	ad 500 ml ddH ₂ O	
MAB (5 x)	100 mM	Maleic acid
	150 mM	NaCl
	adjust pH 7.5	

Buffer/solution	Ingredients	
MBS (1 x)	10 mM	Hepes (pH 7)
	88 mM	NaCl
	1 mM	KCl
	2.4 mM	NaHCO ₃
	0.82 mM	MgSO ₄
	0.41 mM	CaCl ₂
	0.66 mM	KNO ₃
MEMFA	0.1 M	MOPS
	2 mM	EGTA
	1 mM	MgSO ₄
	4 %	Formaldehyde
PBS (10 x)	3.5 M	NaCl
	37 mM	NaH ₂ PO ₄
	150 mM	Na ₂ HPO ₄
	adjust pH 7.3	
Phosphatase Buffer	10 ml	Tris-Cl (1 M, pH 9.5)
	5 ml	MgCl ₂ (1 M)
	2 ml	NaCl (5 M)
	<u>0.5 ml</u>	Tween 20
	ad 100 ml ddH ₂ O	
PTw	1 x	PBS
	0.1 %	Tween 20
SSC (20 x)	0.3 M	Sodium citrate
	3 M	NaCl
	adjust pH 7	
X-Gal staining solution (10 ml)	250 µl	X-Gal (40 mg/ml)
	200 µl	K ₃ Fe(CN) ₆
	200 µl	K ₄ Fe(CN) ₆
	<u>20 µl</u>	MgCl ₂ (1 M)
	ad 10 ml PBS (1 x)	

Table 15: Yeast two-hybrid

Buffer/solution	Ingredients	
Glucose (40 %)	<u>200 g</u> ad 500 ml ddH ₂ O autoclave and filtrate	Glucose
PEG (50 %)	<u>50 g</u> ad 100 ml ddH ₂ O autoclave	PEG 4000
LiAc (10 x)	<u>6.598 g</u> ad 100 ml ddH ₂ O autoclave	LiAc
TE (10 x)	10 ml <u>2 ml</u> ad 100 ml ddH ₂ O autoclave	1 M Tris-HCl (pH 7.4 - 8) 0.5 M EDTA (pH 8)

2.1.7 Media and plates

In table 16 the instructions for the preparation of media and plates for culturing bacteria, yeast and other cells are given.

Table 16: Media and plates

Charge /solution	Ingredients	
DMEM (200 ml) (cell culture)	20 ml <u>2 ml</u> ad 200 ml DMEM	FCS 100 x Penicillin/Streptomycin
LB medium (1 L) (bacteria culture)	10 g 5 g <u>10 g</u> ad 1 L ddH ₂ O autoclave	Peptone Yeast extract NaCl

Charge /solution	Ingredients	
LB plates (bacteria culture)	10 g	Peptone
	5 g	Yeast extract
	10 g	NaCl
	<u>15 g</u>	Agar
	ad 1 L ddH ₂ O	
	autoclave	
Yeast medium (500 ml) (yeast culture)	0.85 g	YNB (Difco)
	0.3 g	DO Supplement
	<u>2.5 g</u>	Ammoniumsulfate
	ad 475 ml ddH ₂ O	
	adjust pH 5.8	
	10 g	Agar
	autoclave at 120 °C for 15 minutes	
	25 ml	40 % Glucose (autoclaved, filtrated)
	500 µl	Streptomycin (100 mg/ml)
	500 µl	Kanamycin (50 mg/ml)
-LT SD plates (yeast culture)	0.85 g	YNB (Difco)
	0.3 g	DO Supplement
	<u>2.5 g</u>	Ammoniumsulfate
	ad 475 ml ddH ₂ O	
	adjust pH 5.8	
	10 g	Agar
	autoclave at 120 °C for 15 minutes	
	25 ml	40 % Glucose (autoclaved, filtrated)
	500 µl	Streptomycin (100 mg/ml)
	500 µl	Kanamycin (50 mg/ml)
	500 µl	Adenine (20 mg/ml)
	500 µl	Histidine (10 mg/ml)

Charge /solution	Ingredients	Charge /solution
-LTHA SD plates (yeast culture)	0.85 g	YNB (Difco)
	0.3 g	DO Supplement
	<u>2.5 g</u>	Ammoniumsulfate
	ad 475 ml ddH ₂ O	
	adjust pH 5.8	
	10 g	Agar
	autoclave at 120 °C for 15 minutes	
	25 ml	40 % Glucose (autoclaved, filtrated)
	500 µl	Streptomycin (100 mg/ml)
	500 µl	Kanamycin (50 mg/ml)
	125 µl	Aureobasidin

2.1.8 Sterilisation

If not indicated differently, sterilisation of solutions and buffers was performed for 20 minutes in the vapour pressure autoclave (Webeco) at 120 °C at 10⁵ Pa. Heat sensitive solutions were sterile filtrated using filtration units of 0.2-0.45 µm pore size. Objects of utility were either autoclaved or heat sterilised for 8-12 hours at 180 °C.

2.1.9 Antibiotics

Ampicillin (50 mg/ml)	AppliChem, Darmstadt
Aureobasidin A	Clontech, Heidelberg
Kanamycin	Roth, Karlsruhe
Penicillin/Streptomycin (100 x)	PAN Biotech, Nuremberg
Streptomycin (100 mg/ml)	ns

2.1.10 Antibodies

All antibodies used in this work are listed in the tables below. Table 17 shows the primary antibodies and table 18 the secondary antibodies.

Table 17: Primary antibodies

antibody	origin	dilution	company
Anti-HA tag	rat monoclonal	1:1,000	Roche, Penzberg
ASH2L	rabbit polyclonal	1:100/1:1,000	Abcam, Cambridge (UK)
CHD7	goat polyclonal	1:100/1: 7,500	Abcam, Cambridge (UK)
CHD8	rabbit polyclonal	1:100/1:8,500	Abcam, Cambridge (UK)
HSC-70	mouse monoclonal	1:10,000	Santa Cruz, Heidelberg
RBBP5	rabbit polyclonal	1:100/1:1,000	Abcam, Cambridge (UK)
SEMA3D	rabbit polyclonal	1:100	Santa Cruz, Heidelberg
WDR5	rabbit polyclonal	1:100/1:1,000	Abcam, Cambridge (UK)

Table 18: Secondary antibodies

antibody	origin	dilution	company
Anti-goat IgG-H&L (Cy3)	donkey polyclonal	1:200	Abcam, Cambridge (UK)
Anti-rabbit IgG (whole molecule), F(ab') ₂ fragment–Cy3	sheep polyclonal	1:200	Sigma, Deisenhofen
Anti-goat IgG-HRP	donkey polyclonal	1:7,500	Santa Cruz, Heidelberg
Anti-mouse IgG (H+L)-HRP	rabbit polyclonal	1:10,000	Dianova, Hamburg
Anti-rabbit IgG (H+L)-HRP	goat polyclonal	1:10,000	Dianova, Hamburg
Anti-rat IgG, (H+L) HRP	goat polyclonal	1:10,000	Thermo Scientific, Rockford (USA)

2.1.11 Morpholinos

The sequence of the Morpholinos used for injections to knockdown gene expression in *Xenopus laevis* are listed in table 19.

Table 19: Morpholinos

name	purpose	sequence
Sema3a	blocking of mRNA	ATGCAATCCAGGTCAGAGAGCCCAT
Sema3d	blocking of mRNA	GACATTTTTGATGCTTCTCTTTCAT

2.1.12 Oligonucleotides

The oligonucleotides were purchased from Eurofins Genomics. In table 20 the sequences of the oligonucleotides and their purpose of use are given.

Table 20: Oligonucleotides

name	purpose	sequence
ASH2LhY2HF	Y2H construct	CCAGATTACGCTCATATGCGCGCGAGAG AAGAGAGTATT
ASH2LhY2HR	Y2H construct	GGCCTCCATGGCCATATGTTCCCAGAAA GTCCTTGACAGA
ASH2L_InFusion_1Rneu	Y2H construct	GGCCTCCATGGCCATATGGCATCTTTGG GAGAACATTTGA
ASH2L_InFusion_2Rneu	Y2H construct	GGCCTCCATGGCCATATGCGGTTGTTGG CTTATGGTACAC
DelSema3a1F	patient screen	TGGGCTGGTTAACTAGGATTGTCTGT
DelSema3a1R	patient screen	GTTGGGAGGGAGTTCAAGGAATTAAG
DelSema3a2F	patient screen	CAATGTTTTGCTTTGTTACCTTGCAG
DelSema3a2R	patient screen	ACATACAGCCTACTCCGTTCCATC
DelSema3a3F	patient screen	CTTTCTTTACTTCAGTTGCCCCAATG
DelSema3a3R	patient screen	TCTTCTGGTGTAAGATACTGGCCACA
DelSema3a4F	patient screen	CAGTCATGCTGATTGCTGAAACTCTT
DelSema3a4R	patient screen	GTTCCACAGGCGTACAAGTGAGTCT
DelSema3a5F	patient screen	CCACAGGACAATATTTTTAAGCTGGAG
DelSema3a5R	patient screen	GCACCTATTAAAAGGGATGCTGTCA
DelSema3a6F	patient screen	GACTTTGCTATCTTCCGAACCTTTGG
DelSema3a6R	patient screen	CATCATGAAGTCACCACCATTAGCTT
DelSema3a7F	patient screen	AAGTTCATTAGTGCCACCTCATCTC
DelSema3a7R	patient screen	AGCGTGAGTAGCTTTTCCAGAGTGTT
DelSema3a8F	patient screen	TCCCTTCTTTCAGAATGACTTTGGAG
DelSema3a8R	patient screen	ACGCAGTTCATCAAAATGAGTGTC
DelSema3a9F	patient screen	TGTTTCAGACTTTGCCATTCCATAAAA
DelSema3a9R	patient screen	CCAAGAGTACACAACAGCTCAAAGGTT
DelSema3a10F	patient screen	AGGGATCAGCCGTGTGTATGTATAGC
DelSema3a10R	patient screen	CTTCCTTGATAAGGCACCCATTGATA
DelSema3a11F	patient screen	GAAGTCATCCAGCCATGTACAATCC

Materials and methods

name	purpose	sequence
DelSema3a11R	patient screen	CATCATACTGTCCATCTTCTGCATCC
DelSema3a12F	patient screen	TAACTTGTGGTCTTCTCCCCACTTTC
DelSema3a12R	patient screen	AAACTGTCATTTCTTCCAGCAGAACC
DelSema3a13F	patient screen	TGTGTCTTATTTCCCAGTCACATTGC
DelSema3a13R	patient screen	AAAGCTCCATTGCTGAAATAGCAGTC
DelSema3a14F	patient screen	TGTCACAGCAGTAAACTCTTTCCACAG
DelSema3a14R	patient screen	TCCTACCTCTTTGCAGTGGGAAAATA
DelSema3a15F	patient screen	TTCAGACGCACAAGACGACAAGATA
DelSema3a15R	patient screen	TTAGCCTGGTCTTAGCAGGTTGAAAG
DelSema3a16F	patient screen	AGCCCTGAAGAGAGAATCATCTATGG
DelSema3a16R	patient screen	TCCTGTACCTCTTCTTTTCGCTCTTC
DelSema3a17F	patient screen	CTGGAAGTCATTGACACAGAGCATTT
DelSema3a17R	patient screen	GAACTCATCCATTGTGTTGAGATTGG
Del_SEMA3A_1Fn	patient screen	GACTAAAGCAGCAAAGGGACCTACAG
Del_SEMA3A_1Rn	patient screen	GTAGGATAATTTACGCCTTGGCACAT
Del_SEMA3A_9Fn	patient screen	TGTTTCAGACTTTGCCATTCCAT
Del_SEMA3A_9Rn	patient screen	CAGCTCAAAGGTTAAAGCAACACTT
Del_SEMA3A_12Fn	patient screen	TTCAAAGATGTTGGGACCGTTCTTA
Del_SEMA3A_12Rn	patient screen	ACTTGTCCATACCAAGTTCAGTGTGC
DelSema3d1F	patient screen	CTAAGCATGACCATGTTGTTTCTTCC
DelSema3d1R	patient screen	CTGATGCCAAAACATTTACAGAAG
DelSema3d2F	patient screen	GGGTTTCATCAGAAGGACTGGATTTT
DelSema3d2R	patient screen	ACAAAACGGGAGAAGAAGAGAGATGA
DelSema3d3F	patient screen	ATTCACCTCTCTGAGCAGAATTGCAGA
DelSema3d3R	patient screen	ACTTACATTGGCATCTTTCCCAGCTA
DelSema3d4F	patient screen	TGATCTACTTGGAACAGGTGGCATA
DelSema3d4R	patient screen	CATATTGGATGAAATGCTCCAGTTCC
DelSema3d5F	patient screen	AGACTGAAATGTCCTTTTCGATCCTCA
DelSema3d5R	patient screen	CAATAGGAAAATGCGGTTTCAGTCAA
DelSema3d6F	patient screen	CATCTTTGGTGTGTCATGCTGTGAAAT
DelSema3d6R	patient screen	TCTGATGTAGTGGTGGTCATGAGTAGG
DelSema3d7F	patient screen	TTGGAACCTTCTTCATACCAGACACCT
DelSema3d7R	patient screen	CAAACCTTCCAACTCGAGAAAGGAT

name	purpose	sequence
DelSema3d8F	patient screen	TGGAAGTGATGGGGCAGATACTTACT
DelSema3d8R	patient screen	CCGTGTACTTTGCGTGTGAATTTTAG
DelSema3d9F	patient screen	ACTCCCCACAAGAGATGAAAGAAATC
DelSema3d9R	patient screen	ATATGCTACTACAAACGCAGGGACAA
DelSema3d10F	patient screen	ATCTTCAAAGGCTCTGCTGTTTGTGT
DelSema3d10R	patient screen	CGTGGATAAGGAATTCTCCCATCATA
DelSema3d11F	patient screen	ATCAGTTTCATAAAGCGGCACTCTGT
DelSema3d11R	patient screen	CATTACATCGTACTGGCCATCTTCTG
DelSema3d12F	patient screen	AAGAGAAGTGAGGGGAATGATTGTC
DelSema3d12R	patient screen	ACTCCTCCAGCACTACCTCTTCCATA
DelSema3d13F	patient screen	CTTGAACATGGAATTGTCTCTGAAGC
DelSema3d13R	patient screen	GCAAGGCTGAAACAATGGTCTCTAAT
DelSema3d14F	patient screen	ATTGTACATTGGTTCCCGAGATGGAT
DelSema3d14R	patient screen	AGTAGGGGTCTCTGGCAAGACAACAG
DelSema3d15F	patient screen	GGAGAGCTAGACGCCAAGATGTAAAA
DelSema3d15R	patient screen	AATTTCTGTGTGCTCTTCCAGAACAC
DelSema3d16F	patient screen	GCTTTCCAGGCATTAGTCATGAAACT
DelSema3d16R	patient screen	ATGACAACAGCTTACCTCCTCTCGAT
DelSema3d17F	patient screen	CAAAACGGAATATGGGCTACTGATTC
DelSema3d17R	patient screen	TATCTCAACCGTGACTCAGCCAATAG
Del_SEMA3D_1Fn	patient screen	GACTTAAAGCCAGAAGCCAAGATTTTC
Del_SEMA3D_1Rn	patient screen	CCTTTGTAGGTTAGCTTGAGTCTTGGA
hCHD7_F1	Y2H construct	GAGGACCTGCATATGAAGATGGCAGATC CAGGAATGA
EphA3mF1	RT-qPCR	AAAGAGGAGGACCCTCCCAGGATGTA
EphA3mR1	RT-qPCR	ATCGGAAGCCTTGTAGAAGCCTGGTC
Gfra2mF1	RT-qPCR	AAACCATCCTGCCAGCTGTTCTTAT
Gfra2mR1	RT-qPCR	ATTGTCCGGTAGGAGGCTCGACAGTT
hCHD7_R1	Y2H construct	CTCCATGGCCATATGCCTTCTGCATCAAC AGATTCTT
hCHD7_F2	Y2H construct	AATTCCCGGGGATCCCACCATCTCCTCCT CCTGAAGAAG
hCHD7_R2	Y2H construct	CAGGTCGACGGATCCCACTGTAGAGCCT GGTCTGCTT
hCHD7_F3	Y2H construct	GAGGACCTGCATATGAAGTGGGCTAAGA AGGCTGAAT
hCHD7_R3	Y2H construct	CTCCATGGCCATATGTGTCCTCACTCCCA CTAATGCT

name	purpose	sequence
hCHD7_F4	Y2H construct	GAGGACCTGCATATGGAAGCAGTGTTGA AAGGCAAAT
hCHD7_R4	Y2H construct	CTCCATGGCCATATGACTTGAACGGAA CTGGTACTG
ifSema3AnewR	cloning	GGATCCGAGCTCGGTACCACTCAGCTGA ATTTCCCACCAT
ifSema3DnewF	cloning	GCTAGTTAAGCTTGGTACCTAACACCAT TTGAAAGAGAACATTG
ifSema3DnewR	cloning	GGATCCGAGCTCGGTACCCAGATTATTG TCTTGTGCCTTAGC
pGADRBBP5F	cloning in pGADT7	CAGATTACGCTCATATGCTCGAGTTGCT GGAGTCCTT
pGADRBBP5R	cloning in pGADT7	GCCTCCATGGCCATATGAAAGGGAAGGG AAGGTCGTA
pGADWDR51F	cloning in pGADT7	CAGATTACGCTCATATGTCCACCCTTGTC TCCTGTGC
pGADWDR51R	cloning in pGADT7	GCCTCCATGGCCATATGGGCAAGAAATG TCACCAGCA
pGADWDR52F	cloning in pGADT7	CAGATTACGCTCATATGTTCTGCATCTCG CTCAACA
pGADWDR52R	cloning in pGADT7	GCCTCCATGGCCATATGGCAAGAAATGT CACCAGCAA
RbBP5pCMV-HA_F	cloning in pCMV-HA	CTTATGGCCATGGAGGCCGGGATGAACC TCGAGTTGCT
RbBP5pCMV-HA_R	cloning in pCMV-HA	ATTCGGGCCTCCATGGCCAAAGGGAAGG GAAGGTCGTA
SEMA3A1F	Sequencing	TCACCTGTTACCTCCAGTTTCC
SEMA3A1R	Sequencing	GGTTTGATGATTTGGGGTTG
SEMA3A2F	Sequencing	TCAGGTTACCATGTACCAACAGTC
SEMA3A2R	Sequencing	TGCATCCATTGATTCATTACTGTC
SEMA3A3F	Sequencing	ACTTCAGTTGCCCCAATGTC
SEMA3A3R	Sequencing	CACATGACCCACAAGTGGAA
SEMA3A4F	Sequencing	CAGTCATGCTGATTGCTGAAA
SEMA3A4R	Sequencing	TGAACCACAAGCAAAATAAACTG
SEMA3A5F	Sequencing	TCTCTGATTAAGTATGTGTTGAAA
SEMA3A5R	Sequencing	TTATTTTCATAATGGAAAATCTTGGT
SEMA3A6F	Sequencing	CATGGTCATAACATGAACTTGC
SEMA3A6R	Sequencing	CCATCATGAAGTCACCACCA
SEMA3A7F	Sequencing	TGGACTGTTCAGAATGGTATTATTT
SEMA3A7R	Sequencing	CCTGTACCTGTATATTTGACTGCG
SEMA3A8/9F	Sequencing	GGAACGATTTCGACCACAAAT
SEMA3A8/9R	Sequencing	TGCAAATTATGAGTACTTGGATAGC
SEMA3A10F	Sequencing	GCCATTTTCACCTATGCCTT
SEMA3A10R	Sequencing	TCTGTCTGTAGCTGCATTGTTTT

name	purpose	sequence
SEMA3A11F	Sequencing	GAACCATTGAGGCCATGTGT
SEMA3A11R	Sequencing	CCAACCCCTGAGATGTTCAA
SEMA3A12F	Sequencing	AAAAGGAAGACCGATATCAAAGG
SEMA3A12R	Sequencing	TGAGAAAACAAAATATGAGCCAAA
SEMA3A13F	Sequencing	AGCAATAACCCCAACTTGGTC
SEMA3A13R	Sequencing	ATCAAAAACATGAGGGCAATG
SEMA3A14F	Sequencing	AGAAGGCCTTTAAAGAAATTAGCA
SEMA3A14R	Sequencing	TTGATGCACTTATTTGAAGAAAGC
SEMA3A15F	Sequencing	TCTGGTAGTGAAAAAGCCATGA
SEMA3A15R	Sequencing	TCTCTTCGGCTGCATTTCTT
SEMA3A16F	Sequencing	TGGCAATAACTTGTCTCCTGAA
SEMA3A16R	Sequencing	TGAATGAGCGATTGATTGGT
SEMA3A17F	Sequencing	ACAGACACGGAGTTTCAGAGC
SEMA3A17R1	Sequencing	AGATTGGGGTGGTTGATGAG
SEMA3A17R2	Sequencing	CCCACCATTTGTAAACATCCA
SEMA3D1F	Sequencing	AACACCATTGTGAAAGAGAACATTG
SEMA3D1R	Sequencing	AATGAGTAATTGGGCTTCGTGT
SEMA3D2F	Sequencing	TTGGCCCTTTTATGCTGTATG
SEMA3D2R	Sequencing	CCAGAATGTGTATCAGAGGCAAT
SEMA3D3F	Sequencing	TCTGAGCAGAATTGCAGAGTG
SEMA3D3R	Sequencing	CCATTAATTCAGTAAAGCCCAAT
SEMA3D4F	Sequencing	ATTTGTCTTGCCTCGTTTGC
SEMA3D4R	Sequencing	TCAAATCTGCCTGTTTTATGTCA
SEMA3D5F	Sequencing	GGAATTTAGTTTGTATCTCCCACA
SEMA3D5R	Sequencing	AATAATGGAAACAAATCGCTTG
SEMA3D6F	Sequencing	GGTGTGATGCTGTGAAATTTGT
SEMA3D6R	Sequencing	TTAAACCAAAGCAAGACAATCAAA
SEMA3D7F	Sequencing	CCCACATCTGGCTTATAGTTCA
SEMA3D7R	Sequencing	AGCATTAACCTTTGGCTTAAACCTT
SEMA3D8Fa	Sequencing	TGATGGTAGTGGTGCCTGTATT
SEMA3D8Ra	Sequencing	TGCATTGTTCAAATCATTTATGC
SEMA3D8Fb	Sequencing	AGACACTACCTGTAATAGCCACCA
SEMA3D8Rb	Sequencing	TGGAGCCAAAGGGAAATAAA

name	purpose	sequence
SEMA3D9F	Sequencing	GCATAATATAGTGCCTCTGTTAATCG
SEMA3D9R	Sequencing	CTACTACAAACGCAGGGACAAA
SEMA3D10F	Sequencing	TGAATGATTGAATGATGATGCT
SEMA3D10R	Sequencing	GTGGCTCTGGTGAATAGCAG
SEMA3D11F	Sequencing	TTCCATATTGACTCTGTTGTCCA
SEMA3D11R	Sequencing	TTTTAAGAAATGCTGACAAGGTTTT
SEMA3D12F	Sequencing	GAGAAAGTGAGGGGAATGATTTG
SEMA3D12R	Sequencing	AAACAAGGGTGCCCTATAACAA
SEMA3D13F	Sequencing	TTTACTTCAGTGATATATGGCATCAG
SEMA3D13R	Sequencing	TTTAACTCCCAATTTCAATGGAT
SEMA3D14F	Sequencing	GTCTGAAAGATGCTTCTAATTCATTT
SEMA3D14R	Sequencing	TTCCTTCCATAGGACATGTTAGTAAT
SEMA3D15F	Sequencing	CATAGTACTGCATCTGCCACTGT
SEMA3D15R	Sequencing	CCAGAACACATGCATTACACAA
SEMA3D16F	Sequencing	TGGCATCTGTTCTGAATCAGTC
SEMA3D16R	Sequencing	TCAATCGTACACTATTTCCCTCAA
SEMA3D17F1	Sequencing	CATTTGCTCTTAGCTCTCTCTGTG
SEMA3D17R1	Sequencing	TCATCCAGGTCTCTGTGATGTC
SEMA3D17F2	Sequencing	AAATCCTTAGCAGCCCCAACTT
SEMA3D17R2	Sequencing	ACTCCATGGGAAGCATTTATGA
SeqhASH2L1F	Sequencing	GGTCGCAAATGCAACAGG
SeqhASH2L1R	Sequencing	GCTTACATCGACCAAGTTTGC
SeqhASH2L2F	Sequencing	ACAGGGACCACCAAGAAGG
SeqhASH2L2R	Sequencing	CCATCTTTGTTAAACGGGTGTT
SeqhASH2L3F	Sequencing	CCATTAACTTTGGACCATGCTT
SeqhASH2L3R	Sequencing	ATGTCACTCATAGGGCGGTAAG
SeqCHD71.1R	Sequencing	ACTGTCTGGCTCCGAGAACTAA
SeqCHD71.2F	Sequencing	GCCTCAATCAGGGAAATCCT
SeqCHD71.2R	Sequencing	CAGGTATCAGTCGTTCCCTGGAT
SeqCHD71.3F	Sequencing	ATCCTCAGCCATCTCACCAG
SeqCHD71.4F	Sequencing	TAGCAGAGGATCCCAGTAAAGG
SeqCHD72.1R	Sequencing	CTGGAGACTCTGCATTGTGTGT
SeqCHD72.2F	Sequencing	GGTGGTCAAGCTAACGTACCTAAC

name	purpose	sequence
SeqCHD73.1R	Sequencing	CTCTCACTGTGCTTACCTGTGG
SeqCHD73.2F	Sequencing	GAACAGACATGCTAGCAGATGG
SeqCHD73.2R	Sequencing	GGATAACTCAGGGTCATTGAGG
SeqCHD74.1R	Sequencing	GGCCTTCTTCCTCTTCTGCT
SeqCHD74.2F	Sequencing	CAATGAAGGATCTACCCAGGTG
seqCHD7_1vectR	Sequencing	GCTGACCCATAGGATTTACTGG
seqCHD7_2vectR	Sequencing	TCCAAGTGGTATTCCCTGAGTT
seqCHD7_3vectR	Sequencing	GATGGTTCTGCAGATGGTTTCT
seqCHD7_4vectR	Sequencing	CCTCTCTTGAGGCCTTTGATAA
SeqCHD7F1new	Sequencing	ATGGCAGATCCAGGAATGAT
SeqCHD7F2new	Sequencing	AGATCAAGCAAAGATCGAGGAG
SeqCHD7F3new	Sequencing	AACCTCACTGCTGCTGATACCT
SeqCHD7F4new	Sequencing	AATGTTTCAGGGTGGAGAAGAA
SeqCHD7F5new	Sequencing	CTTGGATCTGCCAGAGTGGT
SeqCHD7F6new	Sequencing	CAAGAGGCGAAATCTCATGG
SeqCHD7F7new	Sequencing	CTAGTCAAGGAGAACCGGAAGA
seqRbBP5h.F4	Sequencing	GACCCTATTGCTGCCTTCTGTA
SeqxSema3a1F	Sequencing	CTGACCTGGATTGCATTTCTTT
SeqxSema3a1R	Sequencing	TTGTAGGACAATCTGAGCCTTG
SeqxSema3a2F	Sequencing	GGTGGCCACAGAAGCTTAGTTA
SeqxSema3a2R	Sequencing	ACATTCTGACAGTTGAGCCTTG
SeqxSema3a3F	Sequencing	AGCTGAGGATGGTCAATACGAT
SeqxSema3a3R	Sequencing	TGTATCAATGCCATTAGGACCA
SeqxSema3a4F	Sequencing	AATGTCCAGGTTAGCAACACAA
SeqxSema3a4R	Sequencing	CTCAAATTCATGGGTCCTCCTA
seqSEMA3A_F3new	Sequencing	AGACGCACAAGACGACAAGATA
seqSEMA3A_R3new	Sequencing	ATTCTCTCTTCAGGGCTGTGG
SeqSema3d_1F	Sequencing	TTAAACCGCAGCATTCCTCTAC
SeqSema3d_1R	Sequencing	CCGAGGAATATTCTGTTTCAGG
SeqSema3d_2F	Sequencing	TGTTCAATTCCTGGACAAGATG
SeqSema3d_2R	Sequencing	GGATTTCTTTCGTCCTTTGTTG
SeqSema3d_3F	Sequencing	CAATCAGGTGGTTTATTCAGCA
SeqSema3d_3R	Sequencing	GAATCAGAAGCCCGTAGTCTGT

name	purpose	sequence
Sema3AmF1	RT-qPCR	CGGGACTTCGCTATCTTCAGAACACT
Sema3AmR1	RT-qPCR	TCATCTTCAGGGTTGTCACTCTCTGG
Sema3DmF1	RT-qPCR	TTACGTGTGTGGAAGTGGAGCGTTTC
Sema3DmR1	RT-qPCR	AGGCTGCTGAGGATCAAAGGGACAT
SOX10mF1	RT-qPCR	GCTCAGCAAGACACTAGGCAAGCTCT
SOX10mR1	RT-qPCR	CGAGGTTGGTACTTGTAGTCCGGATG
SRY_F	gender PCR	AGCCTGTTGATATCCCCACTG
SRY_R	gender PCR	ATGCTCACCAGTGTGTCAGC
Trp53bp2mF1	RT-qPCR	CCCAGTTGCTGATAACGAACGGATGT
Trp53bp2mR1	RT-qPCR	TCGGTCCACTCACAATGTCCCTGTTA
WDR5hY2HF	Y2H construct	CCAGATTACGCTCATATGTCCACCCTTGT CTCCTGTGC
WDR5hY2HR	Y2H construct	GGCCTCCATGGCCATATGGGTCAACTTC CCGACAGTCTCT

2.1.13 DNA marker

100 bp DNA ladder	Invitrogen, Karlsruhe
1 kb DNA ladder	Invitrogen, Karlsruhe
1 kb DNA ladder	BioLabs, Frankfurt am Main

2.1.14 Protein marker

See Blue Plus 2 Pre-stained Standard	Invitrogen, Karlsruhe
Hi Mark Pre-Stained	Invitrogen, Karlsruhe

2.1.15 Vectors

pBluescript SK (-)	Agilent Technologies, Boeblingen
pcDNA3.1 (+) Flag-6xHis	Invitrogen, Karlsruhe
pCMV-HA	Clontech, Heidelberg
pCMV-Myc	Clontech, Heidelberg
pCS2+MT	ns
pGADT7	Clontech, Heidelberg
pGBKT7	Clontech, Heidelberg
pGEM-T Easy	Promega, Mannheim

2.1.16 Enzymes

Antarctisc Phosphotase	BioLabs, Frankfurt am Main
DNase I (1 U/μl)	Thermo Scientific, Schwerte
Proteinase K	Roth, Karlsruhe
SuperScript® II	Invitrogen, Karlsruhe
T4 Ligase	BioLabs, Frankfurt am Main

2.1.17 Polymerases (Kits)

IMMOLASE™ DNA Polymerase	Bioline, Luckenwalde
In-Fusion™ Advantage PCR Cloning Kit	Clontech, Heidelberg
peqGOLD <i>Pwo</i> -DNA-Polymerase	Peqlab, Erlangen
<i>Pfu</i> Ultra™ Hi-Fidelity DNA polymerase	Stratagene, La Jolla (USA)
Platinum® <i>Taq</i> DNA Polymerase	Invitrogen, Karlsruhe

2.1.18 Restriction enzymes and Buffers

<i>Bam</i> HI	Invitrogen, Karlsruhe
<i>Eco</i> RI	Invitrogen, Karlsruhe
<i>Msc</i> I	BioLabs, Frankfurt am Main
<i>Nde</i> I	BioLabs, Frankfurt am Main
<i>Nru</i> I	BioLabs, Frankfurt am Main
<i>Sfi</i> I	BioLabs, Frankfurt am Main
<i>Xho</i> I	Invitrogen, Karlsruhe
H Buffer	Invitrogen, Karlsruhe
NEBuffer 2	Invitrogen, Karlsruhe
NEBuffer 3	BioLabs, Frankfurt am Main
NEBuffer 4	BioLabs, Frankfurt am Main
React3	Invitrogen, Karlsruhe

2.1.19 Bacterial strains

<i>E. coli</i> DH5α competent cells	Invitrogen, Karlsruhe
Stellar competent cells	Clontech, Heidelberg

2.1.20 Cell line

HeLa cells (human)

2.1.21 Yeast strain

Saccharomyces cerevisiae AH109

Clontech, Heidelberg

Y2HGold Yeast Strain

Clontech, Heidelberg

2.1.22 Model organisms

The *Whirligig* mouse line was generated by ENU (N-ethyl-N-nitrosourea) mutagenesis (Bosman et al., 2005). It was kindly provided from K. P. Steel (Sanger Centre, Cambridge, United Kingdom) and the Helmholtz Zentrum Munich, Germany.

African clawed frog *Xenopus laevis*. Adult frogs were purchased from Nasco (Ft. Atkinson, WI, USA).

2.1.23 Software used

Adobe Photoshop SC4 (compile figures)

AlphaView (capturing and analysing images)

Gen5™ (analysing data, determining protein concentration)

Microsoft Office Excel 2007 (analysing data)

Microsoft Office PowerPoint 2007 (compile figures/tables)

Microsoft Office Word 2007 (compile documents)

Paint (Erstellen und Bearbeiten von Zeichnungen)

SDS Version 2.1, PE Applied Biosystems (analysing RT-qPCR)

4D Tierbase (administration of mice)

Cellsens Dimension (microscopy imaging applications)

2.1.24 Internet platforms used

BLAST (Analysis of DNA sequences)

<http://blast.ncbi.nlm.nih.gov/Blast.cgi>

dbSNP (information about mutations)

<http://www.ncbi.nlm.nih.gov/projects/SNP/>

Ensembl (genetic information)

<http://www.ensembl.org/index.html>

Mutation taster (prediction program)

<http://www.mutationtaster.org/>

NCBI, National Center for Biotechnology Information (biomedical and genetic information)

<http://www.ncbi.nlm.nih.gov/>

NEBcutter V2.0 (recognition sites for restriction enzymes)

<http://tools.neb.com/NEBcutter2/index.php>

OMIM (information about genes and diseases)

<http://www.ncbi.nlm.nih.gov/omim>

PolyPhen2 (prediction program)

<http://genetics.bwh.harvard.edu/pph2/>

Primer3 Input (version 0.4.0) (searching for oligonucleotides)

<http://frodo.wi.mit.edu/primer3/>

Pubmed (searching for publications)

<http://www.ncbi.nlm.nih.gov/pubmed/>

RepeatMasker Web Server (checking for repetitive sequences within genes)

<http://www.repeatmasker.org/cgi-bin/WEBRepeatMasker>

SIFT (prediction program)

<http://sift.jcvi.org/>

2.2 Methods

2.2.1 Isolation of nucleic acids

2.2.1.1 Isolation of genomic DNA for genotyping of mice

To determine the genotype of mouse litters, a tail biopsy was taken at the age of three weeks. To isolate genomic DNA from mouse tail, it was proceeded according to Wieczerszak (2012) with a modified centrifugation step. Therefore, 150 µl of direct lysis buffer (Peqlab) and 5 µl Proteinase K (10 µg/ml) were added and incubated overnight at 55 °C under shaking. Inactivation of proteinase K took place at 85 °C for 50 minutes and the samples were centrifuged at 13,000 rpm for 1 minute. Probes were kept at 8 °C until proceeding with the genotyping PCR using ImmolaseTM DNA polymerase (compare 2.2.7).

2.2.1.2 Isolation of plasmid DNA from bacteria

The plasmid preparation is a procedure to isolate and purify plasmid DNA from bacteria. Three basic steps can be mentioned:

- preparation of a bacterial culture
- lyse the bacteria to extract plasmid DNA
- purification of plasmid DNA

a) Mini-preparation

To extract and purify moderate yields of plasmid DNA from bacteria, the QIAprep[®] Miniprep from Qiagen was used following the company's instructions with some modifications regarding the amount of the buffers and incubation times. The principle of this procedure is based on a modified alkaline lysis method of Birnboim and Doly (1979). Starting material is a 5 ml overnight culture of *E. coli* in LB (Lysogeny Broth) medium with 5 µl of an appropriate antibiotic (50 mg/ml). First, the bacterial cells were pelleted by centrifugation at 4,000 rpm for 10 minutes at 8 °C. The supernatant was discarded and the pellet resuspended in 200 µl Buffer P1 (Resuspension Buffer) with RNase A (Qiagen protocol: 250 µl). Next, 200 µl Buffer P2 (Lysis Buffer) was added and mixed thoroughly by inverting the tube 4-6 times (Qiagen protocol: 250 µl). After incubation for 5 minutes at room temperature, 200 µl Buffer N3 (Neutralisation Buffer) was added (Qiagen protocol: 350 µl). The

solution was immediately mixed by inverting the tubes 4-6 times. Samples were incubated for 5 minutes on ice then centrifuged at 13,000 rpm for 20 minutes at 4 °C (Qiagen protocol: no incubation before the 10 minutes centrifugation step at room temperature). In this protocol no column is utilised; instead, the plasmid DNA is precipitated with isopropanol. The supernatant was carefully transferred to a new tube without taking debris from the pellet. To precipitate the DNA, 420 µl isopropanol was added, mixed and samples incubated for 15 minutes at room temperature before centrifuging at 13,000 rpm for 30 minutes at 4 °C. The supernatant was discarded and the DNA pellet washed with 500 µl 70 % ethanol. After a final centrifugation step at 13,000 rpm for 5 minutes at 4 °C, the supernatant was discarded and the pellet air-dried. Depending on its size the DNA pellet was dissolved in 30-50 µl TE (Tris-EDTA) Buffer or ddH₂O. The DNA concentration was measured with the photometer (Eppendorf) (compare 2.2.2) and stored at -20 °C.

b) Midi-preparation

This method is used to isolate and purify plasmid DNA from bacteria. Here, the PureLink[®] HiPure Plasmid Filter Purification Kit (for midi and maxi preparation of plasmid DNA) from Invitrogen was used which employs a patented anion-exchange resin that ensures high yields of highly pure plasmid DNA. The midiprep was performed according to the manufacturer's instructions with slightly modifications. First, the cell lysate was prepared. Departing from the manufacturer's advice 30 ml instead of 15-25 ml of an overnight LB culture per sample was used for high copy number plasmids containing 30 µl of an appropriate antibiotic (50 mg/ml). The cells were harvested by centrifuging at 4,000 x g for 10 minutes at room temperature. Next, 4 ml Resuspension Buffer (R3) with RNase A was added to the cell pellet which was vortexed until cells were homogenously resuspended (Invitrogen protocol: 10 ml R3 buffer). After that 4 ml Lysis Buffer (L7) was added and tubes were inverted until the lysate composite was homogenously mixed (Invitrogen protocol: 10 ml L7 buffer). Next, the lysate was incubated at room temperature for exactly 5 minutes. Then, 4 ml Precipitation Buffer (N3) was added and tubes were homogeneously mixed by inverting (Invitrogen protocol: 10 ml N3 buffer). While probes were centrifuging at 12,000 x g for 10 minutes at room temperature (not listed in the manufacturer's protocol), the columns were equilibrated by applying 10 ml Equilibration Buffer (EQ1) directly to the filtration cartridge of the column

(Invitrogen protocol: 15 ml EQ1 buffer). After the solution drained by gravity flow, the precipitated lysate was transferred onto the column through a filter to prevent loading any protein remains. The column was washed twice with 10 ml Washing Buffer (W8). The buffer flow through the column by gravity flow until the flow stopped. The flow through was discarded and the DNA was eluted. Therefore, a sterile tube was placed under the column and 5 ml Elution Buffer (E4) was applied to the column. The solution was drained by gravity flow. Next, the DNA was precipitated by adding 3.5 ml isopropanol to the elution, then mixed well and incubated for 2 minutes at room temperature. A centrifugation step was performed at $> 12,000 \times g$ for 30 minutes at 4 °C. The supernatant was removed and the pellet washed with 3 ml 70 % ethanol. After centrifuging at $> 12,000 \times g$ for 5 minutes at 4 °C, the supernatant was removed and the pellet was air-dried for about 10 minutes. Depending on the pellet size the DNA was resuspended in 100-200 μ l TE Buffer or ddH₂O. The concentration of the precipitated DNA was measured with a spectral photometer (Eppendorf) (compare 2.2.2) and stored at -20 °C.

2.2.1.3 RNA isolation from mouse embryos

For the RNA isolation E9.5 old *Whirligig* mouse embryos (wild-type (*Chd7*^{+/+}), heterozygous (*Chd7*^{Whi/+}) and homozygous (*Chd7*^{Whi/Whi})) were used according to the standard protocol of the Transcriptome Analysis Laboratory (TAL), Goettingen. Adding 1 ml TRIzol Reagent (Invitrogen) the entire embryo was lysed in a rotor homogenisator for 5 minutes at 50 oscillations. Next, the homogenate was incubated for 5 minutes at room temperature. To remove insoluble material from the homogenate, samples were centrifuged at $12,000 \times g$ for 10 minutes at 4 °C. The supernatant was transferred to a fresh tube and the sample incubated again for 5 minutes at room temperature. 200 μ l chloroform was added, tubes were vigorously shaken by hand for 15 seconds, then incubated 5 minutes at room temperature. After a 15 minute centrifugation step at $12,000 \times g$ at 4 °C, the upper aqueous phase containing the RNA was transferred to a fresh 2 ml tube. Next, the RNA was precipitated by adding 500 μ l isopropanol and 1 μ l GlycoBlue. Samples were vortexed and incubated at -20 °C for 2 hours or overnight. The samples were centrifuged at $12,000 \times g$ for 30 minutes at 4 °C. The supernatant was removed and the RNA pellet was washed with 1 ml 75 % ethanol. Samples were centrifuged at $12,000 \times g$ for 5 minutes at 4 °C and the supernatant discarded. In case of a DNase

treatment a repetition of the wash step is not necessary. The RNA pellet was air-dried and dissolved in 25 µl DEPC. The concentration of the RNA was determined using a photo spectrometer (Eppendorf) (compare 2.2.2) and stored at -80°C .

2.2.2 Determination of nucleic acid concentration

To measure the concentration of DNA or RNA, a spectral photometer (Eppendorf) was used as described by Nolte (2008). After determining the blank value (solvent, e.g., TE Buffer, DEPC or ddH₂O) the concentration of the nucleic acid could be calculated by measuring the absorbance at 260 nm on the supposition that E_{260} of a 50 ng/µl DNA solution (and 40 ng/µl of a RNA solution) equals 1. The additional quotients E_{260}/E_{280} and E_{260}/E_{230} reflect contaminations with proteins and salt, respectively. The values should be > 1.8 and > 2.0 , respectively. Before the measurement the type of nucleic acid and the dilution factor of the sample were quoted and the concentration in µg/µl was determined.

2.2.3 Reverse transcription

This method was applied to transcribe RNA into complementary DNA (cDNA) using SuperScript II reverse transcriptase (Invitrogen) according to the manufacturer's instructions. In total, 5 µg RNA was used for a total reaction volume of 20 µl. Next, 1 µl Oligo dT (500 µg/ml) and 1 µl dNTP mix (10 mM each) were added to the RNA and ddH₂O was admitted up to 12 µl total. The mixture was incubated at 65°C for 5 minutes then 2 µl of 0.1 M DTT and 4 µl 5 x First-Strand Buffer were added and mixed gently. Next, samples were incubated at 42°C for 2 minutes before adding 1 µl of SuperScript II reverse transcriptase. The reaction sample was gently mixed and incubated at 42°C for 50 minutes. By heating up to 70°C for 15 minutes the reaction was inactivated. The cDNA was kept on ice for 5 minutes and stored at -20°C . To verify whether the transcription was successful, a PCR was performed (compare 2.2.7).

2.2.4 Cloning

Cloning is a method used to create copies of specific DNA fragments. The target DNA is brought into bacterial cells via plasmids. Through cell division (formation of bacterial colonies) the DNA is multiplied.

2.2.4.1 Restriction digestion of plasmid DNA

Restriction endonucleases are enzymes which naturally occur in bacteria and archaea where they have a protecting function against virus invasion (Arber and Linn, 1969; Pingoud et al., 1993). The restriction endonucleases used in this work belong to the type II restriction enzymes. They recognise a specific palindromic sequence of nucleotides and cleave the DNA at the same site (Pingoud and Jeltsch, 2001).

Plasmid DNA was cleaved using restriction enzymes from different companies. In general 10 units (U) enzyme were used to cleave 1 µg DNA in 1-2 hours. The incubation temperature as well as the reaction Buffer depends on the enzyme. To some restriction enzymes 1 x Bovine Serum Albumin (BSA) was added to prevent unspecific bindings. To check whether the cleavage was complete, an aliquote of the reaction was put on an agarose gel (compare 2.2.10).

2.2.4.2 Ligation of DNA fragments into plasmids

For the ligation target DNA fragments (inserts) were amplified by PCR. Inserts and the desired plasmid were digested with appropriate restriction enzymes. For the ligation the T4 Ligase (BioLabs) was used according to the manufacturer's instructions. A reaction volume of 10 µl contained a molar ratio of 1:3 vector to insert, 1 µl T4 ligase and 2 µl 5 x Ligation Buffer. If needed, ddH₂O was supplied to a final volume of 10 µl. The ligation was incubated overnight at 4 °C.

2.2.4.3 Transformation

For the transformation of a ligation reaction, 50 µl competent *E.coli* DH5α-cells (Invitrogen) were defrozen on ice and proceeded according to Hanahan (1983) with some modifications. 10 µl of the ligation mix was carefully added to the DH5α-cells and incubated for 30 minutes on ice. To increase the rate of plasmids adsorbed by the cells, a heat shock was performed at 42 °C for 45 seconds instead of 90 seconds. After that, the samples were incubated on ice for 2 minutes. For proliferation of bacterial cells, 450 µl prewarmed S.O.C. (Super Optimal Broth) medium (Invitrogen) instead of 800 µl was supplied and the samples incubated under continuously shaking at 37 °C for 1 hour. 100 µl of the bacterial mixture was plated on LB plates with an appropriate antibiotic. The plates were incubated overnight at 37 °C.

For a transformation of an In-Fusion™ reaction in DH5 α -cells, 2.5-3 μ l of the reaction was used and proceeded as described previously.

If an In-Fusion™ reaction was transformed into Stella cells, 2.5-3 μ l of the mixture was used, respectively and proceeded as described previously. After 1 hour incubation at 37 °C, 50 μ l of the cell culture was mixed with 50 μ l fresh S.O.C. medium and plated on an LB plate with an appropriate antibiotic. The other 400 μ l S.O.C. medium was centrifuged at 6,000 rpm for 5 minutes at room temperature. The supernatant was discarded and the cell pellet resuspended in 100 μ l fresh S.O.C. medium, then plated on an LB plate with an appropriate antibiotic and incubated overnight at 37 °C.

2.2.5 Cloning by In-Fusion™

In-Fusion™ is a PCR cloning method typically used to clone PCR products into vectors. In this work the In-Fusion™ Advantage PCR Cloning Kit (Clontech) was used according to the company's manual. First, gene-specific In-Fusion primers were designed with 15 bases extensions homologous to the ends of the linearised cloning vector. These primers are used to amplify the gene of interest by PCR. The target fragment was isolated by gel extraction. Then, the In-Fusion™ cloning reaction was set up. For a total reaction volume of 10 μ l, 2 μ l of 5 x In-Fusion™ Reaction Buffer, 1 μ l In-Fusion™ Enzyme, a 2 : 1 molar ratio of insert : vector and the appropriate amount of ddH₂O were used. The cloning reaction was incubated for 15 minutes at 37 °C followed by additional 15 minutes at 50 °C. After that the reaction volume was brought up to 50 μ l with TE buffer (pH 8). Next, the constructs were transformed into either DH5 α or Stella cells (compare 2.2.4.3).

2.2.6 Preparation of glycerin stocks

Every construct has to be maintained as a glycerin stock. Glycerin stocks were prepared according to Wieczerszak (2012). Therefore, a single bacterial colony was picked from an LB plate and inoculated in 5 ml LB medium with 5 μ l of an appropriate antibiotic (50 mg/ml). Inoculated samples were incubated overnight at 37 °C continuously shaking at 120 rpm. 700 μ l of the bacterial culture was mixed with 300 μ l 50 % glycerin and stored at -80 °C.

2.2.7 PCR

The PCR is a method where a polymerase is used to exponentially amplify a desired DNA sequence in vitro (Kleppe et al., 1971; Mullis et al., 1986). As a template a double strand DNA is used which is denaturised by heating up to 94 °C. At a lower temperature the primer hybridisation takes place. Primers are short oligonucleotides which are complementary to a specific region of the template and mark the starting point of the DNA synthesis. An increase of the temperature leads to the activation of the polymerase which binds to the primers and synthesises a new DNA strand complementary to the DNA template strand by using deoxynucleotide triphosphates (dNTPs). This cycle is repeated normally 30-35 times.

a) ImmolaseTM

The ImmolaseTM DNA Polymerase (Bioline) is a thermostable DNA polymerase isolated from a novel organism (Bioline, n.d.). This polymerase is characterised by excellent specificity and robust performance and it is able to eliminate primer-dimers or mis-primed products (Bioline, n.d.). In this work the ImmolaseTM DNA polymerase was used to perform genotyping of mice. Furthermore, this DNA polymerase was used to test the oligonucleotides for RT-qPCR and check transcribed cDNA. The PCR reactions were assembled according to the manufacturer's recommendations. Considering the PCR program the activation conditions were optimised.

Table 21: PCR reaction conditions (ImmolaseTM)

component	volume (µl)
10 x Immo-Puffer	2.5
MgCl ₂ (50 mM)	0.75
dNTPs (je 2,5 mM)	0.5
forward primer (10 pmol/µl)	0.5
reverse primer (10 pmol/µl)	0.5
IMMOLASE TM DNA Polymerase (5 U/µl)	0.2
template DNA	1
ddH ₂ O	to 25

Table 22: PCR program (Immolase™)

step	temperature (°C)	time	cycle
Activation	94	5 min	1
Denaturation	94	30 sec	30-35
Annealing	60/67	45-60 sec	
Extension	72	1 min	
Final extension	72	5-7 min	1
Cooling	4	∞	1

b) peqGOLD *Pwo*-DNA-Polymerase

The peqGOLD *Pwo*-DNA-Polymerase (Peqlab) was originally isolated from the thermophilic archaebacterium *Pyrococcus woesei* and is thermal stable (Peqlab, n.d.). It works highly processive and has a proof-reading function by 3'→5' exonuclease activity (Peqlab, n.d.). This polymerase was used to amplify products which are used to generate constructs for Co-IP and Y2H experiments. Based on the 3'→5' exonuclease activity of the *Pwo*-DNA-Polymerase it is possible that primers and template are destroyed. Therefore, two master mixes are prepared and right before starting the PCR combined according to the company's instructions.

Table 23: PCR reaction conditions (peqGOLD *Pwo*)

component	volume (μl)
Master mix I (25 μl):	
dNTPs (Invitrogen)	4
forward primer (10 pmol/μl)	2
reverse primer (10 pmol/μl)	2
template DNA	1
ddH ₂ O	to 25
Master mix II (25 μl):	
10 x reaction Buffer complete	5
<i>Pwo</i> -DNA-Polymerase (1 U/μl)	3
ddH ₂ O	to 25

Table 24: PCR program (peqGOLD *Pwo*)

step	temperature (°C)	time	cycle
Activation	94	2 min	1
Denaturation	94	15 sec	40
Annealing	54/64	30 sec	
Extension	68	2 min	
Final extension	68	7 min	1
Cooling	4	∞	1

c) *Pfu*UltraTM High-Fidelity DNA Polymerase

The *Pfu* polymerase is found in the hyperthermophilic archaeon *Pyrococcus furiosus*. *Pfu*UltraTM High-Fidelity DNA Polymerase is formulated with the ArchaeMaxx[®] polymerase enhancing factor, resulting in improved overall PCR performance (AgilentTechnologies, n.d.). The *Pfu*UltraTM High-Fidelity DNA Polymerase (Stratagene) was used to amplify products for engineering constructs for Y2H. PCR reaction conditions recommended by the company were optimised by adding 1 μ l of MgSO₄ and modifying the concentration of dNTPs and the polymerase. The annealing and the denaturation cycle were extended from 30 seconds to 45 seconds and the temperature of the extension cycles were set at 72 °C instead of 68 °C.

Table 25: PCR reaction conditions (*PfuUltra*TM High-Fidelity)

component	volume (μl)
10 x <i>PfuUltra</i> HF reaction buffer	2.5
MgSO ₄ (50 mM)	1
dNTPs (2,5 mM each)	0.8
forward primer (10 pmol/μl)	0.5
reverse primer (10 pmol/μl)	0.5
<i>PfuUltra</i> TM high-fidelity DNA polymerase (5 U/μl)	1
template DNA	1
ddH ₂ O	to 25

Table 26: PCR program (*PfuUltra*TM High-Fidelity)

step	temperature (°C)	time	cycle
Activation	95	2 min	1
Denaturation	95	45 sec	35
Annealing	60	45 sec	
Extension	68	2 min	
Final extension	68	10 min	1
Cooling	4	∞	1

d) Platinum[®] *Taq* DNA polymerase

The Platinum[®] *Taq* DNA Polymerase is found in the thermophilic bacterium *Thermus aquaticus* and it has a 5'→3' polymerase and a 5'→3' exonuclease activity (Invitrogen, 2010). The polymerase is complexed with a proprietary antibody that blocks polymerase activity at low temperatures (Invitrogen, 2010). A “hotstart” at 94 °C restores the activity (Invitrogen, 2010). In this work the Platinum[®] *Taq* DNA Polymerase (Invitrogen) was also used to amplify products for engineering constructs for Y2H. Furthermore, it was applied to distinguish the gender of mouse embryos. The PCR reaction was set up according the company’s recommendations.

Materials and methods

The activation, denaturation and annealing cycles were optimised and a final extension step included.

Table 27: PCR reaction conditions (Platinum® *Taq*)

component	volume (µl)
10 x PCR buffer	2.5
MgCl ₂ (50 mM)	0.75
dNTPs (2,5 mM each)	0.5
forward primer (10 pmol/µl)	0.5
reverse primer (10 pmol/µl)	0.5
Platinum® <i>Taq</i> DNA polymerase (5 U/µl)	0.2
template DNA	1
ddH ₂ O	to 25

Table 28: PCR program (Platinum® *Taq*)

step	temperature (°C)	time	cycle
Activation	94/95	5 min	1
Denaturation	94/95	45 sec	35/40
Annealing	59/61	45 sec	
Extension	72	1.5/2 min	
Final extension	72	5/7 min	1
Cooling	4	∞	1

2.2.7.1 Touchdown PCR

The touchdown PCR is a method to avoid amplifying nonspecific sequences by unspecific primer binding. Different annealing temperatures are used starting with high temperatures. The upper limit of the annealing temperature is set by the melting point of the primers used. The increments of annealing temperature decrease as well as the number of cycles can be chosen individually. At temperatures just below the melting point the annealing of primers to the template is most specific while at lower temperatures primers bind less specifically. By the exponential nature of the polymerase amplification the specific sequences amplified in early steps will

overwhelm the nonspecific sequences amplified later (Korbie and Mattick, 2008). For the touchdown PCR applied for mutation screens with human samples the ImmolaseTM DNA polymerase was used.

Table 29: PCR reaction conditions (Touchdown)

component	volume (µl)
10 x Immo-Puffer	2.5
MgCl ₂ (50 mM)	0.75
dNTPs (2,5 mM each)	0.5
forward primer (10 pmol/µl)	0.65
reverse primer (10 pmol/µl)	0.65
IMMOLASE TM DNA Polymerase (5 U/µl)	0.2
template DNA	1
ddH ₂ O	to 25

Table 30: PCR program (Touchdown)

step	temperature (°C)	time	cycle
Activation	95	7 min	1
Denaturation	95	30 sec	5
Annealing	65 -1 until 60	1 min	
Extension	72	1 min	
Denaturation	95	30 sec	30
Extension	72	1 min	
Final extension	72	5 min	
Cooling	4	∞	1

2.2.7.2 Sequencing PCR

The sequence analysis used in this work is modified from the chain determination method by Sanger and Coulson (Sanger and Coulson, 1975). This variation of a PCR uses only one primer. Besides from all four standard deoxynucleotide triphosphates (dNTPs) modified dideoxynucleotide triphosphates (ddNTPs) are used. The four ddNTPs are differently labeled with fluorescent dye and lack a 3'-hydroxy (OH-)

Materials and methods

group that is required for the formation of a phosphodiester bond between two nucleotides which causes termination of DNA strand elongation (Atkinson et al., 1969). The consequences are DNA fragments of different lengths that are separated by size using a capillary electrophoresis (MegaBACETM1000, Amersham). Stimulated by laser the fluorescently labeled ddNTPs emit light at different wavelengths. The sequence is visualised as peaks of different height and shape (chromatogram).

Table 31: PCR reaction conditions (sequencing)

component	volume (µl)
5 x sequencing buffer	2
BigDye [®]	1
forward primer or reverse primer (10 pmol/µl)	1
template DNA	1-6
ddH ₂ O	to 10

Table 32: PCR program (sequencing)

step	temperature (°C)	time	cycle
Activation	95	1 min	1
Denaturation	95	30 sec	30
Annealing/Extension	60	2.5 min	
Final extension	60	5 min	1
Cooling	8	∞	1

After the PCR run, 10 µl ddH₂O was added to each sample.

2.2.8 Quantitative real-time PCR and data analysis

The RT-qPCR is used to amplify and simultaneously quantify cDNA samples reverse transcribed from mRNA (messenger RNA). Therefore, *SYBR Green I*, an asymmetrical cyanine dye that intercalates with double stranded DNA is used (Zipper et al., 2004). In this complex *SYBR Green I* absorbs blue light. The excitation maximum is about 490 nm and it has an emission maximum of approximately

520 nm. This fluorescent signal can be detected by a detection system during qPCR (quantitative real-time PCR) and is proportional to the amplified DNA.

Absolute and relative quantification of nucleic acids are possible by using this method. In this work the relative quantification of gene expression was used. Thereby, an internal reference gene (housekeeping gene) is needed to determine the fold change in expression. ROX (6-Carboxyl-X-Rho-damine) is used as a passive reference dye to normalise the fluorescence signal of *SYBR Green I* (Illumina, 2011). Unspecific influences such as variations caused by pipetting errors can be compensated.

For the RT-qPCR RNA of mouse embryos were reverse transcribed into cDNA. Serial 1:5 dilutions of the cDNA were prepared for each analysed gene which should be analysed to determine the standard curve. To exclude contamination, ddH₂O was used as a blank value for each gene. A triple measurement was performed for all analysed genes, respectively. Samples were applied onto a 384 well plate and analysed with “ABI PRISM® 7900HT Sequence Detection System”. Below the RT-qPCR/qPCR program and the reaction conditions are listed.

Table 33: RT-qPCR/qPCR program

step	temperature (°C)	time	cycle
	50	2 min	1
Activation	95	15 min	1
Denaturation	94	15 sec	40
Annealing	60	30 sec	
Extension	72	1 min	
Dissociation	95	15 sec	1
	60	15 sec	
	95	15 sec	

Table 34: reaction conditions (RT-qPCR/qPCR)

component	volume (µl)
<i>SYBR Green I</i>	5
cDNA or human genomic DNA	2.5
forward primer (1 pmol/µl)	1.25
reverse primer (1 pmol/µl)	1.25

The raw data were evaluated using the sequence-detection software (SDS Version 2.1, PE Applied Biosystems). The SDS software displays the results of the RT-qPCR/qPCR run and plots them in a graph of normalised reporter fluorescence (R_n) versus cycle number (Fig. 4). In table 35 is the definition of terms listed which are used in quantification analysis.

Table 35: Terms used in Allelic Discrimination Analysis.

Term	Definition
Baseline	A line fit to fluorescence intensity values during the initial cycles of PCR, in which there is little change in fluorescence signal.
Threshold cycle (C_T)	The fractional cycle number at which the fluorescence intensity exceeds the threshold intensity.
Passive reference	A dye that provides an internal fluorescence reference to which the reporter dye signal can be normalized during data analysis. Normalization is necessary to correct for fluorescence fluctuations caused by changes in concentration or volume.
Reporter dye	The dye (<i>SYBR Green I</i>) provides a signal that indicates specific amplification.
Normalised reporter (R_n)	The ratio of the fluorescence intensity of the reporter dye signal to the fluorescence intensity of the passive reference dye signal.
Delta R_n (ΔR_n)	The magnitude of the signal generated by a set of PCR conditions. ($\Delta R_n = R_n - \text{baseline}$)

Table modified after AppliedBiosystems (n.d.).

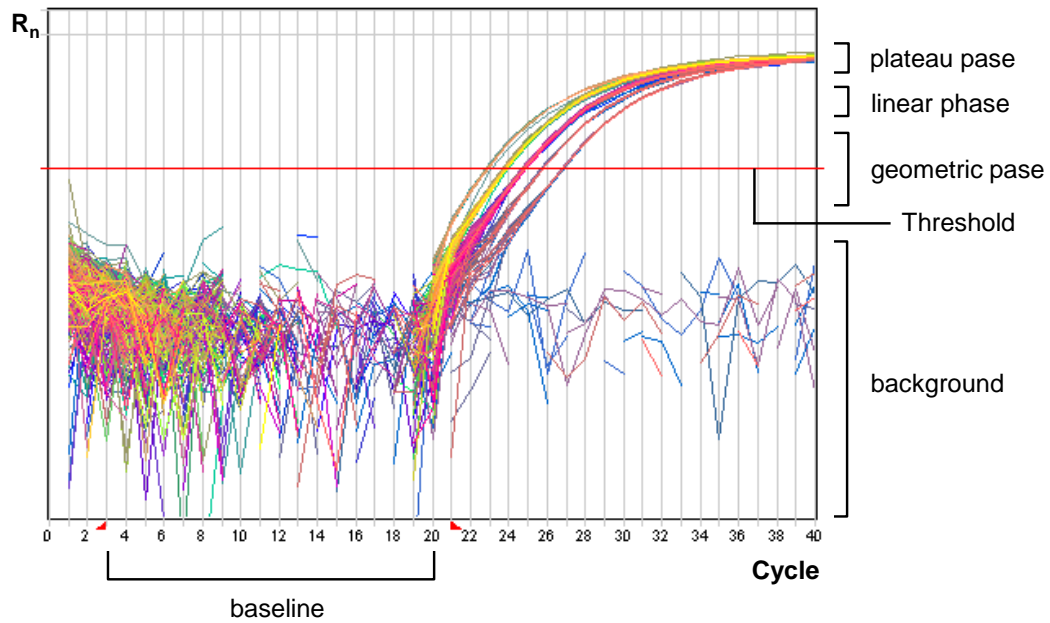


Figure 4: Results after RT-qPCR/qPCR run.

The graph shows the normalised reporter fluorescence (R_n) (ordinate) versus cycle number (abscissa). The threshold is set at a certain R_n value during the exponential amplification phase (geometric phase) slightly above background. Within this phase optimal PCR conditions exists, whereas in the linear and plateau phase the PCR reaction is inhibited due to limited availability of substrates or starting destruction of the polymerase or nucleotides. The number of cycles at which the fluorescence intensity exceeds the threshold intensity is called the threshold cycle (C_t). With the C_t values the quantification of the DNA samples can be determined. Figure modified after AppliedBiosystems (n.d.).

Data were exported to Microsoft Excel and further processed according to Dr. Arne Zibat's instructions. By using the serial 1:5 dilution of the DNA template a standard curve for each target gene was determined. Therefore, the initial concentration of the template DNA has to be known. By plotting the logarithms of the initial concentrations (ordinate) versus the median C_t values (abscissa) the linear equation $y = mx + b$ were achieved for the computation of a standard curve. The constant m is the slope of the straight line, constant b indicates were the straight line intercepts the y-axis and x is the independent variable. Next, the efficiency (E) was determined: $E = 10^{(-1/m)} - 1$. A slope (m) of -3.32 results in an efficiency of 100 %. To analyse the data, the efficiency should be between 85 % and 105 %. Values above 100 % indicate an inhibition of the qPCR. R^2 displays the scattering around the straight line and indicates the reliability of the data. R^2 should be at the minimum of 95 %. Next, the target genes were normalised against three reference genes (housekeeping genes) to compensate variations during qPCR. An ideal control should be easy to detect and

its expression should be stable in different cell types, during the cell cycle or during certain outer influences (Bustin et al., 2009). For the normalisation the logarithms of the initial concentrations of the reference genes were determined by using the formula: $\log(\text{initial concentration}) = (C_t - b) / m$. Next, the logarithms were countermanded and the mean as well as the standard deviation of the initial concentration were determined. Now, the target genes were normalised against the three reference genes. Therefore, the logarithms of the initial concentrations of the target genes were determined and the logarithms countermanded as for the reference genes before. After that, the initial concentration were used for the normalisation (N): $N = \text{initial concentration} / \text{mean of the initial concentration of the reference genes}$. The mean and the standard deviation of the normalisation were determined. Further, the relative change in expression of the target genes was compared to the calibrator (pooled wild-type samples): $N / \text{mean of the initial concentration of the calibrator}$. The mean and the standard deviation of the relative change in expression were determined. Finally, the mean of the relative change in expression of each target gene against the three reference genes were determined and results were represented in a diagram.

For the patient screen to check for duplications and deletions within exons of certain genes, qPCR was performed under adherence of diagnostic standards. Based on the determined concentrations of the DNA samples, patient probes and the wild-type control were brought to a concentration of 1.25 ng/μl using ddH₂O. Using standard DNA (Human DNA Male, ABI) four different concentrations (2.5 ng/μl, 1.25 ng/μl, 0.625 ng/μl and 0.3125 ng/μl) were adjusted. Two reference genes were used and for each analysed probe a no template control (NTC) (DNA volume was replaced by the same volume of ddH₂O) was carried along to check for contaminations. For each probe a double parallel measurement was performed.

A total reaction volume of 10 μl (Tab. 34) was supplied on a 384 well plate. First, 2.5 μl of primer-mix were placed into the wells of a 384 well plate which was then centrifuged for 2 minutes at 1,500 rpm. Next, 7.5 μl of a mixture containing the DNA probe and *SYBR Green I* was added to the wells. To eliminate air bubbles, the plate was centrifuged for 10 minutes at 3,000 rpm and then placed into the “ABI PRISM™ 7900HT Fast Real-Time PCR System” to record the data.

The data were analysed using the software SDS2.3 according to the operating instructions (2012) of the diagnostic department of the Human Genetic Institute,

Goettingen. First, the data were checked for contaminations by using the NTCs. Clear signals indicate a possible contamination and the analysis of this probe has to be repeated. Next, the dissociation curve should show a single peak, which indicates a unified product. If double peaks are present (unspecific side product), the analysis has to be repeated. For each primer pair a standard curve and R^2 value were determined by the SDS software. For R^2 , values should be between 0.99 and 0.98. Next, data were exported and analysed using Microsoft Excel. The multiple of the median (MOM) was determined: $MOM = \text{quantity}/\text{mean quantity of all references}$. For each double measured probe the median of the MOM and the standard deviation were determined and the values rounded to two decimal places after the decimal point. The mean MOM values were presented for each analysed probe in a column diagram. A deletion reveals in the calculation a theoretical value of MOM 0.4-0.6 and duplication a theoretical value of MOM 1.4. The theoretical value of MOM for wild-type is 1.0. Since the qPCR is a sensitive method, the determined values are subjected to variation, so they are often present below or above these theoretical values. Therefore, values below MOM 0.8 and above MOM 1.2 are classified to be suspicious. The reactions have to be repeated.

2.2.9 Purification of DNA

The MSB[®] Spin PCRapace Kit (Invitex) was used for fast and efficient direct purification of PCR products, digested samples and mini preparations according to the manufacturer's instructions with an additional centrifugation step. All centrifugation steps were carried out at room temperature. Up to 50 µl PCR samples 250 µl Binding Buffer was added to the PCR mixture. The sample was mixed vigorously by pipetting, then transferred onto a Spin Filter to bind the PCR fragments. Next, samples were centrifuged at 12,000 rpm for 3 minutes and the flow-through was discarded. An additional centrifugation step at 13,000 rpm for 1 minute was performed to fully remove all ethanol. The flow-through was discarded and the Spin Filter was placed into a new tube. To elute the PCR fragments, at least 10 µl ddH₂O was supplied directly onto the center of the Spin Filter. After 1 minute incubation at room temperature, the samples were centrifuged at 10,000 rpm for 1 minute. Purified samples were stored at -20 °C.

2.2.10 Agarose gel electrophoresis

To separate DNA fragments according to their length after PCR amplification, restriction digestion and ligation reaction, standard agarose gel electrophoresis was used (Fisher and Dingman, 1971; Helling et al., 1974). Depending on the DNA fragment length, 0.5-2 % agarose gels were prepared using agarose (Bio-Budget) and 1 x Tris/Acetate/EDTA (TAE) buffer or 0.5 x Tris/Borate/EDTA (TBE) buffer (Tab. 7). The mixture was boiled in the microwave until the agarose was completely dissolved. As running buffer 1 x TAE buffer or 0.5 x TBE buffer were used. To visualise the DNA under UV light, one drop of Ethidium bromide (AppliChem) (Sharp et al., 1973) or Roti Safe (Roth) was added to the agarose mixture. Gels were placed in horizontal gel chambers (Owl Scientific). Gels were loaded according to Lee et al. (2012).

2.2.11 Gel extraction

The QIAquick Gel Extraction Kit (Qiagen) is used to extract and purify DNA (70 bp-10 kb) from agarose gels in TAE or TBE buffer according to the manufacturer's instructions. All centrifugation steps were carried out at 13,000 rpm at room temperature. The desired DNA fragment was excised from the agarose gel using a clean scalpel. If possible, extra agarose was removed before the gel slice was scaled in a colourless tube. To 1 volume of gel (1 mg is equivalent to 100 µl) 3 volumes of Buffer QG were added to the gel slice. In case of > 2 % agarose gels, 6 volumes Buffer QG were needed. Next, the tube with the gel slice was incubated 10 minutes at 50 °C until the gel slice was completely dissolved. Every 2-3 minutes the tubes were vortexed during incubation to support dissolution. Since the adsorption of DNA to the QIAquick membrane is efficient only at $\text{pH} \leq 7.5$, it is necessary that the colour of the mixture stays yellow indicating the required pH. In case the mixture is orange or violet after the gel has dissolved, 10 µl of 3 M sodium acetate (pH 5) had to be added. To DNA fragments < 500 bp and > 4 kb 1 gel volume of isopropanol was added which increases the yield of DNA fragments. Next, a QIAquick spin column was placed in the provided 2 ml collection tube before the sample was applied to the column to bind DNA. The probes were centrifuged for 1 minute. The column reservoir is 800 µl. For sample volumes > 800 µl, the column was simply loaded and centrifuged again. The flow-through was discarded and the column

placed back in the same collection tube. 500 µl Buffer QG was added to the column and centrifuged for 1 minute. The flow-through was discarded and 750 µl of Buffer PE was added to the column for washing. After 2-5 minutes incubation, the column was centrifuged for 1 minute. The flow-through was removed and the column centrifuged again for 1 minute to completely remove the ethanol from the Buffer PE. To elute the DNA, the column was placed into a new 1.5 ml e-cup and 30-50 µl ddH₂O was added to the center of the QIAquick membrane. After 1 minute incubation the column was centrifuged for 1 minute. The DNA samples were stored at -20 °C

2.2.12 Mouse preparation

One-to-one matings of heterozygous *Whirligig* (*Chd7*^{Whi/+}) females and males were set up. To determine the age of the embryos, a daily check for a vaginal plug (VP check) was performed on female *Whirligig* mice. The day when the copulation plug was observed, was counted as embryonic stage 0.5 (E0.5). At the required day the pregnant *Whirligig* mice were sacrificed by cervical dislocation and the uterus was removed. The embryos were dissected from the yolk sacs and washed with PBS. To determine the gender of the embryos, a tail biopsy was performed. For protein and RNA isolation the embryos were flash frozen on liquid nitrogen and stored at -80 °C. For paraffin sections the embryos were fixed overnight at 4 °C in 4 % paraformaldehyde.

2.2.13 Fixation and dehydration of embryos for paraffin embedding

Fixation and dehydration of mouse embryos have been carried out according to Luxan et al. (2013) with some modifications, such as additional incubation steps and longer incubation times. Mouse embryos isolated from the uterus were fixated overnight in 4 % paraformaldehyde in PBS at 4 °C. The next day embryos were washed for 10 minutes in PBS. If not indicated differently, all steps were carried out at room temperature. By an increasing ethanol row (50 %, 70 %, 80 %, 90 % ethanol/PBS and 100 % ethanol) embryos were dehydrated. In contrast to the procedure performed by Luxan et al. (2013) an additional 50 % ethanol/PBS incubation step was carried out and each concentration step was performed twice for 1 hour. After the dehydration, embryos were incubated overnight instead of 30 minutes in 100 % xylene. Additionally, embryos were incubated in 50 %

paraffin/xylene for 2-6 hours at 65 °C. Embryos were transferred into 100 % paraffin and incubated for 2 days instead of 3 hours at 65 °C. During that time the paraffin was exchanged at least six times. The embryos were ready to be placed into forms to make paraffin blocks for the preparation of sections.

2.2.14 Preparation of paraffin sections of mouse embryos

To prepare paraffin sections, the microtome (JUNG RM 2035, Leica) were used. First, the paraffin block with the fixed embryo was cut to the size needed and clamped onto the microtome. Sections of 6-8 µm thickness were made which were carefully transferred to the surface of water (58 °C) from where they were placed on slides (Thermo Scientific). After the sections were dried, they were stored at 4 °C or room temperature until needed.

2.2.15 Microarray and data analysis

Microarrays are used to measure the expression of a large number of genes (Schena et al., 1995). In this work the microarrays were performed by the TAL in Goettingen as described by Schulz et al. (2014b) using the "Low RNA Input linear Amplification Kit Plus, One Color" protocol (Agilent Technologies, Inc. 2007; Cat. N°: 5188-5339) and the RNA Spike-In Kit for One color (Agilent Technologies, Inc. 2007; Cat. N°: 5188-5282) following the manufacturer's instructions. For the analysis of global gene expression the Mice 4 x 44 K design array from Agilent Technologies (G4846A) was used following the manufacturer's standard protocol. 200 ng of total RNA was used for reverse transcription into cDNA following the company's recommendation. The in vitro transcription was done according to the manufacturer's instructions. To determine the quantity and efficiency of the amplified cRNA that was labeled, the NanoDrop ND-1000 UV-VIS Spectrophotometer version 3.2.1 was used. The hybridisation procedure took place in the Hybridisation Oven (Agilent). Probes were incubated for 17 hours at 10 rpm at 65 °C. The following washing and staining were performed according to the manufacturer's standard protocol. All together the microarray data were generated according to the Minimum Information About a Microarray Experiment (MIAME) guidelines (compare NCBI's Gene Expression Omnibus (GSE46591). The Agilent DNA microarray scanner (G2505B) was used at 5 micron resolution to detect the Cy3 intensities by one-color scanning. Next, the

scanned image files were screened for artefacts and further analysed conforming to Opitz et al. (2010). The Feature Extraction Software Version was changed to 10.7.3.1. DAVID was used to find over-represented functions (Huang da et al., 2009b, a)

2.2.16 Cell biological methods

2.2.16.1 Culturing of eukaryotic cells

In this work human HeLa cells derived from cervical cancer cells were used (Scherer et al., 1953). The adherent cells were cultured in 25 cm² and 75 cm² culture flasks (Sarstedt) in 5 ml and 10 ml medium, respectively. The medium consists of Dulbecco's modified Eagle's media (DMEM) (PAN BIOTECH), 10 % foetal calf serum (PAN BIOTECH) and 1 % penicillin/streptomycin (PAN BIOTECH). Cells were cultured at 37 °C at a humidity of 98 % and CO₂ content of 5 %. Every two days the medium was exchanged.

To split cells, TrypLE Express (Invitrogen) was used to detach cells from the culture flask. First, cells cultured in a 25 cm² flask were washed once or twice with 5 ml DPBS. DPBS was removed completely before adding 1.5 ml TrypLE Express. Cells were incubated at 37 °C for 3 minutes. Then, 3.5 ml medium was added and cells were resuspended and transferred to a 13 ml centrifugation tube and centrifuged at 1,000 rpm for 5 minutes at room temperature. Supernatant was removed and the cell pellet was washed by resuspending in 5 ml DPBS. Tubes were centrifuged again at 1,000 rpm for 5 minutes at room temperature. The supernatant was discarded and the cell pellet was resuspended in medium. A few drops were added to a new 25 cm² culturing flask with 5 ml fresh medium. Cells were equally distributed and incubated at 37 °C.

2.2.16.2 Cryopreservation and revitalisation of eukaryotic cells

For a permanently storage, cells were cultured in 75 cm² flask (Sarstedt) until they reached a confluence of 80 %. They were washed with DPBS and then trypsinised (2.2.16.1). Cells were resuspended in 1.5 ml DMEM, and 1.5 ml of the Cryo-medium consisting of 50 % FKS, 30 % DMEM and 20 % DMSO was added. Cell mixture was transferred in Cryo-tubes and temporarily incubated at -20 °C. Then, cells were kept at -80 °C or liquid nitrogen. For revitalisation, cells were quickly unfrozen at

room temperature and resuspended in 9 ml prewarmed culturing medium. Cells were pelleted twice, washed with culturing medium and cultured in a 25 cm² flask (Sarstedt) with fresh medium (2.2.16.1). After 24 hours the medium was exchanged.

2.2.16.3 Transfection of eukaryotic cells with plasmids

Transfection is the introduction of nucleic acids (DNA or RNA) into cells. In this work HeLa cells were transfected with plasmids containing either a complete gene sequence or certain segments of a gene sequence to overexpress the appropriate DNA sequence in vivo. As transfection reagent lipofectamine 2000 (Invitrogen) was used according to the manufacturer's instructions. Lipofectamine reagent forms cationic liposomes in an aqueous environment which entrap the negatively charged transfection material by forming complexes (Dalby et al., 2004). The cationic lipid molecules are formulated with a neutral lipid that ensures the introduction of the transfection material into the cells (Dalby et al., 2004). HeLa cells were cultured 24 hours before transfection in 75 cm² flasks (Sarstedt) so they have a confluence of 70-90 % at the time of transfection. 30 µg of plasmid DNA was mixed with 1.875 ml Opti MEM (Invitrogen) and incubated for 5 minutes at room temperature. 75 µl lipofectamine 2000 was also mixed with 1.875 ml Opti MEM and incubated for 5 minutes at room temperature. The plasmid DNA and the lipofectamine mixture were combined and incubated for 25 minutes at room temperature. In the meanwhile cells were washed with DPBS and 9 ml DMEM with 1 x NEAA (Gibco) was added. The transfection mixture was added to the cells drop by drop and then incubated at 37 °C. After 4-5 hours, 9 ml DMEM with 20 % FKS and 1 x NEAA was added to the medium. After transfection, cells were incubated at 37 °C for 24 hours total.

2.2.17 Protein chemical methods

2.2.17.1 Protein isolation from HeLa cells

Nuclear proteins from HeLa cells were specifically isolated using the NE-PER Nuclear and Cytoplasmic Extraction Reagents (Thermo Scientific) according to the manufacturer's instruction. First, the medium were removed and cells were washed twice with DPBS and then harvested using TrypLE Express (Invitrogen). To neutralise the trypsin, DMEM medium was added instead of DPBS and the cell suspension was centrifuged at 500 x g for 5 minutes. The supernatant was removed

Materials and methods

and the cell pellet washed by suspending in DPBS. The cell suspension was centrifuged again at 500 x g for 5 minutes. The supernatant was discarded and the cell pellet suspended in 1.5 ml DPBS and then transferred into a 1.5 ml e-cup. Following centrifugation steps were performed at 4 °C, cell samples and extracts were kept on ice. Next, the cells were centrifuged at 500 x g for 2-3 minutes. The supernatant was carefully removed to leave the cell pellet as dry as possible. Depending on the cell volume the reagent volume was determined as shown below.

Table 36: Reagent volumes for different packed cell volume

Packed Cell Volume (µl)	CER I (µl)	CER II (µl)	NER (µl)
10	100	5.5	50
20	200	11	100
50	500	27.5	250
100	1,000	55	500

Right before using CER I and NER protease inhibitors (100 x stock) were added to maintain extract integrity and function. First, ice-cold CER I was added to the cell pellet which was then fully suspended by vortexing on the highest setting for 15 seconds. After 10 minutes incubation, the appropriate amount on ice-cold CER II was added. The tube was vortexed for 5 seconds on the highest setting, then incubated for 10 minutes and vortexed again for 5 seconds on the highest setting. Samples were centrifuged for 5 minutes at maximum speed (~ 16,000 x g). The supernatant consisting of the cytoplasmic extract was transferred to a new prechilled tube. To the pellet which contains the nuclei, the appropriate amount on ice-cold NER was added. For a total of 40 minutes the tube was vortexed every 10 minutes for 15 seconds on the highest setting and then centrifuged for 10 minutes at maximum speed (~ 16,000 x g). The supernatant which contains the nuclear extract was transferred to a new prechilled tube. The protein concentration was determined by Synergy Mx spectrophotometer (BioTek). Extracts were aliquoted and stored at -80 °C.

2.2.17.2 Measurement of protein concentration

After the principle according to Bradford (1976), the concentration of proteins was measured. Therefore, Roti[®]-Nanoquant (Roth) was employed as described by Witt

(2013). This solution contains Coomassie Brilliant Blue that binds under acidic conditions to proteins which leads to a conversion of the red form to the blue form of the dye causing a shift in the absorption spectrum maximum from 365 nm to 595 nm (Bradford, 1976). A standard protein, namely BSA (0-6.7 µg BSA/ml), was used for calibration. Based on the standard curve the protein concentration could be extrapolated. A triple measurement of each sample was performed and the average of the values was determined. First, a 1:100 dilution of the desired protein extract was prepared. 50 µl of the diluted protein extract and 50 µl of ddH₂O as a reference were put in a 96 well plate and 200 µl of the Roti[®]-Nanoquant solution was added. After 5 minute incubation at room temperature, the absorption was measured at 590 and 450 nm by Synergy Mx spectrophotometer.

2.2.17.3 Co-IP

The Co-IP is a technique used to analyse protein-protein interactions. With an antibody a known protein is targeted which is believed to be a member of a protein complex, the protein antigen is precipitated as well as proteins that are bound to it. By western blot analysis and further protein detection methods it might be possible to identify unknown complex members. For Co-IP nuclear cell extract was used and the immunoprecipitation of the target protein was carried out using the Immunoprecipitation Kit (Protein G) from Roche according to the manufacturer's instructions with modifications regarding incubation times, number of washing steps and during centrifugation steps. Depending on the amount of nuclear cell extract, an appropriate amount of the specific antibody was added and the sample incubated on a rotating platform overnight at 4 °C (Roche protocol: 1 hour). The next day 45 µl of the protein G was added to a new tube and centrifuged for 1 minute at 13,000 rpm at room temperature (Roche protocol: 50 µl). The supernatant was removed and the overnight protein solution was added to the remaining protein G. Next, the mixture was incubated on a rotating platform for 2 hours at 4 °C (Roche protocol: 3 hours). Complexes were collected by 3 minutes centrifugation at 3,000 rpm at 4 °C (Roche protocol: 12,000 x g for 20 sec). After the supernatant was removed, the beads were washed using 500 µl of the lysis buffer (Roche protocol: 2 times 1 ml lysis buffer and 20 minutes incubation). The samples were centrifuged again for 3 minutes at 3,000 rpm at 4 °C (Roche protocol: 12,000 x g for 20 sec). The beads were resuspended in 1 ml wash buffer 2 and centrifuged under the same conditions as

before (Roche protocol: centrifugation at 12,000 x g for 20 sec after 20 minutes incubation). After the supernatant was removed, a final washing step using 1 ml wash buffer 3 was performed (Roche protocol: 2 times 1 ml wash buffer 3 and 20 minutes incubation). The following preparation to load the sample on an SDS gel was performed differently. The supernatant was removed after centrifugation and 18 µl DPBS (PAN), 18 µl LDS (Invitrogen) and 4 µl 1M DTT were added to the beads. To denaturise proteins and separate them from the protein G beads, the mixture was incubated for 5 minutes at 95 °C. Beads were centrifuged down and the supernatant was loaded on an SDS gel and further analysed by western blot (2.2.17.5).

2.2.17.4 SDS polyacrylamide gel electrophoresis

By SDS polyacrylamide gel electrophoresis (SDS PAGE) proteins are denaturised and can be separated according to their molecular weight in a polyacrylamide gel by an electric field (Shapiro et al., 1967; Laemmli, 1970). In this work 4-12 % Bis-Tris Gels (Invitrogen) and 3-8 % Tris-Acetate Gels 3-8 % Tris-Acetate Gels (Invitrogen) were used for protein separation (2.2.17.5).

2.2.17.5 Western blot

The western blot is an analytical technique and this method was used to transfer proteins from an SDS gel to a nitrocellulose membrane where the proteins can be detected by different reactions (Towbin et al., 1979; Towbin and Gordon, 1984; Towbin et al., 1992).

Protein extracts used for Co-IP were incubated with 18 µl DPBS (PAN), 18 µl LDS (Invitrogen) and 4 µl 1M DTT for 5 minutes at 95 °C. After spinning down the Protein-G-agarose beads, 30 µl of the supernatant which contains the precipitated protein along with other proteins bound to it in a denaturised form was loaded on an SDS gel. Two different transfer methods were used in this work.

a) semidry

With this transfer variant proteins < 100 kDa were transferred from an SDS gel to a membrane. Using MES SDS Running Buffer (Invitrogen) and a 4-12 % Bis-Tris Gel (Invitrogen), proteins were separated according to their molecular weight. For approximately 2.5-3 hours the gel was running at 100 V. The protein transfer was

performed according to Wiczerzak (2012). The blotting condition was changed to 220 mA instead of 230 mA. 4 Whatman Papers which were soaked in transfer buffer were placed on the TurboblotterTM (Schleicher & Schuell). A nitrocellulose membrane which was wetted in ddH₂O and transfer buffer was put on top of it followed by the SDS gel and another 4 prewetted Whatman Papers. Approximately 50 ml transfer buffer were needed. The blotting was performed at constant 150 mA for 15 minutes followed by 45 minutes at 220 mA.

b) wet blot

This transfer method is appropriate for larger proteins (> 100 kDa). First proteins were separated according to their molecular weight using gel electrophoresis. Therefore, Acetate SDS Running Buffer (Invitrogen) and 3-8 % Tris-Acetate Gels (Invitrogen) were used. The running time of the gel amounted 3-3.5 hours at 100 V. To prevent heating of the buffer, the gel chamber was placed in an ice box. Once the proteins were separated, the “gel-sandwich” was assembled in transfer buffer to avoid bubbles according to BIO-RAD (n.d.). On the grey coloured side of the cassette (Bio-Rad) a foam pad was placed followed by 2 Whatman Papers, a nitrocellulose membrane and the SDS gel. Finally, 2 Whatman Papers and another foam pad were placed on top. The cassette was closed and placed vertically between parallel electrodes in the buffer tank (Bio-Rad) containing a frozen blue cooling unit and the transfer buffer (Tab. 13). To avoid the formation of an ion gradient and to insure the temperature homogeneity, a magnetic stir bar was placed in the buffer tank which was put in a box filled with ice on a magnetic stirrer. For the blotting at 4 °C, the voltage was set on 60 V constant for 2.5 hours.

2.2.17.6 Protein detection using antibodies

Once the protein transfer from the SDS gel to the membrane was completed, the membrane was transferred into a falcon tube (CellSTAR) and unspecific binding sites were blocked by incubating the membrane in TBST with 5 % milk or 5 % BSA for 1-2 hours at room temperature. During incubation steps membranes were placed on a rolling platform. The membrane was then incubated overnight at 4 °C with the appropriate primary antibody. Antibodies were diluted 1:1,000 to 1:2,000 in TBST with 2 % milk or 2 % BSA. Next day the membrane was washed three times for 10 minutes in 20 ml TBST with 2 % milk or TBST if BSA was used. The membrane

was then incubated for 2 hours at room temperature or at 4 °C with a secondary antibody conjugated to horseradish peroxidase (HRP). The antibodies were 1:7,000 to 1:10,000 diluted in TBST with 2 % milk (incubation at room temperature) or 2 % BSA (incubation at 4 °C). After that, the membrane was washed three times for 10 minutes in TBST with 2 % milk and once with TBST for 5 minutes or three times for 10 minutes with TBST at room temperature. To visualise proteins, SuperSignal™ West Pico Chemiluminescent Substrate (Thermo Scientific) was used according to the company's instructions. To prepare the substrate working solution, the two substrate components were mixed in a 1:1 ratio (light sensitive). The membrane was placed between a clear plastic wrap and incubated 5 minutes in the dark with SuperSignal West Pico Substrate Working Solution. HRP produces a detectable light signal in the presence of a substrate which can be either detect on X-ray films or by the detecting system FlourChem® Q (Alpha Innotech).

2.2.18 Direct yeast two-hybrid

The direct Y2H assay is used to identify and investigate protein-protein interactions in vivo using yeast cells. Two proteins of interest are expressed separately. The protein functioning as a bait protein is fused to the Gal4 DNA-binding domain (e.g. pGBKT7 plasmid) while the other one functions as the prey protein which is fused to the Gal4 transcriptional activation domain (e.g. pGADT7 plasmid) (Fields and Song, 1989). Only if a cell contains both proteins that interact with each other, the Gal4 DNA activator is able to bind to the GAL4 DNA binding domain and activates the Gal4-responsive reporters ADE2 and HIS3 (Clontech_Laboratories, 2009a). That means the amino acids adenine and histidine are expressed. Furthermore, the bait plasmid encodes tryptophan (TRP1) (Clontech_Laboratories, 2008) and the prey plasmid encodes leucine (LEU2) (Clontech_Laboratories, 2012). By plating yeast cells on an appropriate synthetic dropout (SD) medium, transformants containing the introduced plasmid(s) can be selected. –LT SD-plates contain every essential amino acid except for leucine and tryptophan. They are used as a transformation control because only cells containing bait and prey plasmids are able to grow. To confirm a direct interaction of two proteins, co-transformed yeast cells are plated on –LTHA SD-plates (the medium includes every essential amino acid except for leucine, tryptophan, histidine and adenine). Only cells are able to grow that harbor bait and

Materials and methods

prey plasmids and additionally express proteins that interact with each other to activate HIS3 and ADE2, so the lacking nutritional factors in the medium can be expressed.

In this work the LiAc method (Ito et al., 1983) modified by Schiestl and Gietz (1989); Hill et al. (1991); Gietz et al. (1992) was used as a simple and highly reproducible method according to the Yeast Protocols Handbook (Clontech_Laboratories, 2009b) with slightly modifications.

Yeast cells (Y2H Gold, Clontech) from a working stock plate were inoculated in 25 ml instead of 50 ml yeast medium. The yeast containing medium was vigorously mixed to disperse the cells and cultured overnight (16-18 hours) at 30 °C shaking at 220 rpm instead of 250 rpm. To get a mid-log phase culture, 4.5 ml of the overnight culture ($OD_{600} > 1.5$) was transferred to 150 ml fresh yeast medium to have an $OD_{600} \sim 0.2-0.3$ and cultured at 30 °C shaking at 220 rpm (Clontech protocol: 230 rpm) for 3-5 hours until the culture had an $OD_{600} \sim 0.5$. The culture was poured into 50 ml tubes and centrifuged at 1,000 x g for 5 minutes at room temperature. The supernatants were discarded and the pellets thoroughly resuspended in ddH₂O and then pooled in one tube with a final volume of 25 ml. The sample was centrifuged again at 1,000 x g for 5 minutes at room temperature and the supernatant discarded. The cell pellet was resuspended in 1 ml freshly prepared, sterile 1 x TE/1 x LiAc (Clontech protocol: 1.5 ml). 1 µg of each plasmid and 0.1 mg of denaturised carrier DNA were mixed with 100 µl of yeast competent cells. 600 µl freshly prepared 40 % PEG/1 x TE/1 x LiAc was added and vortexed. Probes were incubated at 30 °C for 30 minutes shaking at 200 rpm. 70 µl DMSO were added and mixed by gentle inversion. Next, a heat shock was performed at 42 °C for 15 minutes to promote the intake of plasmids into cells. After that, samples were incubated on ice for 1–2 minutes. Cells were centrifuged for 5 seconds at 14,000 rpm at room temperature, the supernatant was discarded and the cells resuspended in 300 µl ddH₂O (Clontech protocol: 500 µl TE buffer). Cells were plated on –LT SD agar plates as transformation control and on a –LTHA SD agar plate. Plates were incubated up-side-down at 30 °C for 3-7 days.

2.2.19 Cytological and histological methods

2.2.19.1 Immunocytochemistry with eukaryotic cells

Immunocytochemistry (ICC) is a common method to detect proteins in cells using primary antibodies against the protein of interest. With a secondary antibody conjugated with a fluorophore, the localisation of the target protein can be visualised by a fluorescence microscope. The ICC was performed according to the ICC protocol from abcam with some modifications according to incubation times and concentrations (Abcam, n.d.).

One day before, HeLa cells were cultured on slides (BD Biosciences). The medium was removed and cells were washed twice with PBS. After that, cells were fixated for 20 minutes with 4 % formaldehyde in PBS (abcam protocol: 15 minutes). If not indicated differently, all steps were carried out at room temperature. After the fixation cells were washed twice for 5 minutes with PBS and then permeabilised for 10 minutes using 0.1 % Triton X-100 in PBS (abcam protocol: 0.25 % Triton X-100). After washing the cells twice with PBS for 5 minutes (abcam protocol: 3 times for 5 minutes), 3 % BSA in PBS were added to the cells to block unspecific binding sides (abcam protocol: 1 % BSA in PBST). After 20-30 minutes the blocking solution was removed and the primary antibody 1:100 diluted in 3 % BSA/PBS was added to the cells and incubated overnight at 4 °C (abcam protocol: 1 % BSA in PBST). The next day the primary antibody dilution was removed and cells were washed twice for 10 minutes with PBS (abcam protocol: 3 times 5 minutes). The secondary antibody conjugated with Cy3 was diluted 1:200 in 3 % BSA/PBS and added to the cells which were incubated afterwards for 2 hours (abcam protocol: 1 % BSA for 1 hour). The last steps of the abcam protocol were performed differently. After washing the cells three times for 10 minutes in PBS and once with ddH₂O, Vectashield containing DAPI were added to the cells to stain the nuclei. The cells on the slide were closed by a cover slip and edges were sealed with nail polish.

2.2.19.2 Duolink PLA

The Duolink PLA method can be used to detect, visualise and quantify protein interaction in cells and tissues prepared for microscopy. The principle of this assay is based on *in situ* PLA[®], a proximity ligation assay technology (OlinkBiosciences,

2010). Two primary antibodies are used which are raised in two different species to detect the protein of interest. As secondary antibodies serve PLA probe PLUS and PLA probe MINUS which are conjugated with oligonucleotides (OlinkBiosciences, 2010). The two PLA probes generate a signal only when they bind to primary antibodies which have bound the target in close proximity (OlinkBiosciences, 2010). The signal is visible as an individual fluorescent spot.

In this work adherent human HeLa cells were used cultured in 8-well chamber slides (BD Biosciences) one day before starting the Duolink PLA method according to the manufacturer's instructions with some modifications. All steps were carried out at room temperature unless otherwise described. Cells were carefully washed twice with PBS to fully remove the medium. Next, the cells were fixed for 20 minutes in PBS with 3.7 % formaldehyde. After cells were washed twice for 5 minutes in PBS, a permeabilisation step was performed for 10 minutes using PBS with 0.1 % Triton X-100 to ensure access of the antibodies. Again, cells were washed twice for 5 minutes in PBS. To ensure that all non-specific binding sites are neutralised, cells were blocked in a preheated humidity chamber for 30 minutes at 37 °C with Blocking Solution (1 drop per reaction area), a component of the Duolink reagents. Primary antibodies were diluted 1:100 in Antibody Diluent which is another Duolink reagent. Cells were incubated overnight in a humidity chamber at 4 °C with diluted primary antibody combinations (30 µl per reaction area): The next day the primary antibodies were tapped off the slides which were then washed three times instead of two times for 5 minutes with gentle shaking in cuvettes containing at least 70 ml of Buffer A (prepared according to the manufacturer's instructions, Tab. 10). The two PLA probes were diluted 1:5 in Antibody Diluent and added to the cells (25 µl per reaction area). The slides were incubated in a preheated humidity chamber for 1 hour at 37 °C. After the incubation, the PLA probe solution was tapped off the slides. Before adding the ligation-ligase solution to the cells, slides were washed three times instead of two times for 5 minutes with Buffer A. The 5 x ligation stock was diluted 1:5 in ddH₂O. It contains two oligonucleotides that hybridise to the conjugated oligonucleotides of the PLA probes as well as all components necessary for ligation, except for the ligase. The ligase (1 U/µl) was diluted 1:40. The ligation-ligase solution was added to the cells (25 µl per reaction area) which were then incubated in a preheated humidity chamber for 30 minutes at 37 °C. The hybridised oligonucleotides will join to a close circle if the two PLA probes are in close

proximity, acting as a template for the following amplification step. The slides were washed twice for 2 minutes in Buffer A. Next, the amplification solution consisting of the 1:5 diluted amplification stock (light sensitive!) and the 1:80 diluted Polymerase (10 U/ μ l) were added (30 μ l per reaction area) and slides were incubated in a preheated humidity chamber for 100 minutes at 37 °C. During the amplification reaction the ligated circle of oligonucleotides acts as a template for rolling-circle amplification (OlinkBiosciences, 2010). The oligonucleotide of one PLA probe functions as a primer (OlinkBiosciences, 2010). Fluorescently labeled oligonucleotides hybridise to the amplified product which will be visible as a distinct fluorescent spot under the fluorescence microscope indicating a protein interaction (OlinkBiosciences, 2010). After that slides were washed twice for 10 minutes in minimum 70 ml Buffer B (prepared according to the manufacturer's instructions, Tab. 10) followed by an additional wash step with 0.1 x Buffer B for 1 minute. Divergent from the manufacturer's protocol the cytoskeleton of the cells were stained with FITC Phalloidin (Sigma-Aldrich) using a 1:700 dilution in Antibody Diluent (20 μ l per reaction area) for 30 minutes. After two final wash steps with 0.1 x Buffer B for 10 minutes, the slides were air dried in the dark before they were mounted with cover slips and Mounting Medium containing DAPI (Vector) to stain the nuclei. The edges were sealed using nail polish. Slides were incubated at least 15 minutes in the dark before documented using a fluorescence microscope (Olympus) and a confocal laser scanning microscope (Olympus).

2.2.19.3 Immunohistochemistry (3,3'-Diaminobenzidine (DAB) staining)

For immunohistochemistry the NovocastraTM Novostain Universal Detection Kit (Leica) and DAB (Roche) were used after Batsukh et al. (2012) with slightly modifications. Paraffin sections on slides were deparaffinised by incubating 10 minutes in xylene followed by two additional incubating steps in fresh xylene for 5 minutes, respectively. Next, tissue samples were hydrated by a decreasing ethanol row (100 %, 95 %, 90 %, 80 %, 70 % and 50 % ethanol/H₂O). Additionally to the procedure conducted by Batsukh et al. (2012), slides were rinsed carefully with ddH₂O and then incubated for 5 minutes instead of 2 minutes in PBS. Next, slides were placed in a cuvette with an antigen retrieval buffer (Tab. 9) and boiled for 10 minutes in a steam cooker. Then, the cuvette with the slides was placed on ice for approximately 10-20 minutes. To block the endogenous peroxidase activity, the

tissue samples were incubated with 3 % H_2O_2 in methanol instead of 6 % H_2O_2 in H_2O for 15 minutes in a humidity chamber. After that, non-specific binding sites were blocked using prediluted horse serum (Leica). After 10 minutes incubation, the primary antibodies (1:50 to 1:100 diluted in 1:1 horse serum and TPBS (PBS + 0.2 % Tween 20) were added on the tissue samples. Samples were incubated overnight (maximum 16 hours) at 4 °C in a humidity chamber. The next day the slides were taken from 4 °C and incubated for 1 hour at room temperature before they were washed for 5 minutes in PBS with 0.1 % Tween 20. The prediluted biotinylated universal secondary antibody (Leica) was added to the tissue samples which were incubated for 10 minutes. After washing the slides for 5 minutes in PBS with 0.01 % Triton X-100, tissue samples were incubated for 5 minutes in a prediluted Streptavidin peroxidase complex reagent (Leica). Streptavidin has a high affinity to biotin, so it binds to the biotinylated universal secondary antibody. Slides were washed again for 5 minutes in PBS with 0.1 % Tween 20 and then tissue samples were incubated up to 2 minutes in 1 x DAB solution (Roche). DAB is oxidised by the peroxidase conjugated to Streptavidin which causes a brown colour. After washing the slides for 5 minutes in PBS with 0.1 % Tween 20 instead of water, the nuclei were stained with haematoxylin. The slides were washed three times with dd H_2O , then covered with Aqua-Poly/Mount Coverslipping Medium (Polysciences) and a cover slip and the samples were analysed using a BX60 microscope (Olympus).

2.2.20 Mutational analysis

To screen for mutations in genes, the sequence of all coding exons and flanking intronic areas of the concerning gene was analysed by touchdown PCR (2.2.7.1). The PCR products were cleaned up by vacuum purification using MultiScreen Filter Plates (Merck Millipore). Each well of the plate was equilibrated with 100 µl TE buffer. Another 100 µl TE buffer was added to the 25 µl PCR reactions and mixed by pipetting. Then, each mixture was put onto a well of the plate. The vacuum pump (Merck Millipore) was turned on and the liquid in the wells were sucked off. To elute the DNA, 50 µl dd H_2O was added to each well and pipetted up and down several times. Next, the purified DNA was sequenced in both directions (2.2.7.2). Oligonucleotides used for touchdown PCR and sequencing are listed in table 20.

To screen for large deletions or duplications within a gene, qPCRs were performed for each coding exon (Tab. 33).

2.2.21 Molecular biological methods concerning the model organism *Xenopus laevis*

2.2.21.1 In vitro transcription of sense RNA

To synthesise large amount of capped RNA that mimics most eukaryotic mRNAs in vivo, the mMESSAGE mMACHINE[®] SP6 or T7 Transcription Kits (Ambion) were used. These synthesised capped RNAs are ideal for oocyte microinjection (Ambion, 2012). The transcription reaction was assembled at room temperature according to the company's instructions. A 20 µl transcription mixture was prepared using 1 µg linearised plasmid template, 10 µl 2 x NTP/CAP, 2 µl 10 x reaction buffer and 2 µl 10 x enzyme mix containing the appropriate RNA polymerase. The mixture was brought to a final volume of 20 µl with nuclease free H₂O and then mixed thoroughly and incubated 2 hours at 37 °C. Next, the template DNA was removed by adding 1 µl TURBO DNase (2 U/µl) during a 15 minutes incubation at 37 °C. After the DNase treatment, the sense RNA was purified.

2.2.21.2 Purification of sense RNA

To purify sense RNA for oocyte microinjection, the Illustra[™] RNAspin Mini (GE Healthcare) was used according to the manufacturer's instructions. All centrifugation steps were carried out at room temperature. To purify a 20 µl transcription reaction, 3.5 volume of Buffer RA1 (70 µl) and 95-100 % ethanol (70 µl), respectively were added, mixed and supplied on a column (blue). Next, samples were centrifuged at 8,000 x g for 30 seconds and the flow through was discarded. 200 µl Buffer RA2 was added onto the column which was centrifuged at 11,000 x g for 1 minute. The column was placed in a new collection tube and 600 µl Buffer RA3 was added. After centrifugation at 11,000 x g for 1 minute, the flow through was discarded and 250 µl of Buffer RA3 was supplied onto the column. To dry the membrane, the column was centrifuged at 11,000 x g for 2 minutes. The column was placed into a new 1.5 ml tube. 33-35 µl preheated RNase free H₂O was added directly to the center of the membrane. The column was incubated for 2 minutes at 80 °C and then centrifuged at 11,000 x g for 1 minute. The concentration of sense RNA was determined using the NanoDrop 2000c spectrometer (Thermo Scientific) and stored at -80 °C.

2.2.21.3 In vitro transcription of labeled anti-sense RNA

For whole mount *in situ* hybridisation (WMISH) experiments digoxigenin (DIG) labeled anti-sense RNA was synthesised using a DIG-RNA labeling mixture (Roche) according to Hedderich (2012) with additional use of Pyrophosphatase, different amount of polymerases and modification of DNase incubation time. For a total transcription reaction of 25 µl following chemicals were assembled (Tab. 37).

Table 37: Reaction conditions (in vitro transcription of labeled anti-sense RNA)

volume	chemicals
5 µl	5 x transcription buffer (Fermentas)
0.5 µl	Pyrophosphatase (4 U/ml)
4 µl	DIG-mix (ATP, CTP, GTP, UTP/digoxigenin UTP (Roche)
1 µl	0.75 M DTT
1 µl	RNaseOut (40 U/µl, Invitrogen)
0.2-1 µg	linearised template DNA
1 µl	T7 or SP6 RNA polymerase (20 U/µl, Fermentas)
to 25 µl	RNase free H ₂ O

The transcription reaction was incubated at 37 °C for 2 hours. To remove the template DNA, 1 µl TURBO DNase (2 U/µl) was added and the sample was incubated at 37 °C for 15 minutes. Next, the anti-sense RNA was purified.

2.2.21.4 Purification of labeled anti-sense RNA

To clean up labeled anti-sense RNA for oocyte microinjection, the RNeasyTM Mini Kit (Qiagen) was used according to manufacturer's manual. All centrifugation steps were carried out at room temperature. First, the transcription mixture was adjusted to a volume of 100 µl using RNase free H₂O. Next, 350 µl Buffer RLT was added and mixed well. After that, 250 µl ethanol (96-100 %) was added to the diluted RNA and mixed well. The solution was transferred immediately onto an RNeasy Mini spin column that was centrifuged at 10,000 rpm for 15 seconds. The flow-through was discarded and 500 µl Buffer RPE was added to the column for washing. The column

was centrifuged at 10,000 rpm for 15 seconds and the flow-through was discarded. Again, 500 µl Buffer RPE was added to the column that was centrifuged at 10,000 rpm for 2 minutes. The column was placed into a new 2 ml collection tube and centrifuged at full-speed for 1 minute. The column was placed into a new 1.5 ml receiver tube. 50 µl preheated RNase free H₂O was added to the center of the membrane and the column was incubated at 80 °C for 2 minutes. To elute the RNA, the column was centrifuged at 10,000 rpm for 1 minute. To determine the concentration of the anti-sense RNA, the NanoDrop 2000c spectrometer (Thermo Scientific) was used. The anti-sense RNA was stored at -80 °C.

2.2.21.5 Morpholino oligonucleotides

The Morpholino oligonucleotides (MO) were purchased from Gene Tools, LLC. The MO were dissolved at 65 °C in RNase free H₂O and diluted to a final concentration of 8 µg/10 nl. MO were stored at 4 °C and heated up for 10 minutes at 65 °C before usage.

2.2.21.6 Preparation of *Xenopus laevis* testis and fertilisation of oocytes

The preparation of the testis and fertilisation of oocytes have been carried out by Dr. Peter Wehner according to Wehner (2012). To isolate sperm from testis, male *Xenopus laevis* were put into a 0.05 % benzocaine/water solution for 30 minutes at room temperature. Frogs were decapitated and the testis was removed, then washed three times with MBS and stored in 1 x MBS buffer at 4 °C. To stimulate the egg deposition, female *Xenopus laevis* frogs were injected into the dorsal lymph sac with 1,000 units human chorionic gonadotropin (hCG) hormone (Sigma-Aldrich). Approximately 12 hours after injection the female frogs lay eggs. These eggs were fertilised in vitro. Therefore, a piece of testis was macerated in 0.1 x MBS. To remove the jelly coat from fertilised eggs, they were incubated for 3-5 minutes with 2 % cysteine hydrochloride (pH 8).

2.2.21.7 Microinjection of *Xenopus laevis* embryos and culture

Microinjections of *Xenopus laevis* blastomeres have been performed by Dr. Peter Wehner according to Wehner (2012). For microinjection fertilised eggs were put into injection buffer and placed on a cooling plate. Glass capillaries that were prepared with a needle puller were loaded with the substances needed for microinjection. The

injection was carried out using the Microinjector 5242 (Eppendorf). 4-10 nl β -galactosidase (*lacZ*) mRNA (W. C. Smith and Harland, 1991) and MO were injected animally into one blastomere of a two-cell stage embryo. The MO used are short oligonucleotides that interfere with the target mRNA to block translation. To allow the healing after injection, embryos were kept for 1-2 hours in injection buffer. After that, they were washed twice with 0.1 x MBS. Embryos were cultured to the desired stage in 0.1 x MBS at 12.5 to 18 °C. The developmental stages were determined according to Nieuwkoop and Faber (Hubrecht-Laboratorium (Embryologisch Instituut) et al., 1967).

2.2.21.8 Fixation of injected *Xenopus laevis* embryos and X-gal staining

Fixation and X-gal staining of *Xenopus laevis* embryos have been performed by Dr. Peter Wehner and me according to Wehner (2012). This procedure is used for WMISH to determine the *lacZ* mRNA injected region of the embryo (Hardcastle et al., 2000). The *lacZ* mRNA is co-injected as a lineage tracer with the appropriate MO. After injected embryos developed to the desired stage, they were fixated for 1 hour in MEMFA. All steps were carried out at room temperature. After the fixation, embryos were washed three times for 10 minutes with 1 x PBS and then stained with X-gal solution in the dark until the requested intensity of staining was achieved. The X-gal solution was removed and embryos were washed three times for 10 minutes in 1 x PBS. Next, embryos were fixed again for 1 hour in MEMFA. Afterwards, embryos were washed three times with 100 % ethanol. Embryos were long term stored in 100 % ethanol at -20 °C.

2.2.21.9 Whole mount in situ hybridisation

With this technique the localisation of mRNA within an embryo can be visualised using a labeled specific complementary RNA probe. The WMISH was performed as described by Harland (1991) with some modifications.

Detailed procedure of the WMISH on *Xenopus laevis*:

Day 1

All incubation steps were performed under gentle shaking. *Xenopus laevis* embryos were rehydrated by a decreasing ethanol row (75 % EtOH/H₂O, 50 % EtOH/H₂O,

25 % EtOH/PTw) followed by five washing steps with PTw. Each step was carried out for 5 minutes at room temperature.

To permeabilise the embryos to ensure fully penetration of RNA probes, embryos were treated with proteinase K (10 µg/ml) in PTw as described in table 38.

Table 38: Proteinase K treatment of *Xenopus laevis* embryos

Developmental stage of <i>Xenopus laevis</i> embryos	Incubation time (min)	Temperature
9-10.5	6-8	room temperature
14-16	8-10	room temperature
20-25	15-18	room temperature
36	22-25	room temperature
40	17-20	37 °C
42-43	27-30	37 °C
46	32-35	37 °C

The following acetylation step increases the specific binding of the probe to mRNA. Therefore, the embryos were washed twice in 0.1 M Triethanolamine (pH 7.5) for 5 minutes, respectively. After that, embryos were incubated for 5 minutes in 4 ml Triethanolamine with 12.5 µl Acetic Anhydride. Additional 12.5 µl Acetic Anhydride was added followed by two 5 minute washing steps with PTw.

Subsequent to the acetylation embryos were fixed for 20 minutes in PTw containing 4 % formaldehyde and then washed five times with PTw buffer for 5 minutes, respectively.

For the following hybridisation embryos were left in 1 ml PTw and 250 µl prewarmed Hybmix was added and carefully mixed. The solution was replaced by 1 ml fresh Hybmix and after 10 minutes incubation at 60 °C replaced again by 1 ml Hybmix. After 4-5 hours incubation at 60 °C, the Hybmix was exchanged and the embryos hybridised over night at 60 °C with the desired antisense RNA probe diluted in Hybmix.

Day 2

The next day the RNA probe was removed and preheated Hybmix was added to the embryos which were incubated for 10 minutes at 60 °C. After that, the embryos were incubated three times for 15 minutes in 2 x SSC at 60 °C. An RNase mix containing 2 x SSC, 10 µg/ml RNase A and 0.01 U/ml RNase T1 was added to the embryos to degrade mismatched double stranded RNA. After an incubation time of approximate 40 minutes at 37 °C and 30 rpm, the RNase mix was washed away with 2 x SSC for 5 minutes at room temperature followed by two additional washing steps with 0.2 x SSC for 30 minutes at 60 °C as well as two further wash steps with 1 x MAB for 15 minutes at room temperature.

Next, the antibody reaction took place. First, embryos were washed once with MAB containing 2 % of the blocking reagent BMB for 15 minutes at room temperature followed by 40 minutes incubation in MAB containing 2 % BMB and 20 % horse serum at room temperature. The next 4 hours the embryos were treated with MAB containing 2 % BMB, 20 % horse serum and 1:5,000 diluted Sheep Alkaline phosphatase-coupled anti-Dig antibody at room temperature. After the antibody incubation, the embryos were washed three times with MAB for 10 minutes at room temperature. Embryos were kept in fresh MAB over night at 4 °C.

Day 3

The next day, the washing with MAB was continued five times for 5 minutes at room temperature, respectively. In preparation to the colour reaction the embryos were washed twice for 5 minutes at room temperature with fresh prepared APB. For the colour reaction itself the embryos were incubated up to 3 days at 4 °C in 3 ml APB solution containing 2.4 µl NBT (100 mg/ml) and 10.5 µl BCIP (50 mg/ml).

To reduce background after staining, a decreasing methanol row (one minute or longer in 100 % methanol, one minute in 75 %, 50 % and 25 % methanol/H₂O, respectively) can be performed. After removing the background, the pigmented embryos were bleached at room temperature to remove the pigmentation which can interfere the staining. Therefore, the embryos were fixated in MEMFA for 30 minutes and washed twice for 5 minutes in 5 x SSC. Next, the embryos were bleached up to 30 minutes in 5 x SSC containing 50 % formamide and 2 % H₂O₂. Finally, embryos were washed twice for 5 minutes in 5 x SSC and 30 minutes in

Materials and methods

MEMFA. Before documentation, the embryos were washed three times for 5 minutes in PTw. Embryos were stored in 100 % ethanol at -20 °C.

2.2.22 OVERVIEW

Co-IP

- generation of constructs (recloning of the gene of interest in the pCMV-HA vector)
 - PCR to amplify the plasmid with gene of interest
 - gel extraction
 - restriction digestion
 - ethanol precipitation
 - cloning by In-FusionTM or ligation
 - transformation
 - mini-preparation of plasmid with appropriate insert
 - test digestion
 - purification of mini-preparation
 - sequencing
 - midi-preparation of plasmid with appropriate insert
- transfection of HeLa cells
- isolation of nuclear proteins from HeLa cells
- Co-IP
- separation according to the molecular weight on SDS gel
- western blot
- antibody treatment
- detection of protein signals

Immunocytochemistry

- culture HeLa cells on slides
- fixation of cells
- permeabilisation of cells
- blocking
- antibody treatment
- data analysis

Duolink

- culturing HeLa cells on 8-well chamber slides
- fixation of cells

- permeabilisation of cells
- Duolink
- staining the cytoskeleton of cells with FITC Pallocidin and the nuclei with DAPI
- data analysis (fluorescence microscope/confocal laser scanning microscope)

Yeast two-hybrid

- generation of constructs
 - PCR to amplify the gene of interest
 - gel extraction
 - restriction digestion of the plasmid
 - if necessary ethanol precipitation and treatment with Antarctic phosphatase
 - cloning by In-FusionTM
 - transformation
 - mini-preparation of plasmid with appropriate insert
 - test digestion
 - purification of mini-preparation
 - sequencing
 - (midi-preparation of plasmid with appropriate insert)
- Yeast two-hybrid

Transcriptome, micro array

- mating heterozygous (*Chd7*^{Whi/+}) female and male mice
- preparation of E9.5 embryos
- tail biopsy for genotyping and shock freezing of the embryo
- determination of the genotype
 - isolating of genomic DNA
 - genotyping PCR
 - test agarose gel
 - purification of genotyping PCR samples
 - sequencing PCR
- determination of gender by PCR
- RNA isolation of E9.5 embryos
- micro array

- data analysis

Confirmation of micro array by RT-qPCR

- mating heterozygous (*Chd7*^{Whi/+}) female and male mice
- preparation of E9.5 embryos
- tail biopsy for genotyping and shock freezing of the embryo
- determination of the genotype
- determination of gender by PCR
- RNA isolation of E9.5 embryos
- reverse transcription (cDNA synthesis)
- test primer for RT-qPCR by PCR
- RT-qPCR
- data analysis

DAB staining

- mating wild-type female and male mice of the CD-1 strain
- preparation of E12.5 embryos
- fixating embryos overnight in 4 % paraformaldehyde/PBS
- prepare embryos for embedding in paraffin
- paraffin sections
- preparing the sections for immunostaining with DAB
 - Xylenel treatment and rehydration
 - boiling in EDTA
 - blocking step and antibody incubation
 - DAB staining
- data analysis

Patient screen

Mutation screen

- generate primers for each exon of the gene of interest
- PCR to amplify each exon of the gene of interest
- purify PCR samples
- sequencing
- data analysis

Deletion/Duplication screen

- generating primers for each exon of the gene of interest
- test primers in a qPCR using wild-type genomic DNA
- measurement of DNA concentration of patient samples
- qPCR
- data analysis

Whole mount *in situ* hybridisation

- generating sense and labeled anti-sense probes
 - digestion of plasmid with the appropriate gene
 - purification of digested plasmids
 - in vitro transcription of sense and labeled anti-sense RNA
 - purification of sense and labeled anti-sense RNA
 - measurement of RNA concentration of sense and labeled anti-sense RNA
- injection of one blastomere of a two-cell *Xenopus laevis* oocytes with MO
- collection of embryos at the desired stage
- fixation and X-gal staining of embryos
- whole mount *in situ* hybridisation
- data analysis

3 Results

3.1 CHD7 interacts with components of the WAR complex

Chromatin remodelling enzymes are known to form large multi-subunit complexes (Mohrmann and Verrijzer, 2005; Ho et al., 2009a). It was shown that CHD7 interacts with the chromatin remodelling enzyme CHD8, which in turn interacts with components of the WAR complex (Batsukh et al., 2010; Yates et al., 2010). The following described data are published by us (Schulz et al., 2014a). To prove whether CHD7 also interacts with the members of the WAR complex WDR5, ASH2L and RBBP5, Co-IP experiments on human HeLa cells were performed (Fig. 5).

HeLa cells were single transfected with pCMV-HA plasmids containing the human full-length sequence of ASH2L (NP_004665.2) or RBBP5 (NP_005048.2). Untransfected HeLa cells were used as a negative control. Using a CHD7 antibody, endogenous CHD7 was precipitated. With an HA antibody the overexpressed proteins ASH2L (Fig. 5A, lane 1) and RBBP5 (Fig. 5A, lane 2) were detected. As expected no band was observed for the negative control (Fig. 5A, lane 3). Bands of the appropriate size were observed after detecting the overexpressed proteins ASH2L and RBBP5 with an HA antibody, confirming the successful transfection (Fig. 5A, lane 4+5). Co-IPs where endogenous CHD8 was precipitated with a CHD8 antibody and overexpressed ASH2L (Fig. 5B, lane 1), RBBP5 (Fig. 5B, lane 2) and the CHD7 fragment (amino acids 1591-2181, NP_060250.2) (Fig. 5B, lane 3) were detected with an HA antibody confirmed the known interaction of CHD8 and CHD7 as well as CHD8 and the WAR complex members. The reciprocal experiment was performed by single transfection of HeLa cells with pCMV-HA plasmids containing either ASH2L or RBBP5. Untransfected HeLa cells served as a negative control. Next, the overexpressed proteins were precipitated using an HA antibody. With a CHD7 antibody endogenous CHD7 was detected at ~320 kDa. A band at the estimated size was observed after ASH2L (Fig. 5C, lane 1) and RBBP5 single transfection (Fig. 5C, lane 2). No band was observed for the negative control, showing that endogenous CHD7 does not bind unspecifically to the beads (Fig. 5C, lane 3). Untransfected HeLa cells were used to precipitate endogenous WDR5 using a WDR5 antibody. With a CHD7 antibody the estimated size of endogenous CHD7

(~320 kDa) was detected (Fig. 5C, lane 4). Furthermore, endogenous CHD7 was detected in untransfected HeLa cells used as an input control (Fig. 5C, lane 5). In conclusion, the data obtained by Co-IP experiments demonstrate that CHD7 interacts with WDR5, ASH2L and RBBP5.

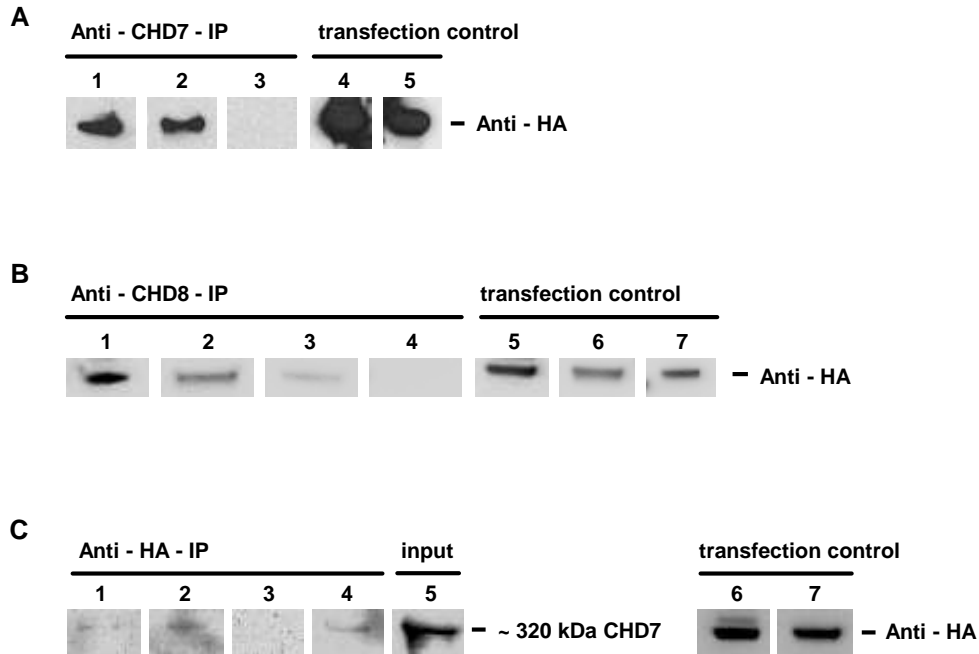


Figure 5: Co-immunoprecipitation experiments with HeLa cells.

(A) HeLa cells were single transfected with the pCMV-HA plasmids containing either the human full-length sequence of ASH2L (NP_004665.2) (lane 1) or RBBP5 (NP_005048.2) (lane 2). Endogenous CHD7 was precipitated using a CHD7 antibody. With an HA antibody bands of the estimated size of ASH2L (~ 76 kDa; lane 1) and RBBP5 (~ 59 kDa; lane 2) were observed. Untransfected HeLa cells served as a negative control (lane 3). After precipitating endogenous CHD7, no band was detected with an HA antibody. Lane 4 and 5 represent the transfection controls: input after ASH2L-pCMV-HA single-transfection of HeLa cells (lane 4); input after RBBP5-pCMV-HA single transfection of HeLa cells (lane 5). Overexpressed ASH2L and RBBP5 were detected with an HA antibody. (B) Positive control, confirming the interaction of CHD8 with ASH2L, RBBP5 and CHD7. HeLa cells were single transfected with ASH2L-pCMV-HA (lane 1), RBBP5-pCMV-HA (lane 2) or CHD7-CR1-3-pCMV-HA (NP_060250.2) (lane 3). The pCMV-HA plasmids contain the human full-length sequence of ASH2L or RBBP5 or a part of CHD7 (amino acids 1591-2181). A CHD8 antibody was used for precipitation of endogenous CHD8 and an HA antibody for detection of the overexpressed proteins. A band at ~ 76 kDa corresponding to the estimated size of ASH2L (lane 1), a band (~ 59 kDa) of the predicted size of RBBP5 (lane 2) and a band (~ 70 kDa) of the CHD7 part was detected. As a negative control untransfected HeLa cells were used (lane 4). Endogenous CHD8 was precipitated with a CHD8 antibody. No band was observed by using an HA antibody for detection (lane 4). Lane 5-7 show the transfection controls. Input after single transfection of HeLa cells with ASH2L-pCMV-HA (lane 5), RBBP5-pCMV-HA (lane 6) and CHD7-CR1-3-pCMV-HA (lane 7). The overexpressed

proteins were detected with an HA antibody. (C) Vice versa experiment to experiment A. HeLa cells were single transfected with the plasmids ASH2L-pCMV-HA (lane 1) or RBBP5-pCMV-HA (lane 2). The overexpressed proteins were precipitated with an HA antibody and endogenous CHD7 (~ 320 kDa) was detected using a CHD7 antibody. Untransfected HeLa cells were used as a negative control (lane 3). No CHD7 was detected after precipitation with an HA antibody, indicating that endogenous CHD7 does not bind unspecifically to the beads. Endogenous WDR5 was precipitated with a WDR5 antibody using untransfected HeLa cells and a ~ 320 kDa band was observed with a CHD7 antibody (lane 4). The transfection controls are shown in lane 6 and 7. Overexpressed ASH2L (lane 6) and RBBP5 (lane 7) were detected with an HA antibody after single transfection of HeLa cells with either ASH2L-pCMV-HA or RBBP5-pCMV-HA. Three biological replicates were performed for each Co-IP experiment (A - C). Figure modified after Schulz et al. (2014a).

3.2 CHD7 and the members of the WAR complex are co-localised in the nucleus

To confirm the Co-IP data and determine where in the cell interactions occur, the Duolink PLA method was used. The antibodies used to detect the target proteins were tested in an immunocytochemistry performed on untransfected HeLa cells. The results are shown in figure 6. The cell nuclei were stained with DAPI. Primary antibodies were used to detect CHD7, CHD8, WDR5, ASH2L and RBBP5. With secondary antibodies conjugated with Cy3 the localisation of the proteins was visualised (Fig. 6B, E, H, K, L). Merging the DAPI (nuclei) and the Cy3 channel (detected target proteins) revealed that all analysed proteins were localised specifically in the nucleus: CHD7 (Fig. 6C), CHD8 (Fig. 6F), WDR5 (Fig. 6I), ASH2L (Fig. 6L), RBBP5 (Fig. 6O).

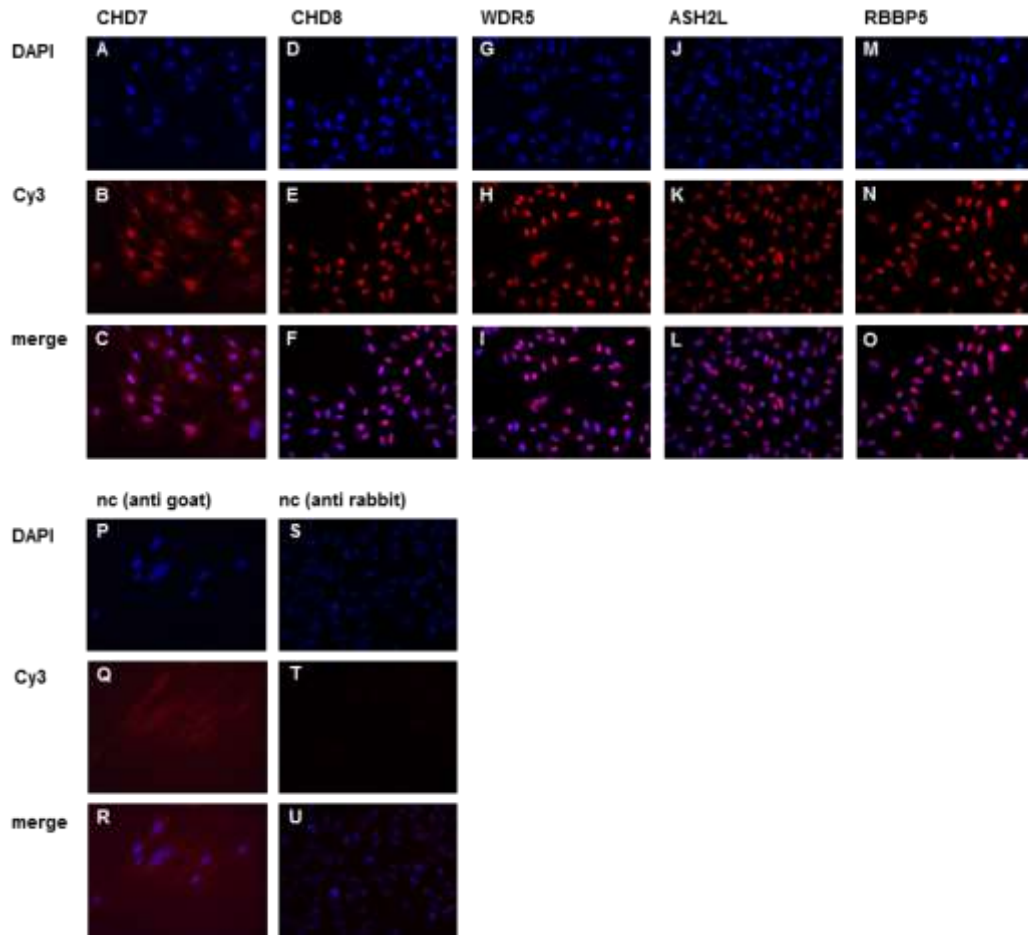


Figure 6: Protein localisation after immunocytochemistry performed with HeLa cells.

Untransfected HeLa cells were incubated overnight with following antibodies to detect the target proteins CHD7 (B, C), CHD8 (E, F), WDR5 (H, I), ASH2L (K, L) and RBBP5 (N, O). Cy3 conjugated secondary antibodies (anti-goat: B, C and anti-rabbit: E, F, H, I, K, L, N, O) were used for visualisation. All proteins analysed were detected in the nucleus. The nuclei of cells were stained with DAPI (A, D, G, J, M, P, S). To validate the specificity of the secondary antibody, HeLa cells were incubated only with the Cy3 conjugated antibody (anti-goat: P-R and anti-rabbit: S-U). It was shown that the anti-goat Cy3 antibody causes a slightly background (Q, R).

For analysing protein interactions by the Duolink PLA method, untransfected HeLa cells were used. The results are presented in figure 7 and published by us (Schulz et al., 2014a). Cell nuclei were stained with DAPI and the cytoskeleton of cells with FITC Phalloidin. PLA signals (red dots) indicate the protein interactions. By merging the channels the localisation of the protein interaction within the cells could be determined. Positive PLA signals were detected in the nucleus using antibodies against CHD7 and WDR5 (Fig. 7C, D, E), CHD7 and ASH2L (Fig. 7H, I, J), CHD7 and RBBP5 (Fig. 7M, N, O), CHD7 and CHD8 (Fig. 7R, S, T). The known interaction between CHD7 and CHD8 were used as a positive control. Cells only

treated with one primary antibody served as a negative control. Only few PLA signals were observed in the cytoplasm and nuclei showing no specific preference, indicating that nearly no unspecific binding of the PLA probes to the antibodies is present (Fig. 7U, V, W, X, Y). In summary, the interaction of CHD7 with the members of the WAR complex WDR5, ASH2L and RBBP5 was confirmed by Duolink PLA. Furthermore, it was shown that the interactions were localised in the nuclei of HeLa cells.

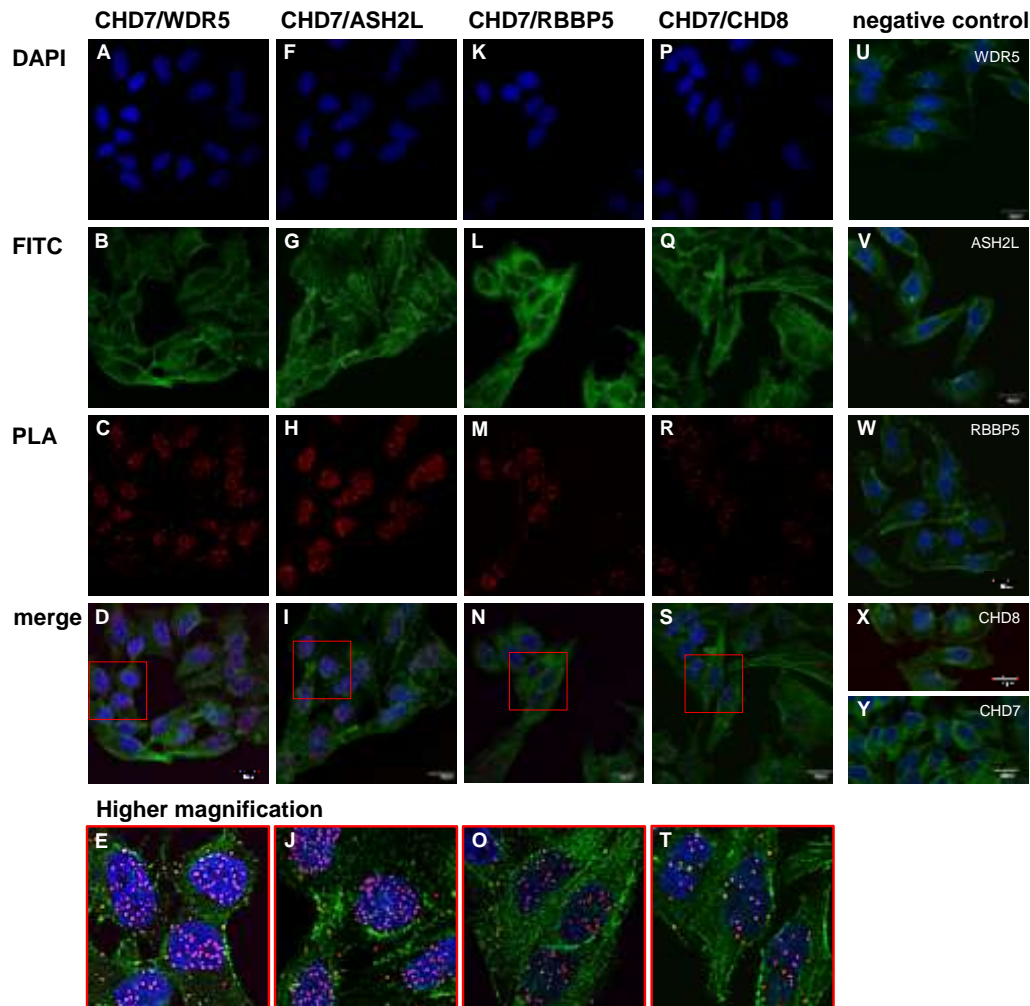


Figure 7: Analysing protein interactions in HeLa cells using the Duolink PLA method.

The nuclei of cells were stained with DAPI (A, F, K, P) and the cytoskeleton of cells were stained with FITC Phalloidin (B, G, L, Q). Positive PLA signals (red dots) indicate protein interactions. PLA signals were mainly detected in the nuclei using antibodies against CHD7 and WDR5 (C, D, E), CHD7 and ASH2L (H, I, J), CHD7 and RBBP5 (M, N, O) and CHD7 and CHD8 (R, S, T) which was used as a positive control. A higher magnification of the merged pictures is shown (E, J, O, T). Only few PLA signals were observed in the cytoplasm and nuclei with no specific preference using an antibody against WDR5 (U), ASH2L (V), RBBP5 (W), CHD8 (X) or CHD7 (Y). These results indicate that there is nearly no unspecific binding of the PLA probes to the antibodies. The Duolink

PLA experiment was carried out three times. Scale bars indicated in the merged pictures correspond to 20 μ m. Figure modified after Schulz et al. (2014a).

3.3 CHD7 shows no direct interaction with WAR complex members

To further analyse whether the identified interactions of CHD7 with components of the WAR complex are direct ones, Y2H experiments were carried out (Fig. 8) and published by us (Schulz et al., 2014a). The recently described constructs CHD7-CR1-3-pGBKT7 containing the CHD7 fragment spanning the amino acids 1591-2181 (NP_060250.2) and the CHD8-pGBKT7 plasmid containing a CHD8 part (amino acids 1789-2302, NP_065971.2) were used as bait plasmids (Batsukh et al., 2010). WDR5-pGADT7 (NP_060058.1), ASH2L-pGADT7 (NP_004665.2) and RBBP5-pGADT7 (NP_005048.2) served as prey plasmids, respectively. Colonies on the –LT plates indicated a successful transformation (Fig. 8A, C, D, F). As a positive control the CHD8-pGADT7-Rec prey plasmid and the CHD7-CR1-3-pGBKT7 bait plasmid were used (Batsukh et al., 2010). The auto activation test using the empty pGBKT7 plasmid and pGADT7 with WDR5, ASH2L or RBBP5 revealed no auto activation of the yeast strain reporter genes (Fig. 8C, E, G). While the direct interaction of the recently described CHD8 fragment (Batsukh et al., 2010) and WDR5, ASH2L and RBBP5 was confirmed, the direct Y2H experiments revealed no direct interaction of the CHD7-CR1-3-part with the WAR complex members (Fig. 8B, E, G).

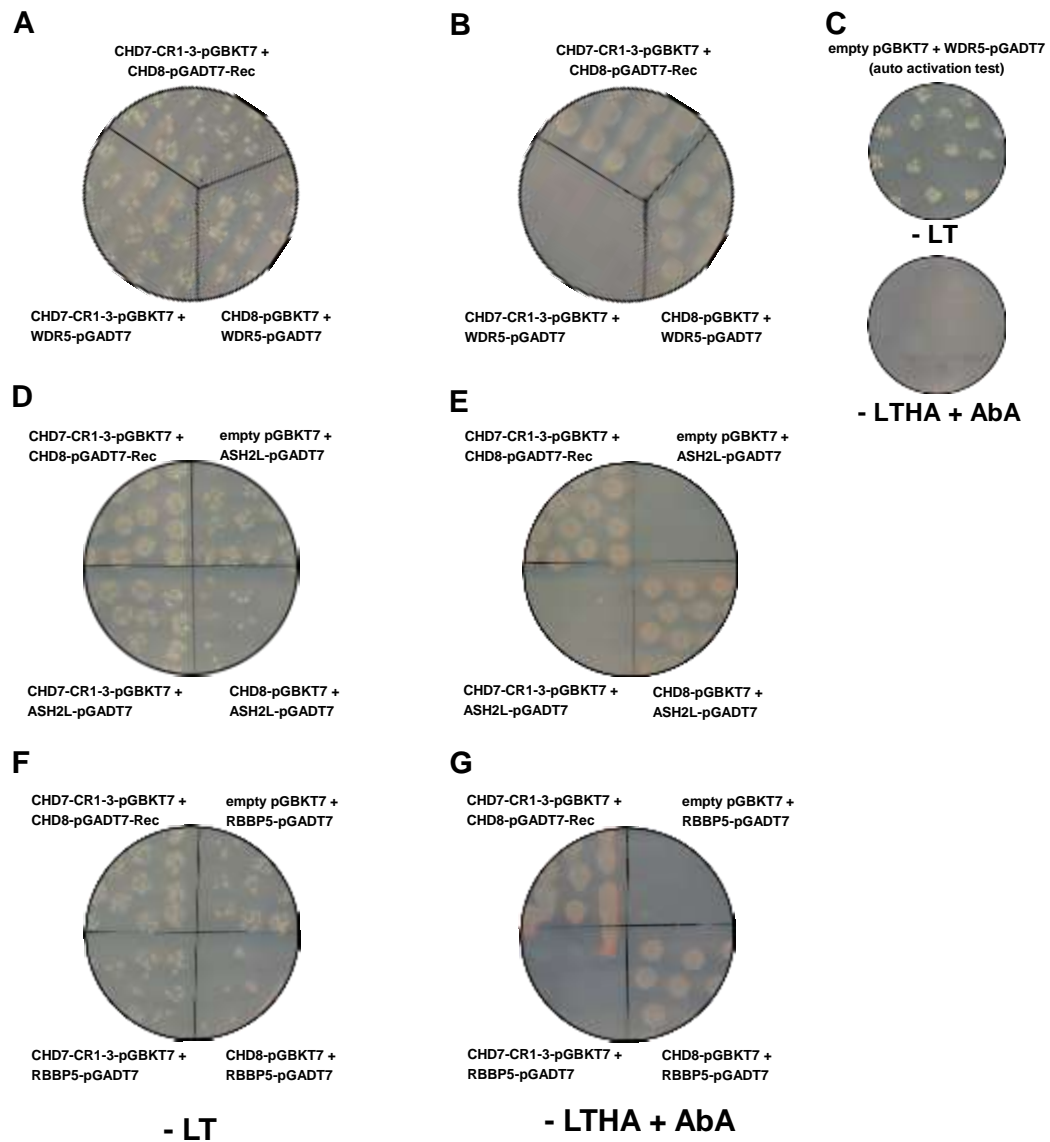


Figure 8: Results of the direct yeast two-hybrid assay.

CHD7-CR1-3-pGBKT7 was used as a bait plasmid to analyse a direct interaction of the CHD7 part (amino acids 1591-2181, NP_060250.2) and the components of the WAR complex (WDR5, ASH2L and RBBP5). The pGADT7 prey plasmid contained either the full-length sequence of WDR5 (NP_060058.1), ASH2L (NP_004665.2) or RBBP5 (NP_005048.2). CHD7-CR1-3-pGBKT7 and CHD8-pGADT7-Rec (containing CHD8 amino acids 1789-2302, NP_065971.2) were used as a positive control. Colonies for each sample on the –LT plate indicated a successful transformation (A, C, D, F). No colonies were detected on –LTHA + AbA (Aureobasidin A) plates using the empty pGBKT7 plasmid and the pGADT7 plasmid with WDR5, ASH2L or RBBP5, showing no auto activation of the yeast strain reporter genes (C, E, G). The direct interaction of the CHD8 part (CHD8-pGBKT7, amino acids 1789-2302, NP_065971.2) and the WAR complex members was confirmed whereas no direct interaction was detected for CHD7-CR1-3-pGBKT7 and the components of the WAR complex (B, E, G). Three biological replicates were performed. Figure modified after Schulz et al. (2014a).

Considering the fact, that the interaction region could be located outside of the analysed CHD7-CR1-3 fragment, further constructs for CHD7 were generated. Therefore, the whole *CHD7* gene was divided into four overlapping fragments without interrupting any known functional domain (Fig. 9).

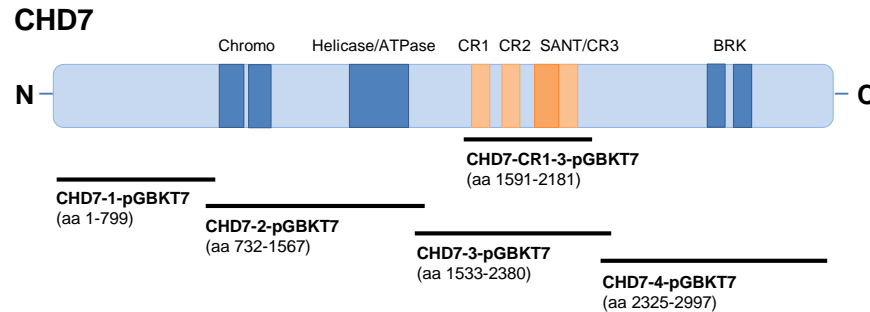


Figure 9: Schematic representation of the CHD7 constructs for yeast two-hybrid experiments.

The ATP-dependent chromatin remodelling enzyme CHD7 belongs to the CHD family and consists of two N-terminal located chromodomains, a helicase/ATPase domain, three conserved regions (CR1-CR3), a SANT domain and two BRK domains at the C-terminus. As indicated, the *CHD7* gene was divided into four overlapping parts without interrupting any known functional domains (CHD7-1-pGBKT7, 1-799 aa; CHD7-2-pGBKT7, 732-1567 aa; CHD7-3-pGBKT7, 1533-2380 aa; CHD7-4-pGBKT7, 2325-2997 aa). In addition, the CHD7-CR1-3-pGBKT7 plasmid is shown (Batsukh et al., 2010). Figure modified after Schulz et al. (2014a).

In conclusion, the data from the direct Y2H experiments revealed no direct interaction of CHD7 with the WAR complex members and the known direct interaction of CHD8 with the components of the WAR complex was confirmed. At the same time the region which is responsible for the direct interaction was identified to be located within the CHD8 fragment spanning the amino acids 1789-2302, NP_065971.2.

3.4 Genome-wide expression analysis demonstrates a misregulation of NCC guidance genes in case of CHD7 loss of function

Already in 1985 Siebert et al. (1985) assumed that the malformations and defects seen in CHARGE syndrome patients result from abnormalities during NCC development. Chd7 knockdown experiments in *Xenopus laevis* demonstrated that Chd7 is essential for the formation of NCCs (Bajpai et al., 2010). However, only a few Chd7 target genes involved in the formation and migration of NCCs were described (Bajpai et al., 2010). Because nothing is known about the role of Chd7 in

the guidance of migrating NCCs and the process of EMT, a genome-wide microarray expression analysis was performed with embryos of the *Whirligig* mouse line at E9.5 at the time of NCCs migration (Schulz et al., 2014b). Animals were kindly provided by K. P. Steel (Sanger Centre, Cambridge, United Kingdom) and the Helmholtz Zentrum, Munich, Germany. The *Whirligig* mouse line was generated by a large-scale ENU mutagenesis programme (Hrabe de Angelis et al., 2000; Hawker et al., 2005). In exon 11 of the *Chd7* gene a nonsense mutation (p.W973X) leads to a premature stop codon (Bosman et al., 2005). Heterozygous (*Chd7*^{Whi/+}) mice reveal symptoms which are also present in CHARGE syndrome patients, therefore providing a good model to study features of CHARGE syndrome (Bosman et al., 2005).

The data presented below are published by us (Schulz et al., 2014b). The microarray analysis was performed on four female wild-type (*Chd7*^{+/+}), four heterozygous (*Chd7*^{Whi/+}) and four homozygous (*Chd7*^{Whi/Whi}) mouse embryos. 98 differentially expressed genes showing more than two-fold differences (\log_2 fold-change (FC) ≤ -1 or ≥ 1) and a false discovery rate (FDR) $< 5\%$ were identified by comparing homozygous (*Chd7*^{Whi/Whi}) and wild-type (*Chd7*^{+/+}) embryos. For 71 of these genes the expression was decreased and 27 genes were found with increased expression. The heat map shown in figure 10 displays some of the genes recognised by microarray analysis. Interestingly, many of these differentially expressed genes are known to play a role in NCC migration and axon guidance. Examples are members of the semaphorin family like *Sema3a* (*sema domain, immunoglobulin domain (Ig), short basic domain, secreted, (semaphorin) 3A*), *Sema3c* (*sema domain, immunoglobulin domain (Ig), short basic domain, secreted, (semaphorin) 3C*) or *Sema3d* (*sema domain, immunoglobulin domain (Ig), short basic domain, secreted, (semaphorin) 3D*) which are required for guiding migrating NCCs (Eickholt et al., 1999; Brown et al., 2001; Gitler et al., 2004; Lepore et al., 2006; Sato et al., 2006) and *Epha3* (*Eph receptor A3*), *Epha5* (*Eph receptor A5*) and *Epha7* (*Eph receptor A7*) belonging to the family of ephrin receptors. Ephrin receptors are also involved in the guidance of NCCs (Kuriyama and Mayor, 2008). Furthermore, transcription factors like *Sox10* (*SRY (sex determining region Y)-box 10*) and *Foxd3* (*forkhead box D3*) which play a role in the early migration process of NCCs were found to be upregulated. A complete list of the 98 differentially expressed genes is shown in table 39 in the appendix.

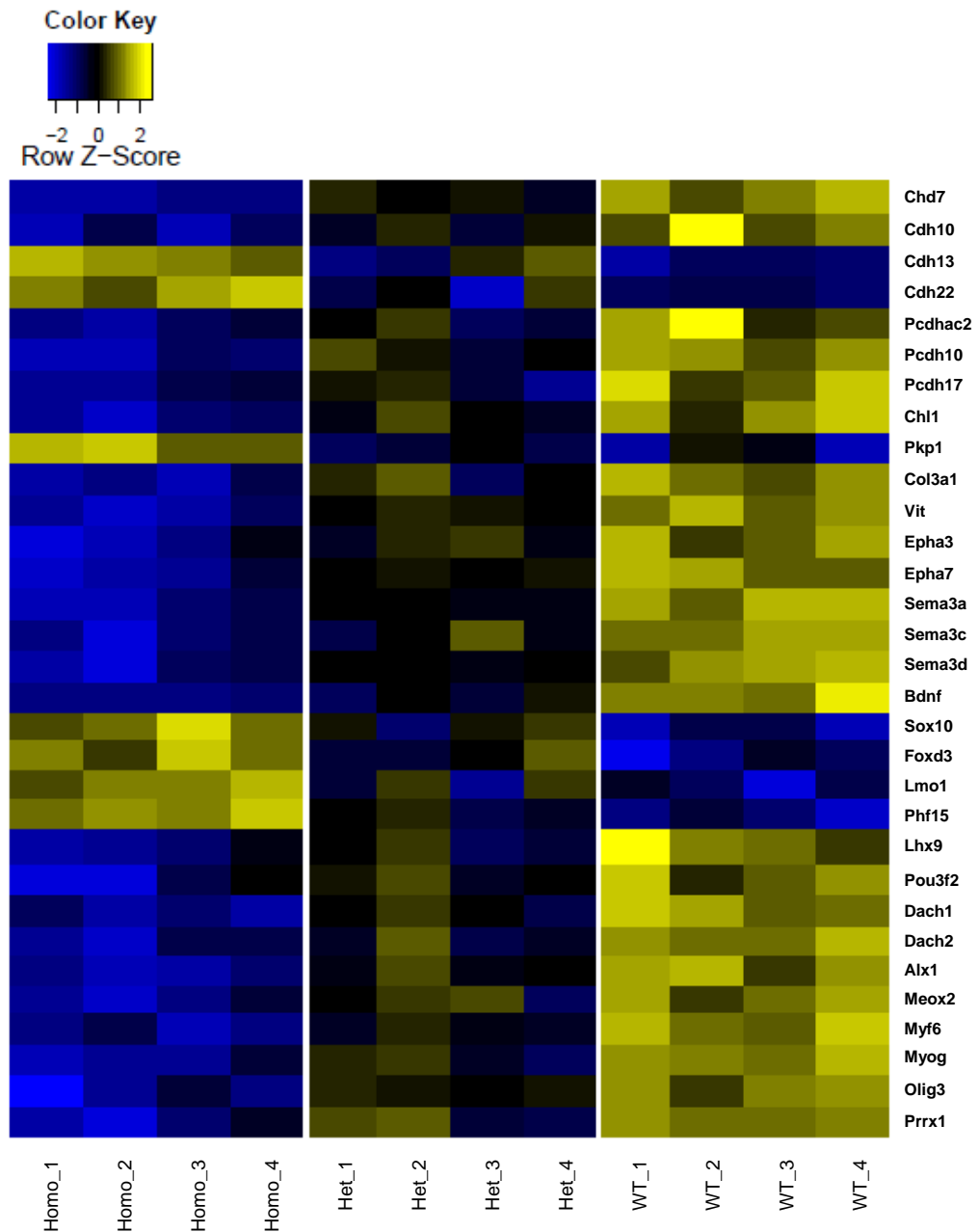


Figure 10: Heatmap of differentially expressed genes found by microarray.

The heatmap shows some of the differentially expressed genes found by comparison of the expression profile of four female mouse embryos (E9.5) per genotype (wild-type (*Chd7^{+/+}*): WT 1-4, heterozygous (*Chd7^{Whi/+}*): Het 1-4 and homozygous (*Chd7^{Whi/Whi}*): Homo 1-4). The results illustrate a regulating function of CHD7 of genes involved in NCC and axon guidance and transcription factors. Figure modified after Schulz et al. (2014b).

3.5 Expression analysis by RT-qPCR confirms the results of the microarray

To validate the data of the genome-wide microarray analysis, the expression of genes involved in NCC guidance, namely *Sema3a*, *Sema3d*, *Epha3*, *Sox10* and the two further genes *Trp53bp2* (*transformation related protein 53 binding protein 2*) and *Gfra2* (*glial cell line derived neurotrophic factor family receptor alpha 2*) were analysed by RT-qPCR. Furthermore, these genes were chosen to have a complete validation of upregulated, nonregulated and downregulated genes. The relative expression of these genes is shown in figure 11 and published by us (Schulz et al., 2014b). The same RNA used for the microarray analysis was employed for the RT-qPCR. Four biological replicates for heterozygous (*Chd7^{Whi/+}*) and homozygous (*Chd7^{Whi/Whi}*) mice were analysed. Four wild-type (*Chd7^{+/+}*) embryos were pooled and used as a calibrator. Data were normalised against three reference genes (*Tbp* (*TATA box binding protein*), *Sdha* (*Succinate dehydrogenase complex, subunit A*) and *Hprt* (*Hypoxanthin-phosphoribosyl-transferase*)). The microarray expression analysis revealed a clear upregulation of *Sema3a*, *Sema3d* and *Epha3*. The results of the RT-qPCR showed that in heterozygous (*Chd7^{Whi/+}*) animals the relative expression of *Sema3a* was decreased up to 50 %. Homozygous (*Chd7^{Whi/Whi}*) mice showed a reduction of *Sema3a* expression between 60-70 %. A similar decrease in expression was observed for *Sema3d*. The relative expression of *Epha3* was reduced more than 50 % in heterozygous (*Chd7^{Whi/+}*) embryos and 60-80 % in homozygous (*Chd7^{Whi/Whi}*) embryos. The average relative expression of *Trp53bp2* remained mostly unchanged in heterozygous (*Chd7^{Whi/+}*) and homozygous (*Chd7^{Whi/Whi}*) embryos compared to wild-type (*Chd7^{+/+}*). According to the microarray data the expression of the transcription factor *Sox10* and *Gfra2* was upregulated (appendix, Tab. 39). The relative expression of *Sox10* measured by RT-qPCR was increased about 35 % in heterozygous (*Chd7^{Whi/+}*) mice. The increase in expression of *Sox10* was even stronger in the homozygous (*Chd7^{Whi/Whi}*) stage where in half of the embryos *Sox10* was double as high as in wild-type (*Chd7^{+/+}*) embryos. The *Gfra2* expression was in half of the heterozygous (*Chd7^{Whi/+}*) embryos 0.7-2.3 times higher compared to the wild-type (*Chd7^{+/+}*) control embryos. In the majority of homozygous (*Chd7^{Whi/Whi}*) embryos the *Gfra2* expression was markedly more than double as the

expression in the wild-type ($Chd7^{+/+}$) embryos. Altogether, the results of the RT-qPCR reflect the data of the genome-wide microarray analysis.

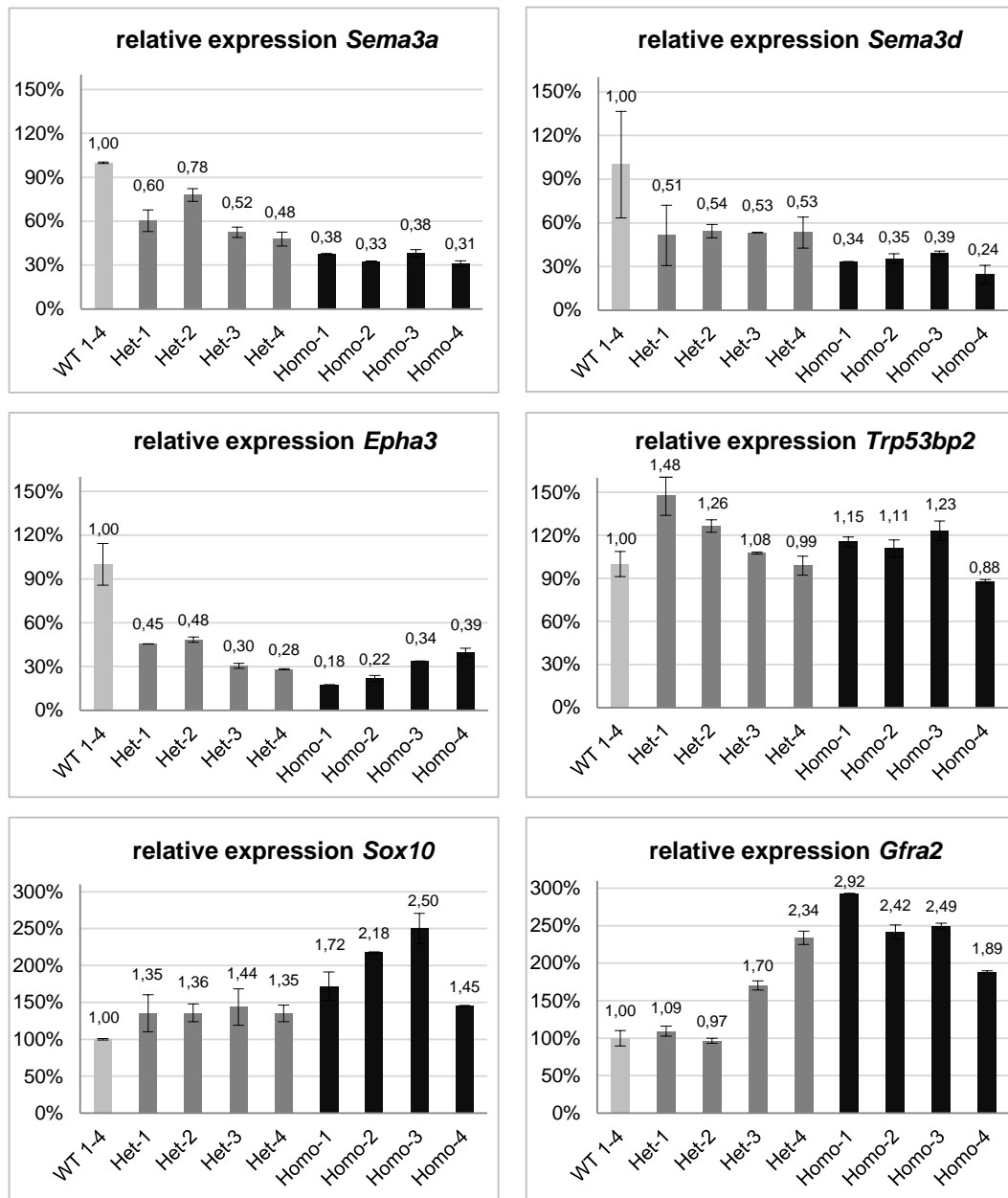


Figure 11: Results of the gene expression analysis by RT-qPCR.

A selection of six genes (*Sema3a*, *Sema3d*, *Epha3*, *Trp53bp2*, *Sox10* and *Gfra2*) was used to validate the microarray data by RT-qPCR. The same RNA from female embryos of the *Whirligig* mouse line was used as for the microarray. The experiment was performed on four biological replicates per genotype ($Chd7^{Whi/+}$ and $Chd7^{Whi/Whi}$). The RNA from the four wild-type ($Chd7^{+/+}$) embryos was pooled and utilised as a calibrator. The data were normalised against the three reference genes *Tbp*, *Sdha* and *Hprt*. The expression of *Sema3a*, *Sema3d* and *Epha3* is downregulated, *Trp53bp2* is mostly unaffected and *Sox10* and *Gfra2* are upregulated. These results confirm the data from the whole-genome microarray analysis. Figure modified after Schulz et al. (2014b).

3.6 There is no gender specific effect on the expression of *Sema3a*, *Sema3d*, *Epha3*, *Trp53bp2*, *Sox10* and *Gfra2* in Whirligig mouse embryos

To further validate whether the data from the microarray and the RT-qPCR are female specific, the same genes were analysed by another RT-qPCR approach using RNA extracted from male wild-type (*Chd7*^{+/+}), heterozygous (*Chd7*^{Whi/+}) and homozygous (*Chd7*^{Whi/Whi}) mouse embryos (E9.5). The results described below are published by us (Schulz et al., 2014b). Three biological replicates for each genotype were analysed. The three wild-type (*Chd7*^{+/+}) embryos were pooled and served as a calibrator. The data were normalised against the reference genes *Tbp*, *Sdha* and *Hprt*. The results are represented in figure 12. The relative expression of *Sema3a* was downregulated in all embryos. Homozygous (*Chd7*^{Whi/Whi}) mice showed with a decrease of more than 50 % up to 70 % the most precise effect. In the majority of heterozygous (*Chd7*^{Whi/+}) individuals *Sema3d* expression was about half reduced compared to wild-type (*Chd7*^{+/+}) embryos. The *Sema3d* expression was even more decreased (> 70 %) in homozygous (*Chd7*^{Whi/Whi}) mice. *Epha3* was also found to be downregulated in the majority of heterozygous (*Chd7*^{Whi/+}) and homozygous (*Chd7*^{Whi/Whi}) embryos with about 70 %. While the expression of *Trp53bp2* remained unaffected, the expression of *Sox10* and *Gfra2* was increased. Especially homozygous (*Chd7*^{Whi/Whi}) mice showed a three times higher expression level of *Gfra2* than wild-type (*Chd7*^{+/+}) embryos. In summary, it can be stated that female and male embryos showed a similar expression of the analysed genes which corresponds to the results of the microarray.

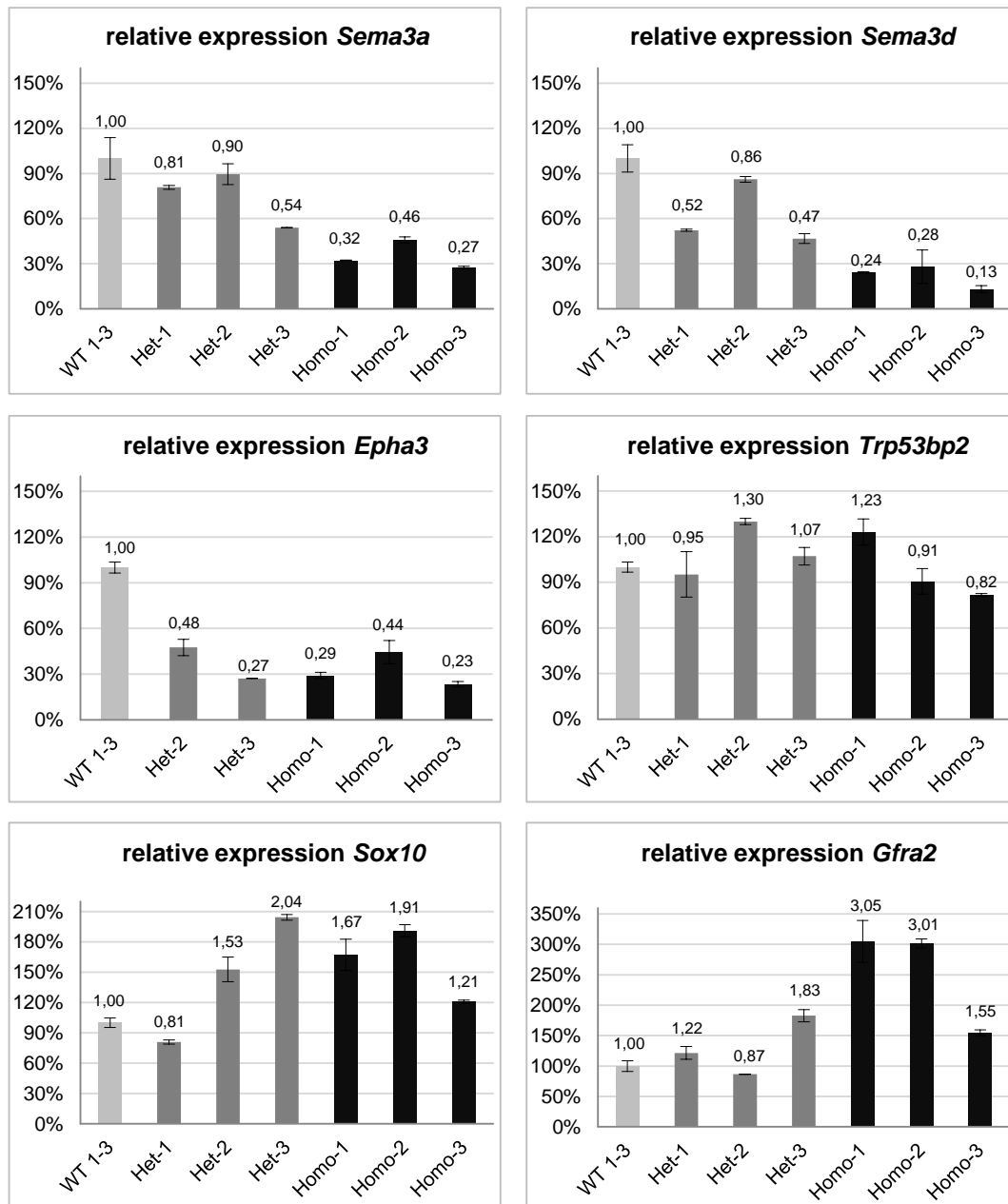


Figure 12: Repetition of RT-qPCR.

RNA from male E9.5 embryos was used. Three biological replicates were performed for each genotype ($Chd7^{Whi/+}$ and $Chd7^{Whi/Whi}$). Pooled RNA from three wild-type ($Chd7^{+/+}$) embryos served as a calibrator. Data were normalised against the three reference genes *Tbp*, *Sdha* and *Hprt*. The same genes were analysed under identical conditions as described before (Fig. 11). The *Sema3a*, *Sema3d* and *Epha3* expression is found to be downregulated. *Trp53bp2* expression is mostly unaffected and the *Sox10* and *Grfa2* expression is upregulated, demonstrating that there is no gender specific CHD7 regulation of the analysed genes. One of the biological replicates of the heterozygous ($Chd7^{Whi/+}$) mouse embryos analysing the *Epha3* expression was excluded due to technical issues. Figure modified after Schulz et al. (2014b).

3.7 CHD7 and SEMA3D show a similar expression pattern in mouse embryos

The data from the genome-wide microarray analysis revealed a high number of differentially expressed genes which play a role in NCC migration (Schulz et al., 2014b). It was shown that CHD7 has a regulatory effect on some members of the semaphorin family (Fig. 10) (Schulz et al., 2014b). Therefore, the expression pattern of CHD7 and SEMA3D was analysed on paraffin sections of wild-type mouse embryos (E12.5) and compared with each other. Figure 13 shows three serial made sagittal sections from the embryo (Fig. 13A, B, C) after immunohistochemistry (DAB staining). Picture A shows the negative control, picture B represents the expression pattern of CHD7 and the expression profile of SEMA3D can be seen in picture C. CHD7 is expressed mainly in the brain, heart, vertebrae and nerves along the spine and the sensory nerve ends above the eye. SEMA3D is also expressed in the brain, heart and different structures of the nervous system like CHD7. While CHD7 seems to be more restricted to a specific area, SEMA3D is expressed also in the surrounding epithelium. Unfortunately, further investigation of SEMA3D and CHD7 expression in wild-type (*Chd7*^{+/+}) and heterozygous (*Chd7*^{Whi/+}) mouse embryos of the *Whirligig* mouse line failed as well as the expression analysis of SEMA3A due to technical issues affecting the colour reaction. Several repetitions with different mouse embryos were performed, solutions, such as paraffin, fixating solution and the DAB staining solutions were exchanged but the technical problem could not be solved. It would be interesting to analyse the changes in the expression pattern of semaphorins in CHD7 deficient mouse embryos.

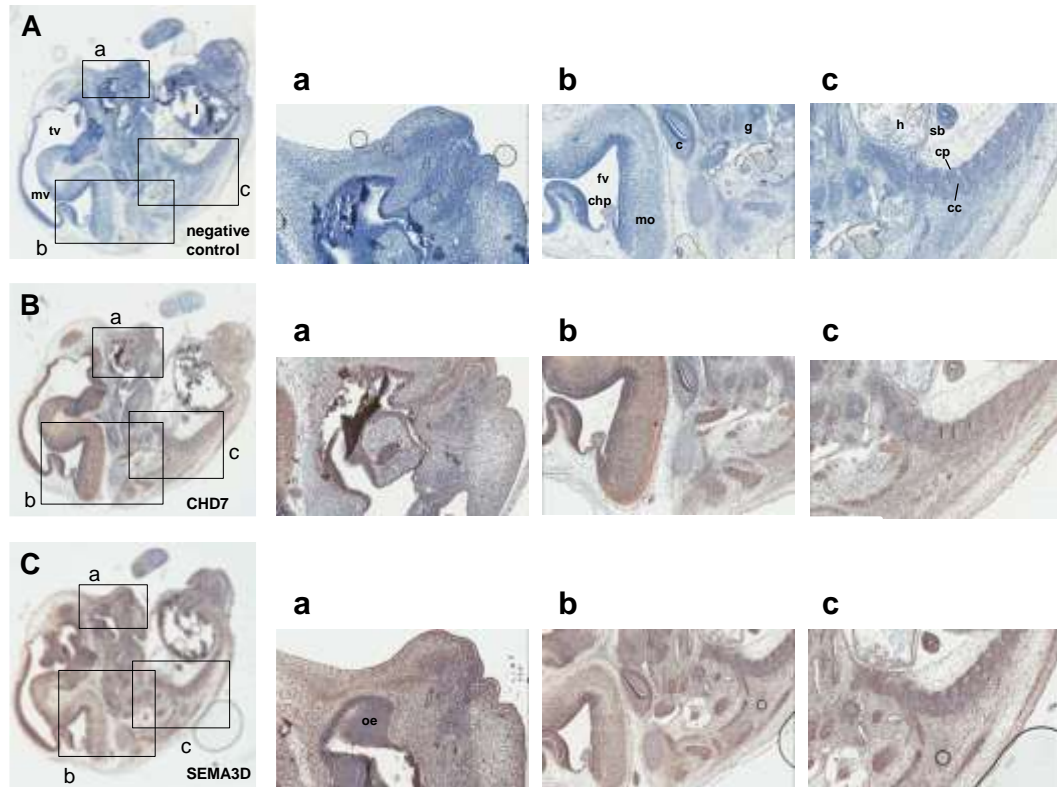


Figure 13: CHD7 and SEMA3D expression analysis using paraffin sections of mouse embryos stained with DAB.

Serial sagittal paraffin sections were prepared using wild-type mouse embryos (E12.5). The expression pattern of CHD7 (**B**) and SEMA3D (**C**) were analysed by DAB staining. No primary antibody was used for the negative control (**A**). Different regions of the embryos are shown in higher magnification: front head (**a**), neck (**b**) and dorsum (**c**). The negative control showed no unspecific staining, indicating that the universal secondary antibody does not bind unspecifically to the tissue of the embryos (**A**). CHD7 expression was found in the medulla oblongata, choroid plexus differentiating from roof of fourth ventricle, cochlea, heart, cartilage primordium of body of vertebra and in different ganglia e.g. along the spine and above the eye (**B**). The SEMA3D expression pattern resembles the expression of CHD7 in the medulla oblongata, choroid plexus differentiating from roof of fourth ventricle, cochlea, heart, cartilage primordium of body of vertebra and in different ganglia (**C**). c = cochlea, cc = cartilage condensation being primordium of vertebral body, chp = choroid plexus differentiating from roof of fourth ventricle, cp = cartilage primordium of body of vertebra, fv = forth ventricle, g = ganglia, h = heart, l = liver, mo = medulla oblongata, mv = mesencephalic vesicle, oe = olfactory epithelium, sb = segmental bronchus within accessory lobe of right lung, tv = right telencephalic vesicle.

3.8 Results of *SEMA3A* and *SEMA3D* mutation screens in patients with CHARGE syndrome

CHARGE syndrome is a phenotypically heterogeneous disorder, so it is possible that there are other genes which might act as modifiers leading to a more severe phenotype when they are mutated. In 5-10 % of typical CHARGE patients and 40-60 % of patients suspected of having CHARGE the underlying cause remains unknown (Janssen et al., 2012) so it could be possible that other “CHARGE genes” exist. For that reason 45 CHARGE syndrome patients without a mutation in the *CHD7* gene were screened for mutations in *SEMA3A* (GenBank accession number: NM_006080.2) and *SEMA3D* (GenBank accession number: NM_152754.2). All 17 coding exons and flanking intronic sequences of *SEMA3A* and *SEMA3D* were analysed by amplifying these regions by PCR and screening for mutations by sequencing. The results from the *SEMA3A* mutation screen are published by us (Schulz et al., 2014b). For *SEMA3A* three non-synonymous variants were found: c.196C>T (p.R66W), c.2002A>G (p.I668V) and c.2062A>G (p.T688A). Sequences are shown in figure 14. The variants are indicated by red arrows. The variant p.R66W was located in the sema domain, a conserved module of ligand-receptor interaction, also present in other proteins like plexins (Antipenko et al., 2003) and was predicted to be damaging (Polyphen 2, SIFT and mutation taster). By screening the parents of the patient carrying the c.196C>T (p.R66W) variant it was shown that this variant was inherited from the healthy father. The two other identified variants p.I668V and p.T688A were predicted to be benign (Polyphen 2). The parents were not available for a further clarification.

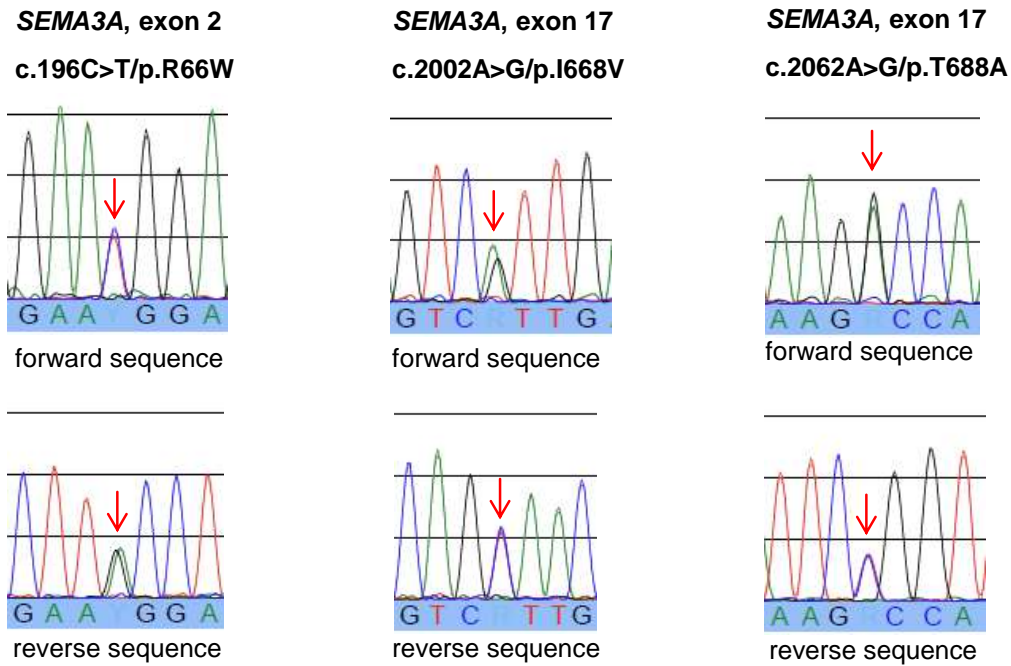


Figure 14: Results of the *SEMA3A* mutation screen.

All coding exons of the *SEMA3A* gene were sequenced in 45 *CHD7* negative patients diagnosed with CHARGE syndrome. Three non-synonymous variants were identified: c.196C>T (p.R66W), c.2002A>G (p.I668V) and c.2062A>G (p.T688A). The mutations are indicated by red arrows in the forward and reverse sequence, respectively.

Sequencing of *SEMA3D* revealed following non-synonymous variants: c.193T>C (p.S65P), c.1272C>A (p.H424Q) and c.2101A>C (p.K701Q) (Fig. 15). While the non-synonymous SNP p.K701Q is a common variant with an allele frequency of 0.346 in the ESP cohort population (SNPdev, n.d.), the variant p.S65P is less common. In the ESP cohort population it has an allele frequency of 0.017 (SNPdev, n.d.). Both variants are predicted to be benign (Polyphen and Polyphen 2). The variant p.H424Q is quite rare. It was observed in the ESP cohort population with an allele frequency of 0.002 (SNPdev, n.d.) and it was found to be located in a highly conserved domain. In silico programmes predicted the variant p.H424Q as a protein “damaging” variant (Polyphen, Polyphen 2, SIFT). For further clarification the parents of the patients were screened. It was shown that the variant p.H424Q was inherited from the healthy father.

Furthermore, in ten *CHD7* negative CHARGE patients all 17 coding exons of *SEMA3A* and *SEMA3D* were analysed for copy number defects (large deletions and duplications) by qPCRs. In these patients copy number defects were excluded.

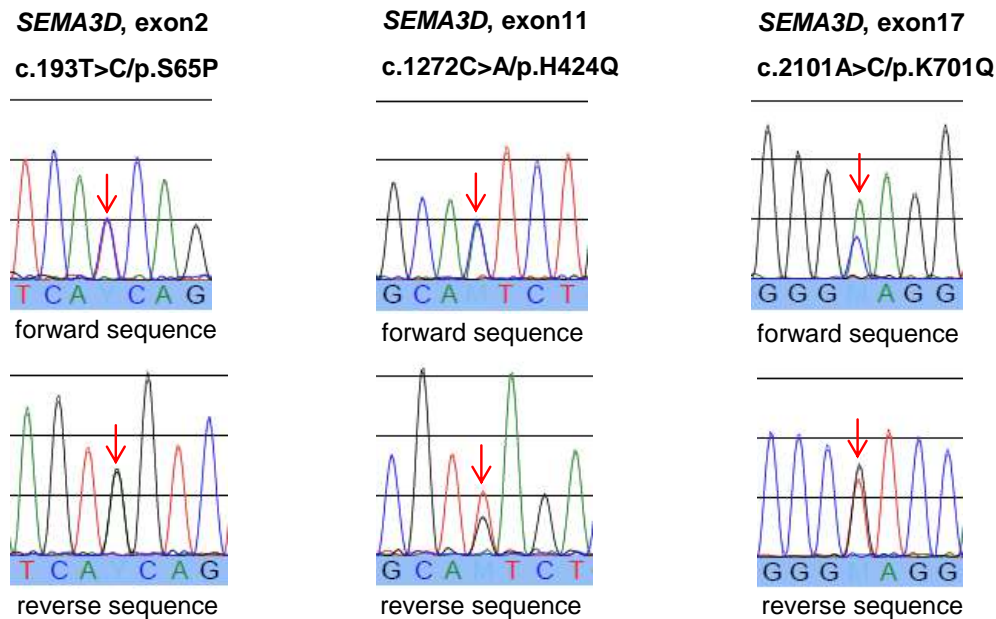


Figure 15: Results of the *SEMA3D* mutation screen.

The 17 exons of the *SEMA3D* gene were sequenced in 45 *CHD7* negative CHARGE patients. Three non-synonymous variants were found: c.193T>C (p.S65P), c.1272C>A (p.H424Q) and c.2101A>C (p.K701Q). The mutations are shown in the forward and reverse sequence indicated by red arrows.

3.9 Knockdown of *Chd7* causes alteration in *sema3a* expression in *Xenopus laevis*

Chd7 is highly conserved throughout different species (Bosman et al., 2005; Bajpai et al., 2010; Schnetz et al., 2010). It was shown that *Chd7* deficient *Xenopus laevis* embryos mimic basic features of CHARGE syndrome (Bajpai et al., 2010). To study the effect of *Chd7* on the expression of *sema3a* in another species, *Chd7* was downregulated in *Xenopus laevis* mediated by *Chd7* MO. The data below are published by us (Schulz et al., 2014b). The *sema3a* expression pattern was analysed by WMISH at the neurula stage 20 (Fig. 16) and the tailbud stage 27 (Fig. 17). Embryos were injected with a MO in combination with *lacZ* RNA as a lineage tracer in one blastomere at a two-cell stage. The injected side is indicated by the blue *lacZ* staining (Fig. 16A-F; Fig. 17B, D, F). Control embryos were injected with 20 ng control MO (Co MO) which has no target RNA. Embryos injected with the Co MO showed as expected a normal *sema3a* expression pattern in the midbrain-hindbrain boundary (mh) (Fig. 16A; Fig. 17A, B) and somites (s) (Fig. 16B; Fig. 17A, B). Tailbud stages showed an additional expression in the splanchnic mesoderm (sm)

(Fig. 17A, B). After Chd7 was downregulated by injecting 10 ng Chd7 MO, in about 70 % of the embryos a reduction of *sema3a* expression were detected. Approximately 60 % of these embryos showed a severe downregulation of the *sema3a* expression pattern in general or the expression in one district region was completely missing (Fig. 16C, D; Fig. 17D). After injecting 20 ng Chd7 MO, in almost all analysed embryos of the neurula and tailbud stage the *sema3a* expression was dramatically decreased or completely absent (Fig. 16E, F; Fig. 17F).

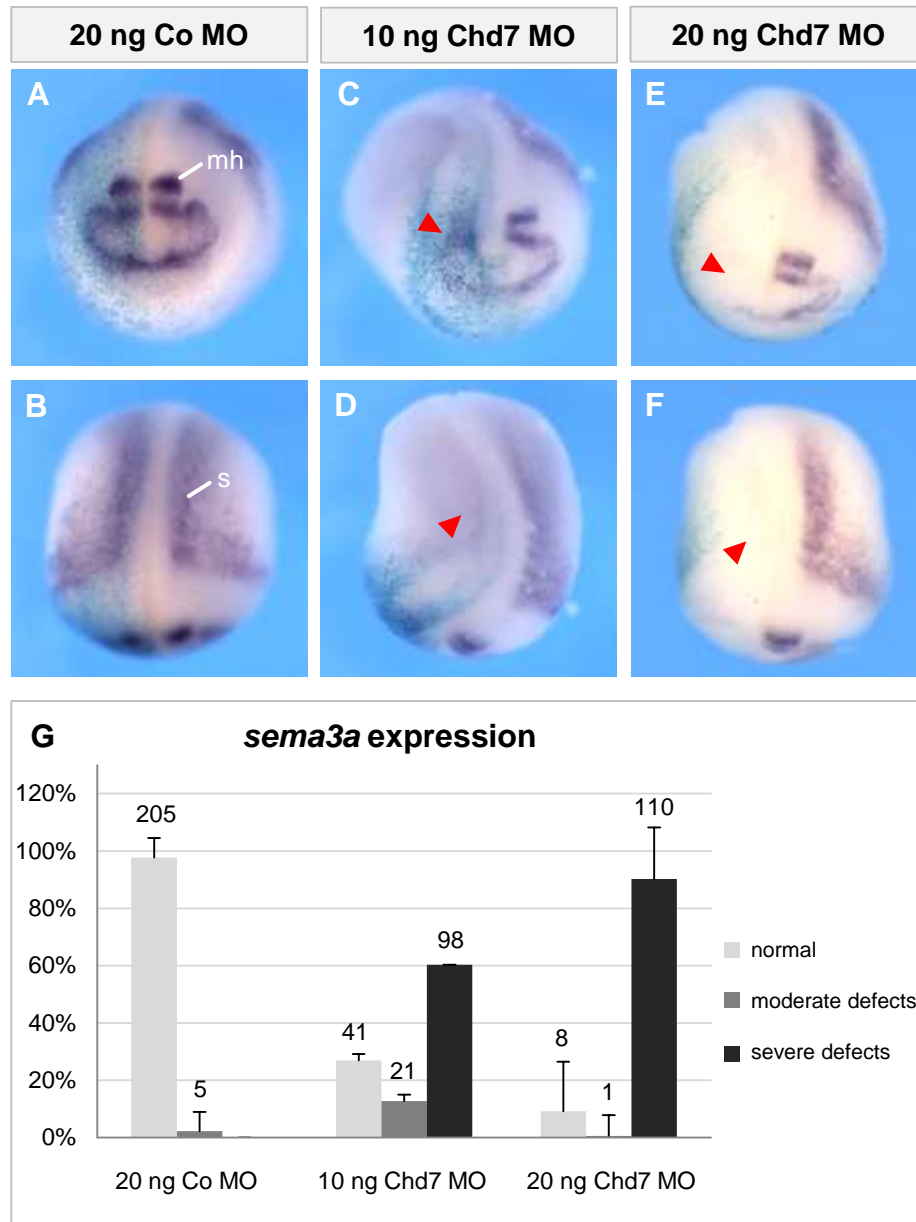


Figure 16: *Sema3a* expression analysis by whole mount *in situ* hybridisation after Chd7 knockdown in *Xenopus laevis* (neurula stage 20).

One blastomere of the two-cell stage embryos was injected with a MO and *lacZ* RNA as a lineage tracer. Embryos were injected with 20 ng control MO (A, B), 10 ng Chd7 MO (C, D) or 20 ng CHD7

MO (E, F). The injected side of the embryo is indicated by a blue *lacZ* staining. The expression pattern of *sema3a* (purple staining) was analysed. Nearly all control embryos showed a normal expression pattern of *sema3a* (A, B); midbrain hindbrain boundary (mh); somites (s). After knocking down Chd7 with 10 ng Chd7 MO, in about 60 % of the embryos a clear reduced *sema3a* expression in the somites and the head region was observed (C, D). An injection of 20 ng Chd7 MO led to a complete loss of *sema3a* expression or to a drastic reduced expression pattern in 90 % of the embryos (E, F). The graph summarises three independent experiments (G). The diagram reflects the percentage of the embryos showing a normal *sema3a* expression pattern (light grey columns), moderate (grey columns) or severe defects (black columns). Standard error of the means is shown. On top of each column the total number of the embryos counted in the different categories is listed. Figure modified after Schulz et al. (2014b).

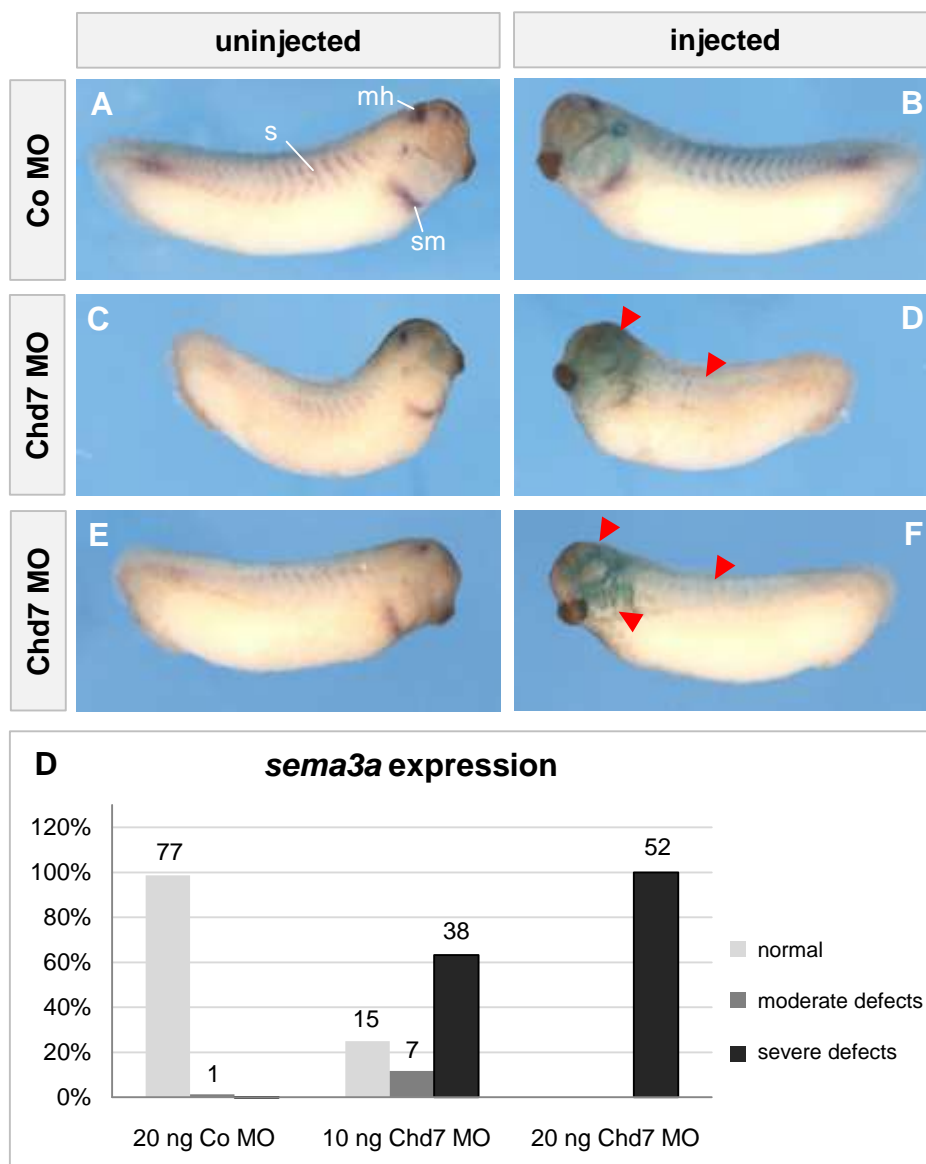


Figure 17: *Sema3a* expression after Chd7 knockdown in *Xenopus laevis* (tailbud stage 27).

One blastomere of two-cell embryos was injected with a MO (20 ng control MO (A, B), 10 ng Chd7 MO (C, D) or 20 ng CHD7 MO (E, F)) in combination with *lacZ* RNA for lineage tracing. A blue

lacZ staining indicates the injected side of the embryo (**B, D, F**). The expression pattern of *sema3a* (purple staining) was analysed by whole mount *in situ* hybridisation. In 99 % of the control embryos the expression pattern of *sema3a* remained unchanged (**A, B**); midbrain hindbrain boundary (mh); somites (s); splanchnic mesoderm (sm). After the knockdown of Chd7 with 10 ng Chd7 MO 60 % of the embryos showed a reduced *sema3a* expression in the somites and the head region (**C, D**). A complete loss of *sema3a* expression or a drastic reduced expression was observed in all embryos after 20 ng Chd7 MO injections (**E, F**). The columns of the diagram show the percentage of embryos with normal *sema3a* expression (light grey), moderate (grey) or severe changes in the expression pattern (black). On top of each column the amount of embryos obtained in the different categories are listed. The data refer to one biological replicate. Figure modified after Schulz et al. (2014b).

3.10 The Chd7 MO phenotype was successfully rescued by human *CHD7* RNA

Rescue experiments were performed to check whether human *CHD7* RNA is able to rescue the Chd7 MO phenotype. The human *CHD7* full-length plasmid was kindly provided by J. Wysocka (Department of Developmental Biology, Stanford University School of Medicine, Stanford, California). The following data are published by us (Schulz et al., 2014b). *CHD7* DNA was transcribed into sense RNA to obtain the rescue construct (h*CHD7* RNA). *Xenopus laevis* embryos were injected as described before. A WMISH was performed at neurula stages 20 and 21 to analyse the expression of *sema3a*. Embryos injected with Co MO and the rescue construct and uninjected embryos were used as controls. More than 95 % of these embryos showed a normal *sema3a* expression (Fig. 18A-D; Fig. 19A-D). After injecting 10 ng Chd7 MO, half of the embryos showed a massively reduced *sema3a* expression and more than 30 % a moderate reduction (Fig. 18E, F). For the rescue experiments embryos were injected with 10 ng of Chd7 MO to knockdown Chd7 in combination with 1 ng of the rescue construct h*CHD7* RNA which is not recognised by the MO. The embryos of the Chd7 knockdown were compared with the embryos after the rescue. The percentage of embryos showing a severe reduction of *sema3a* expression was reduced from 53 % down to 6 %. At the same time the percentage of embryos with a normal expression pattern was increased from 13 % to 52 % (Fig. 18I). The rescue of the Chd7 MO phenotype was slightly more effective after injecting 1.5 ng h*CHD7* RNA (Fig. 19I). The percentage of severe alterations in *sema3a* expression was decreased from 61 % to 4 % and the percentage of embryos showing a normal phenotype was increased from 24 % to 56 %.

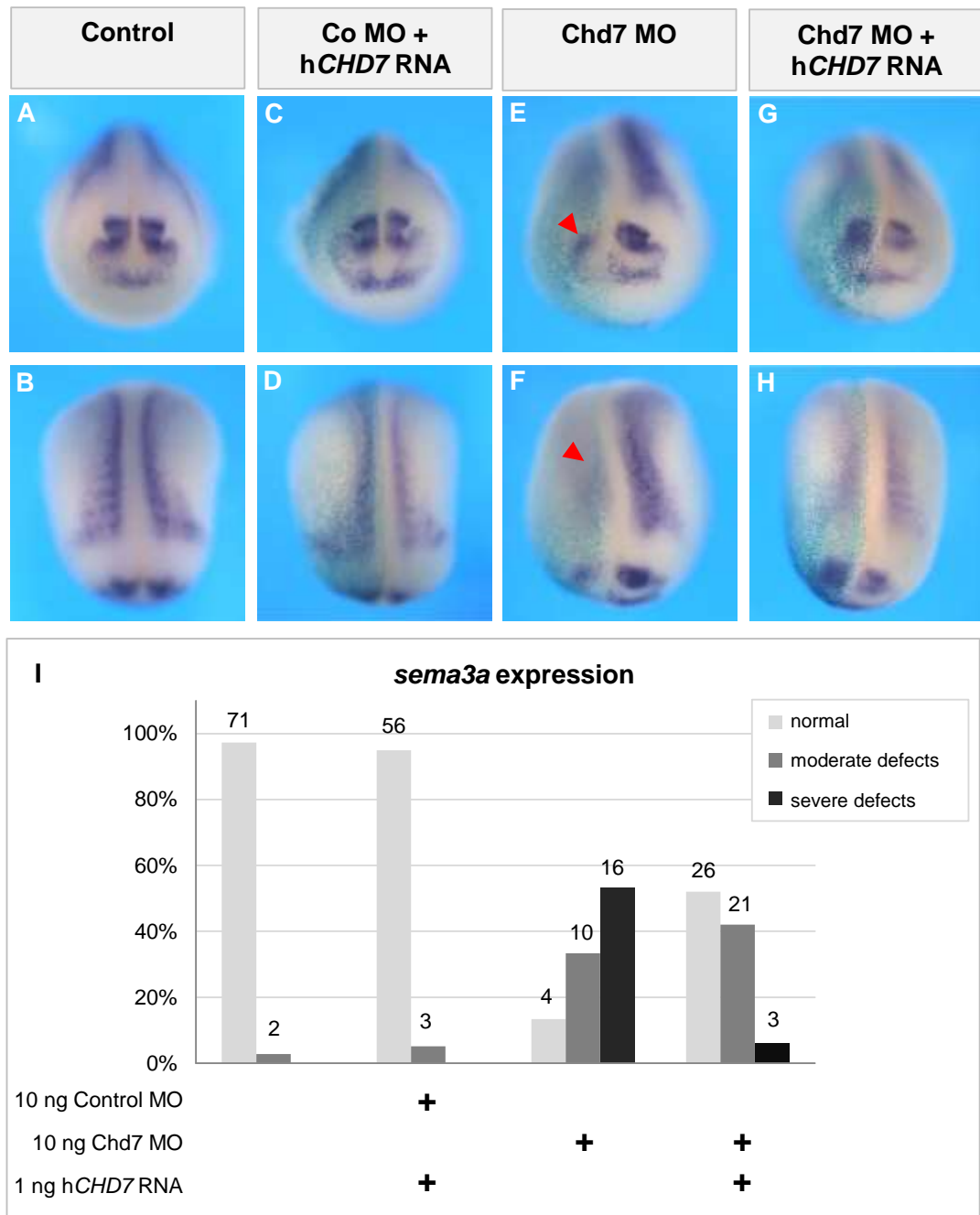


Figure 18: Rescue of the Chd7 MO phenotype in *Xenopus laevis* (neurula stage 21).

As a rescue construct human *CHD7* RNA (hCHD7 RNA) was used which is not recognised by the Chd7 MO. Embryos were injected (one blastomere of a two-cell stage) with either 10 ng of a Co MO and 1 ng hCHD7 RNA for the rescue (C, D), 10 ng Chd7 MO (E, F) or 10 ng Chd7 MO and 1 ng hCHD7 RNA (G, H). All embryos were co-injected with *lacZ* RNA as lineage tracer. By whole mount *in situ* hybridisation the *sema3a* expression was analysed (purple staining). Uninjected embryos were used as a control. Nearly all uninjected embryos showed the normal *sema3a* expression pattern (A, B). In more than 90 % of the embryos co-injected with a Co MO and hCHD7 RNA the *sema3a* expression pattern remained unchanged (C, D). After downregulation of Chd7 by injecting 10 ng Chd7 MO, more than 50 % of the embryos showed severe defects, meaning a clear reduced *sema3a* expression pattern and/or missing *sema3a* expression in either somites or head region (E, F).

Results

In more than 30 % of these embryos moderate reduction of *sema3a* was detected and in about 10 % of the embryos the *sema3a* expression pattern remained unaltered. More than half of the embryos co-injected with 10 ng Chd7 MO to knockdown Chd7 and 1 ng h*CHD7* RNA to rescue the Chd7 MO phenotype showed a normal *sema3a* expression pattern (**G**, **H**) and about 40 % had a moderate reduced *sema3a* expression pattern. (**I**) Graph summarises the percentage of embryos obtained from one biological replicate with normal *sema3a* expression (light grey columns), moderate (grey columns) or severe changes in the expression pattern (black columns). Numbers on top of each column represent the amount of embryos counted in the different categories. Figure modified after Schulz et al. (2014b).

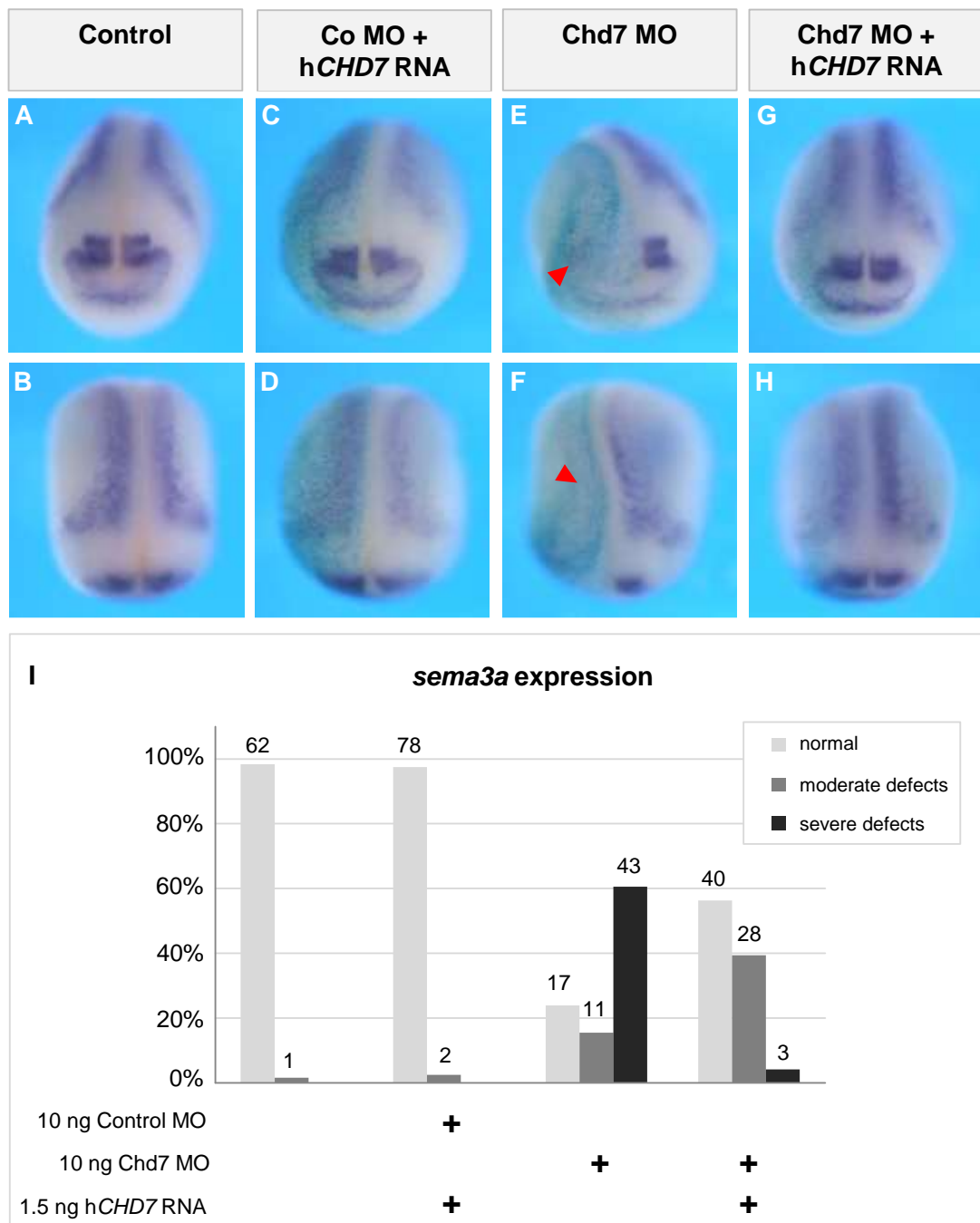


Figure 19: Repetition of the rescue of the Chd7 MO phenotype in *Xenopus laevis* (neurula stage 20).

Single blastomeres of two-cell stages were injected with either 10 ng of a control MO and 1.5 ng human rescue *CHD7* RNA (h*CHD7* RNA) (C, D), 10 ng Chd7 MO (E, F) or 10 ng Chd7 MO and 1.5 ng h*CHD7* RNA (G, H). Co-injection of *lacZ* RNA served as a lineage tracer. *Sema3a* expression was analysed by whole mount *in situ* hybridisation (purple staining). Nearly all uninjected control embryos showed a normal *sema3a* expression pattern (A, B). In more than 95 % of the embryos co-injected with a Co MO and h*CHD7* RNA the *sema3a* expression pattern remained unchanged (C, D). After injection of 10 ng Chd7 MO, more than 60 % of the embryos showed severe changes in the *sema3a* expression pattern (E, F). After co-injection of 10 ng Chd7 MO to knockdown Chd7 and 1.5 ng h*CHD7* RNA to rescue the Chd7 MO phenotype, in about 60 % of the embryos a normal *sema3a* expression pattern was observed (G, H) and 40 % showed moderate changes in the *sema3a* expression pattern. (I) The graph summarises the data obtained from one biological replicate. Columns represent the percentage of embryos with normal *sema3a* expression (light grey), moderate (grey) or severe reduction of the expression pattern (black). Numbers on top of each column indicate the amount of embryos counted in the different categories. Figure modified after Schulz et al. (2014b).

3.11 Knockdown of Sema3a and Sema3d causes migration defects of NCCs in *Xenopus laevis*

It was shown in *Xenopus laevis* embryos that a MO mediated downregulation of Chd7 leads to migration defects of NCCs (Bajpai et al., 2010). Semaphorins are involved in the process of NCC guidance (Kuriyama and Mayor, 2008). Because *Sema3a* and *Sema3d* were found to be downregulated in *CHD7* deficient mice (Schulz et al., 2014b), these genes were chosen for knockdown experiments in *Xenopus laevis* to analyse the effect on NCC migration. Embryos were injected in one blastomere of a two-cell stage. The expression of the NCC marker *twist* was analysed by WMISH at the neurula stage 21 in three independent experiments (Fig. 20) and the tailbud stage 26 in two independent experiments (Fig. 21). Control embryos injected with 20 ng Co MO showed as expected a normal *twist* expression of the three cranial-crest segments: mandibular (m), hyoid (h) and branchial (b) (Fig. 20A; Fig. 21A, B). By injecting 20 ng Chd7 MO to knockdown Chd7 almost 80 % of the analysed embryos of the neurula and tailbud stage showed severe migration and induction defects of NCCs highlighted by red arrowheads (Fig. 20B; Fig. 21C, D). About half of the embryos at the neurula stage revealed moderate migrating defects of NCCs (yellow arrowheads) after *Sema3a* (Fig. 20C) and *Sema3d* (Fig. 20D) downregulation. Furthermore, in about 5 % of the analysed

embryos severe migration defects were detected after a Sema3a knockdown. If Sema3d is downregulated, 10 % of the embryos revealed severe defects of migrating NCCs. About 20 % of the embryos at the tailbud stage showed moderate migration defects after Sema3a was downregulated (Fig. 21E, F) and in almost 40 % of the embryos moderate defects of migrating NCCs were observed after downregulation of Sema3d indicated by yellow arrowheads (Fig. 21G, H). A rescue of the Chd7 MO phenotype (*twist* expression) was successfully performed using the same human *CHD7* RNA as a rescue construct as described before on page 109 (results not shown). This data confirms the results of the rescue experiment with *Xenopus laevis* embryos performed by Bajpai et al. (2010). In conclusion, a loss of function of Chd7 severely affects the NCC induction and migration in the majority of analysed embryos while a loss of function of either Sema3a or Sema3d led in about half of the embryos to moderate NCC migration defects.

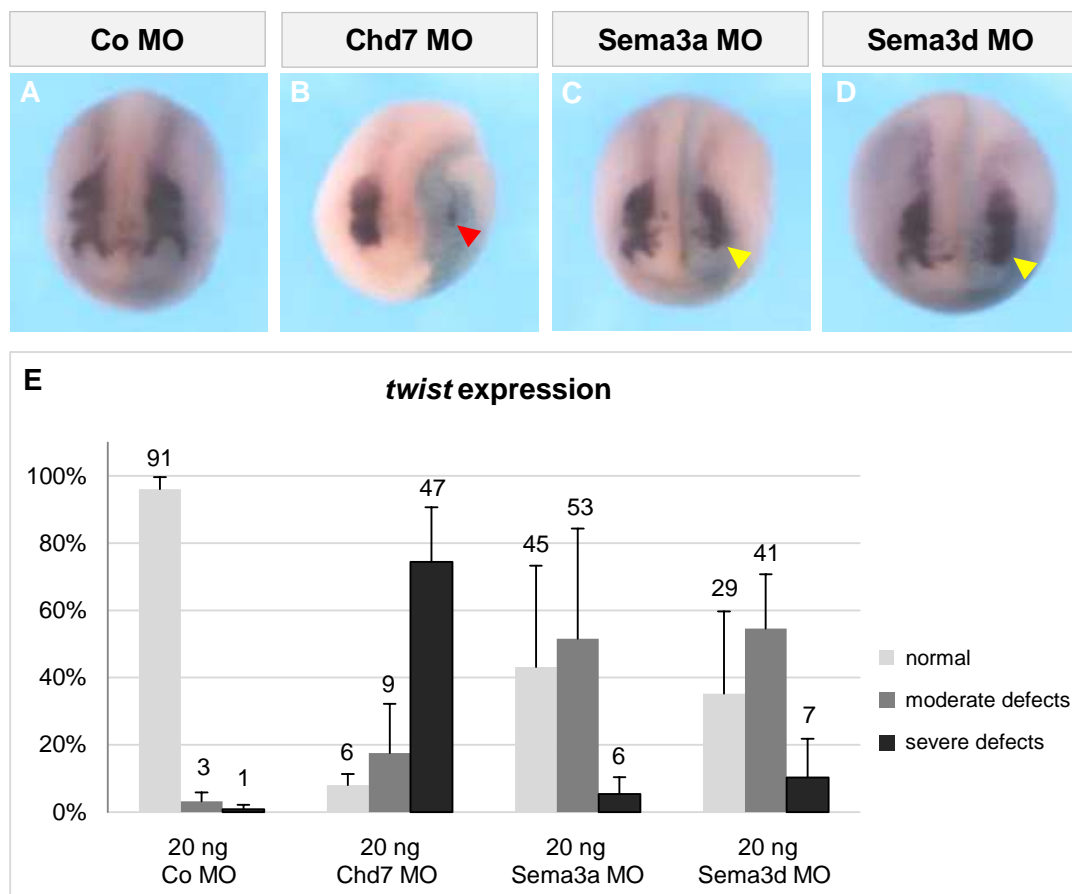


Figure 20: *Twist* expression analysis after knockdown of Chd7, Sema3a or Sema3d in *Xenopus laevis* (neurula stage 21).

Embryos were injected with 20 ng Co MO (A), 20 ng Chd7 MO (B), 20 ng Sema3a MO (C) or 20 ng Sema3d MO (D) in one blastomere of a two-cell stage. *LacZ* RNA was co-injected as a lineage tracer.

Results

At the neurula stage 21 a whole mount *in situ* hybridisation was performed to analyse the expression of the NCC marker *twist* (purple staining). The injected side is indicated by the blue *lacZ* staining (**B**, **D**, **F**, **H**). More than 90 % of the embryos injected with 20 ng Co MO revealed a normal *twist* expression (**A**). After injecting 20 ng Chd7 MO more than 70 % showed severe defects in form of extreme migration or induction defects of NCCs (red arrowhead) (**B**). A knockdown of Sema3a and Sema3d led in about 50 % of the embryos to moderate migration defects of NCCs (yellow arrowheads) (**C**, **D**). The diagram represents the percentage of embryos after injection of MO showing normal *twist* expression indicating normal NCC migration (light grey), moderate (grey) or severe migration defects (black) of NCCs (**E**). (**I**) The data include three independent experiments. Standard error of the means is given. Total numbers of animals dedicated to each category are shown on top of each column.

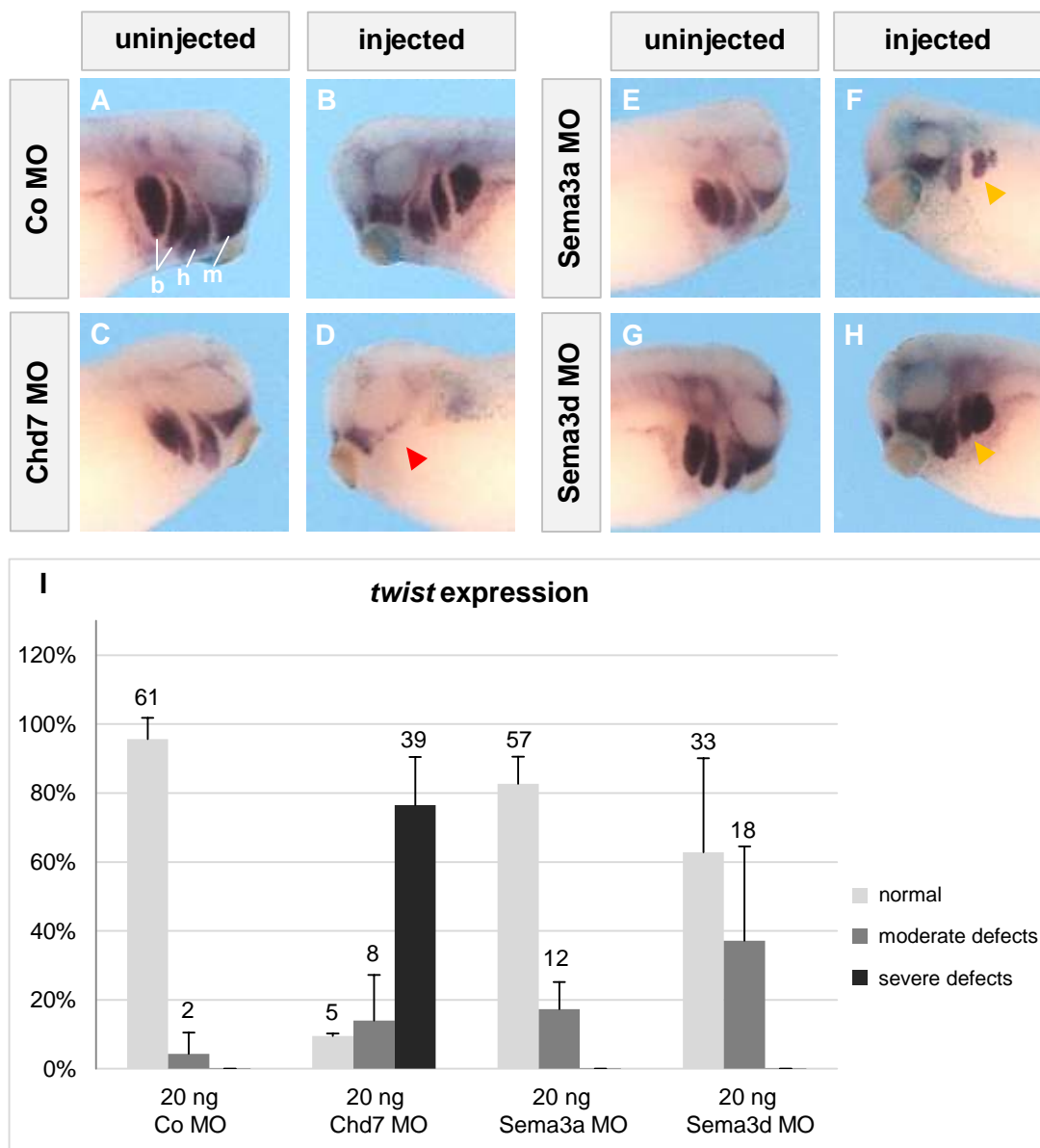


Figure 21: Effect of Chd7, Sema3a or Sema3d knockdown on NCCs (*twist* expression) in *Xenopus laevis* (tailbud stage 26).

One blastomere of a two-cell stage was injected with a MO in combination with *lacZ* RNA. The injected side of the embryo is recognisable by the blue *lacZ* staining (**B**, **D**, **F**, **H**). Control embryos were injected with 20 ng of Co MO (**A**, **B**). For the knockdown 20 ng Chd7 MO (**C**, **D**), 20 ng Sema3a MO (**E**, **F**) or 20 ng Sema3d MO were injected (**G**, **H**). At the tailbud stage 26 a whole mount *in situ* hybridisation was performed to analyse the expression pattern of the NCC marker *twist*. Most embryos (> 90 %) injected with 20 ng Co MO showed a normal *twist* expression pattern of the three cranial-crest segments: mandibular (m), hyoid (h) and branchial (b) (**A**, **B**). After injecting 20 ng Chd7 MO to knockdown Chd7, in almost 80 % of the analysed embryos severe defects were observed like massive migration and induction defects (red arrowhead) of NCCs (**D**). About 20 % of the embryos injected with 20 ng Sema3a MO (**F**) and 40 % of those injected with 20 ng Sema3d MO (**H**) showed moderate migration defects of NCCs (yellow arrowhead). In the diagram the results of two independent experiments are shown (**I**). The columns represent the percentage of embryos showing a normal NCC migration indicated by a normal *twist* expression (light grey), moderate migration defects (grey) or severe migration or induction defects of NCCs (black). The total number of embryos obtained in each category is shown on top of the columns. Standard error of the means is given.

3.12 Double knockdown of Chd7 and Sema3a or Sema3d has no clear synergistic effect on *twist* expression in *Xenopus laevis*

To determine whether the Chd7 MO phenotype on *twist* expression can be increased, double knockdown experiments on *Xenopus laevis* embryos were performed. Chd7 was downregulated in combination with either Sema3a or Sema3d. Embryos were injected in one blastomere of a two-cell stage. *Twist* expression was analysed by WMISH at the neurula stage 20 (Fig. 22A) and the tailbud stage 27 (Fig. 22B), respectively. Uninjected embryos as well as embryos injected with 10 ng Co MO served as controls showing a normal *twist* expression. Chd7 alone was downregulated by injecting 10 ng Chd7 MO. 35 % of the embryos at the neurula stage revealed moderate migration defects and further 35 % showed severe migration defects of NCCs (Fig. 22A). At the tailbud stage about 60 % of the analysed embryos revealed severe alteration in *twist* expression after Chd7 was downregulated (10 ng Chd7 MO) (Fig. 22B). Embryos co-injected with 5 ng Chd7 MO and 5 ng Co MO were used as a reference control. Compared to the reference control, embryos (neurula stage) co-injected with 5 ng Chd7 MO and 5 ng Sema3a MO showed a slightly increase in moderate migration defects in NCCs. While no severe migration defects were detected in the reference control, 4 % of the embryos revealed severe migration defects after the Chd7/Sema3a knockdown (Fig. 22A). In 28 % of the

reference control embryos (tailbud stage) moderate defects in migrating NCCs were observed, while 48 % were detected after a double knockdown of Chd7 and Sema3a (Fig. 22B). The combination of 5 ng Chd7 MO and 5 ng Sema3d MO led in 75 % of the embryos of the neurula stage to moderate migration defects while in the reference control only 63 % of the embryos were detected with moderate migration defects of NCCs (Fig. 22A). In tailbud stage embryos the percentage of embryos showing moderate defects of migrating NCCs was increased (39 %) compared to the reference control (28 %). Furthermore, 5 % showed severe migration and induction defects whereby none of the reference control embryos were detected with this phenotype (Fig. 22B).

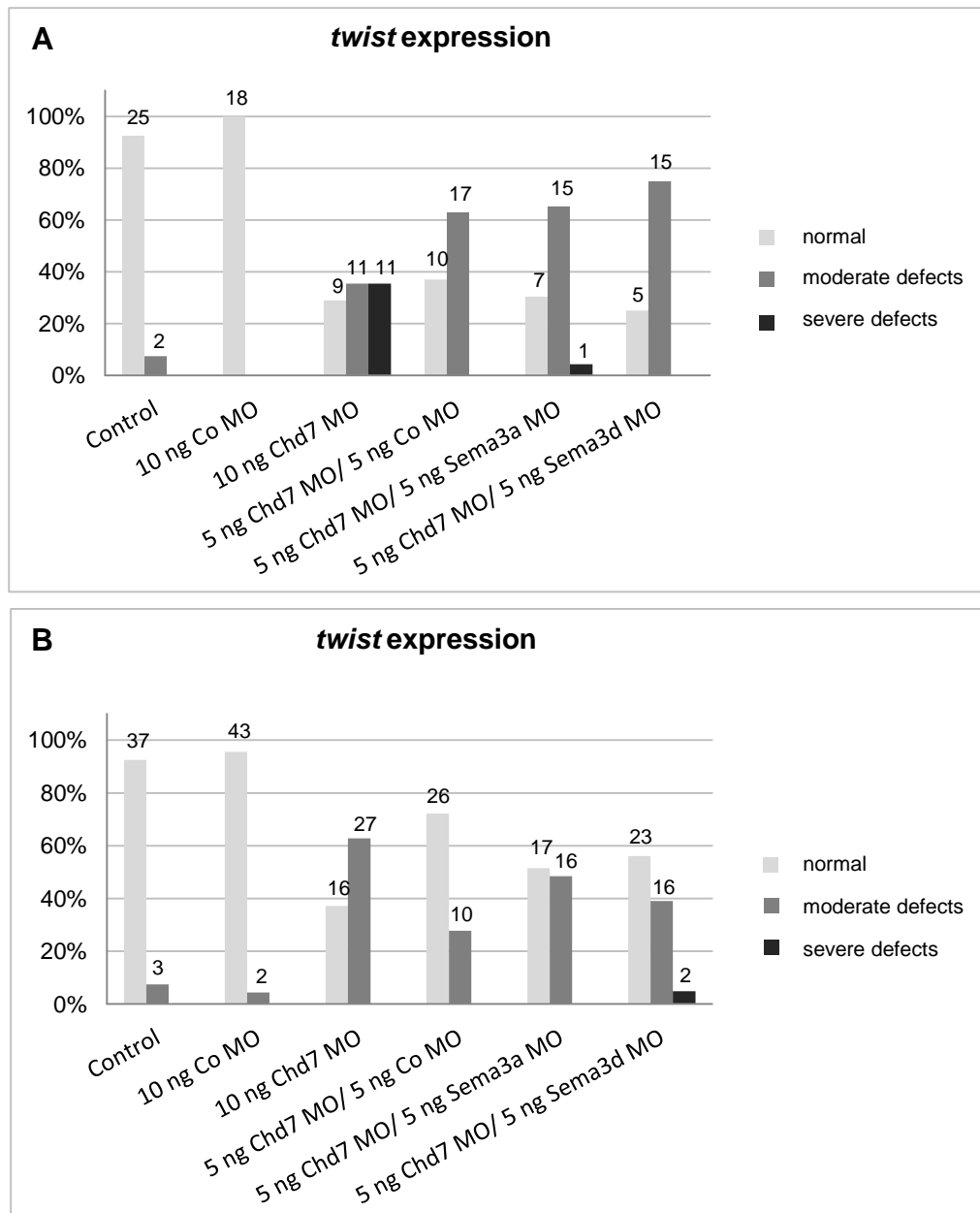


Figure 22: Effect on *twist* expression after Chd7 knockdown, Chd7/Sema3a and Chd7/Sema3d double knockdown in *Xenopus laevis*.

Embryos from one batch were either not injected or injected with 10 ng of Co MO, 10 ng Chd7 MO or co-injected with 5 ng Co MO and 5 ng Chd7 MO, 5 ng Chd7 MO and 5 ng Sema3a MO or 5 ng Chd7 MO and 5 ng Sema3d MO. At neurula stage 20 a whole mount *in situ* hybridisation was performed to analyse the expression of the NCC marker *twist* (A). The diagram summarises the results of one experiment. The columns represent the percentage of the embryos showing a normal expression of *twist* (normal NCC migration) (light grey), moderate migration defects (grey) or severe migration and induction defects of NCCs (black). Numbers on top of each column indicate the number of embryos found in the different categories. Nearly all control embryos (uninjected and injected with 10 ng Co MO) showed a normal *twist* expression. After injecting 10 ng Chd7 MO, 35 % of the embryos showed severe migration and induction defects of NCCs and 35 % had moderate migration defects. In about 60 % of embryos co-injected with 5 ng Co MO and 5 ng Chd7 MO moderate migration defects of

NCCs were observed but no severe defects. After co-injection of 5 ng Chd7 MO and 5 ng Sema3a MO, more than 60 % of the embryos showed moderate migration defects. In 4 % severe migration defects were detected. A co-injection of 5 ng Chd7 MO and 5 ng Sema3d MO led in almost 80 % of the embryos to moderate migration defects of NCCs. Another whole mount *in situ* hybridisation (one biological replicate) was performed at the tailbud stage 27 (**B**). More than 95 % of the uninjected embryos and embryos injected with 10 ng Co MO showed a normal *twist* expression pattern. After an injection of 5 ng Co MO and 5 ng Chd7 MO, about 30 % of the embryos had moderate migration defects. An injection of 10 ng Chd7 MO led in approximately 60 % of the embryos to moderate migration defects of NCCs. Half of the embryos showed moderate defects in migrating NCCs if 5 ng Chd7 MO and 5 ng Sema3a MO were injected. After co-injection of 5 ng Chd7 MO and 5 ng Sema3d MO, about 40 % of the embryos revealed moderate migration defects and 5 % showed severe migration defects of NCCs.

To analyse whether the increase of defects seen of NCC migration and induction after the double knockdown (Chd7 and Sema3a or Sema3d) can be intensified, the MO concentration were doubled to 10 ng. The expression pattern of *twist* was analysed in four independent experiments in neurula stages 20/21 (Fig. 23) and the tailbud stages 27, respectively (Fig. 23B). About 80 % of the embryos showed severe migration and induction defects of NCCs after a downregulation of Chd7 by injecting 20 ng Chd7 MO. Embryos, co-injected with 10 ng Chd7 MO and 10 ng Co MO were used as a reference control. In comparison of embryos of the reference control to embryos injected with either 10 ng Sema3a MO or Sema3d MO instead of the Co MO, the percentage of embryos showing defects of NCC migration was increased.

After a Chd7/Sema3a double knockdown, more embryos (neurula stage) revealed severe migration and induction defects (68 %) as the reference control (56 %). The percentage of embryos with moderate defects of NCC migration was also increased (23 %) in comparison to the reference control (12 %). No changes in the percentage of embryos with defects of NCC migration were observed in tailbud stages.

Comparing the embryos after a double knockdown of Chd7/Sema3d to the reference control, it was observed that the percentage of embryos showing severe migration and induction defects was increased from 56 % to 73 %. The percentage of embryos with moderate migration defects were slightly increased as well. In the tailbud stages a higher percentage of severe migration and induction defects was detected after Chd7/Sema3d double knockdown (62 %) compared to the reference control (48 %).

Furthermore, it was observed in the neurula and tailbud stages that a double knockdown mediated by an injection of 10 ng Chd7 MO + 10 ng Sema3a MO or Sema3d MO did not reach the percentage of embryos showing defects in the migration of NCCs detected after single knockdown of Chd7 by injecting 20 ng Chd7 MO. Although, a higher percentage of embryos showed defects of NCC migration and induction after downregulation of Chd7 in combination with Sema3a or Sema3d the effect is too less to conclude a clear synergistic effect. All experiments with the model organism *Xenopus laevis* were performed within the collaboration with Prof. Dr. Annette Borchers and Dr. Peter Wehner in the Department of Developmental Biochemistry, Goettingen. Handling of *Xenopus laevis*, including fertilisation, injecting embryos and caring until embryos reached the desired developmental stage has been undertaken by Dr. Peter Wehner.

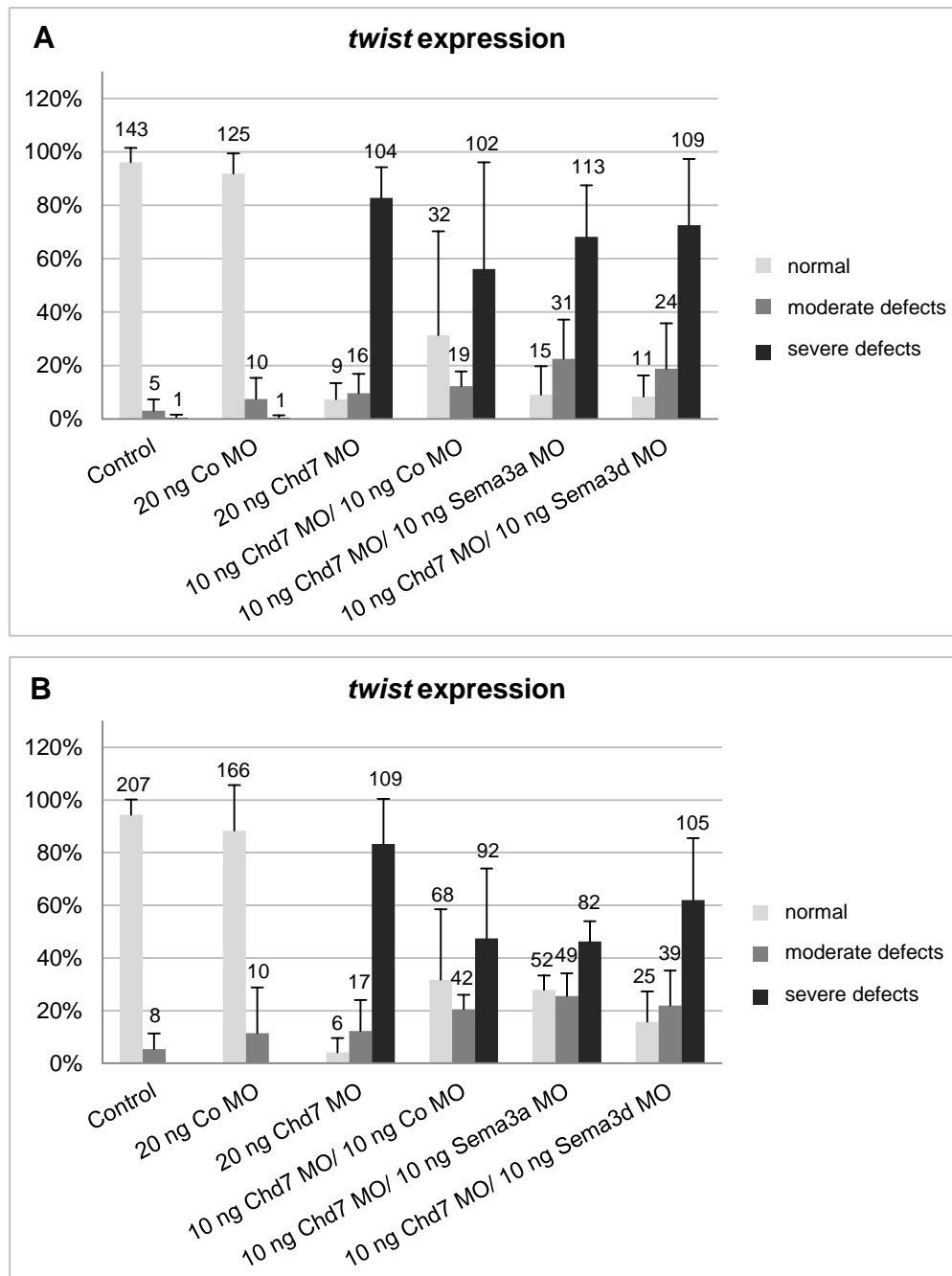


Figure 23: Effect on the NCC marker *twist* after Chd7 knockdown, Chd7/Sema3a and Chd7/Sema3d double knockdown in *Xenopus laevis*.

The graphs summarise four independent experiments where knockdowns were performed and the expression pattern of *twist* was analysed at the neurula stage 20/21 (A) and the tailbud stage 27 (B). The columns represent the percentage of the embryos showing a normal expression of *twist* indicating normal NCC migration (light grey), moderate migration defects (grey) or severe migration and induction defects of NCCs (black). Numbers on top of each column indicate the number of embryos obtained in the different categories. Standard error of the means is shown. At a two-cell stage embryos were injected in one blastomere with 20 ng Co MO, 10 ng Co MO and 10 ng Chd7 MO, 20 ng Chd7 MO, 10 ng Chd7 MO and 10 ng Sema3a MO or 10 ng Chd7 MO and 10 ng Sema3d MO. The *twist* expression pattern remained unchanged in more than 90 % of the uninjected embryos and after

injection of 20 ng Co MO. An injection of 10 ng Co MO and 10 ng Chd7 MO led in more than 50 % of the embryos to severe defects of migrating NCCs. In more than 80 % of the embryos injected with 20 ng Chd7 MO severe migration and induction defects were observed. After double knockdown of Chd7 and Sema3a, about 70 % of the embryos showed severe migration and induction defects of NCCs and more than 20 % were observed with moderate migration defects. An injection of 10 ng Chd7 MO and 10 ng Sema3d MO led in more than 70 % of the embryos to severe migration and induction defects and about 20 % showed moderate defects of migrating NCCs. The whole mount *in situ* hybridisation performed at the tailbud stage revealed for the majority of uninjected and the injected embryos with 20 ng Co MO a normal expression pattern of *twist*. More than 40 % of embryos co-injected with 10 ng Co MO and 10 ng Chd7 MO showed severe defects of migrating NCCs and about 20 % were detected with moderate migration defects. After downregulation of Chd7 by injecting 20 ng Chd7 MO, more than 80 % of the analysed embryos showed severe migration and induction defects of NCCs. More than 40 % of the embryos were detected with severe migration and induction defects after a double knockdown of Chd7 and Sema3a by injecting 10 ng of each MO and more than 20 % showed moderate migration defects. A co-injection of 10 ng Chd7 MO and 10 ng Sema3d MO led in about 60 % of the embryos to severe migration and induction defects and more than 20 % revealed moderate defects of migrating NCCs.

4 Discussion

4.1 Short summary

It was shown in two independent experiments performed with HeLa cells that CHD7 interacts with WDR5, ASH2L and RBBP5 (WAR complex). By Co-IP experiments the interaction of CHD7 with members of the WAR complex was shown in two ways: by precipitation of endogenous CHD7 and detection of overexpressed ASH2L and RBBP5 (Fig. 5A) as well as by precipitation of endogenous WDR5 and overexpressed ASH2L and RBBP5 and detection of endogenous CHD7, respectively (Fig. 5C) (Schulz et al., 2014a). With the Duolink PLA method these interactions were confirmed and at the same time the localisation of the interactions was found to be in the nuclei of HeLa cells (Fig. 7) (Schulz et al., 2014a). Furthermore, Y2H experiments revealed no direct interaction of the analysed CHD7 fragment (amino acids 1591-2181) with full-length constructs of WDR5, ASH2L and RBBP5 (Fig. 8) (Schulz et al., 2014a).

The genome-wide microarray analysis performed with embryos of the *Whirligig* mouse line which carry a nonsense mutation in the *Chd7* gene, revealed 98 genes showing a differential expression (compare appendix, Tab. 39) (Schulz et al., 2014b). Interestingly, a lot of these genes are involved in the process of axon and NCC guidance, such as members of the semaphorin family SEMA3A, SEMA3C and SEMA3D (Fig. 10) (Schulz et al., 2014b).

Knockdown experiments of *Chd7* carried out with embryos of the African clawed frog *Xenopus laevis* resulted in severe reduction or complete absence of *sema3a* expression (Fig. 16; Fig. 17) (Schulz et al., 2014b). Furthermore, the negative effect of a *Chd7* downregulation on NCCs formation (*twist* expression) observed by Bajpai et al. (2010) was confirmed. After *Chd7* downregulation, severe migration and induction defects of NCCs were determined (Fig. 20; Fig. 21). Downregulation of either *Sema3a* or *Sema3d* in *Xenopus laevis* embryos resulted in moderate migration defects (Fig. 20; Fig. 21). A double knockdown of *Chd7* in combination with either *Sema3a* or *Sema3d* led to a higher number of *Xenopus laevis* embryos with more severe defects of migrating NCCs (Fig. 22; Fig. 23).

4.2 CHARGE syndrome shows phenotypical overlap with other syndromes

CHARGE syndrome is a highly heterogeneous disorder and shows a phenotypical overlap with other syndromes (Sanlaville and Verloes, 2007; Jongmans et al., 2009; Bergman et al., 2011). An example is the Kabuki syndrome (OMIM 147920) which is a rare developmental disorder characterised by a typical facial gestalt, short stature, skeletal abnormalities, cardiac malformations, immunological defects and intellectual disabilities (Ng et al., 2010; Li et al., 2011; Bogershausen and Wollnik, 2013). Heterozygous mutations in the *KMT2D* (*MLL2*) gene are described as the major genetic cause of Kabuki syndrome (Ng et al., 2010). *KMT2D* is a methyltransferase responsible for histone 3 lysine 4 (H3K4) di- and trimethylation (Song JJ, 2008).

Our working group described a patient who was initially diagnosed as having CHARGE syndrome because he fulfilled the diagnostic criteria for CHARGE provided by Pagon et al. (1981) (five of six features) and Blake et al. (1998) (three of four major and three of seven minor signs). According to the CHARGE syndrome criteria from Verloes (2005), the patient fulfilled the criteria for having an atypical CHARGE syndrome (one of three major and three of five minor signs). To confirm the clinical diagnosis, a *CHD7* mutation analysis was performed but no mutation was found. Further clinical examinations of the patient revealed emerging facial features, such as long palpebral fissures, long dense eyelashes and arched eye-brows, leading to the clinical diagnosis of Kabuki syndrome. A *KMT2D* mutation analysis revealed in exon 22 a heterozygous nonsense mutation confirming the clinical diagnosis of Kabuki syndrome (Schulz et al., 2014a).

4.3 CHD7 is associated with the WAR complex

KMT2D, the gene mutated in patients with Kabuki syndrome, belongs to the SET1 family of enzymes which are commonly associated with multi-subunit complexes to be able to activate the methyltransferase (Miller et al., 2001; Yokoyama et al., 2004; Wysocka et al., 2005; Steward et al., 2006; Ernst and Vakoc, 2012). In *Drosophila* the homologous gene of *KMT2D* is *trx* (*trithorax*) of the trithorax group which maintains the homeotic gene expression (Ringrose and Paro, 2004). The counterpart

of trithorax group proteins are polycomb group proteins which are most commonly linked to the repression of homeotic genes (Ringrose and Paro, 2004).

One of the “core” complexes of KMT2D consists of WDR5, ASH2L and RBBP5 (WAR complex) (Steward et al., 2006; Song JJ, 2008; Yates et al., 2010). The ATP-dependent chromatin remodelling enzyme CHD8 interacts with the components of the WAR complex in the absence of MLL (Steward et al., 2006; Thompson et al., 2008; Thompson BA, 2008; Yates et al., 2010). Yates et al. (2010) suggested a role of CHD8 in the regulation of gene transcription at the *HOXA* locus. They demonstrated a negative regulation of *HOXA2* gene expression by CHD8 (Yates et al., 2010). Furthermore, it was shown by our working group that CHD7 interacts directly and indirectly with CHD8 (Batsukh et al., 2010), both proteins belong to the same subgroup of the CHD family (Flaus et al., 2006).

Co-IP experiments performed with HeLa cells demonstrated an interaction of CHD7 with WDR5, ASH2L and RBBP5 (Fig. 5) (Schulz et al., 2014a). Luisa Freese (PhD student of our group) completed successfully the Co-IP experiment using the pCMV-HA-WDR5 construct, which was generated during writing my thesis. Full-length WDR5 was overexpressed in HeLa cells, endogenous CHD7 was precipitated and the overexpressed WDR5 was detected using an HA antibody (data not shown).

The interaction between CHD7 and members of the WAR complex was confirmed by the Duolink PLA method (Fig. 7) (Schulz et al., 2014a). Further, it was demonstrated that the interaction takes place in the nuclei of HeLa cells (Fig. 7) (Schulz et al., 2014a) where eukaryotic gene transcription takes place (Georgiev, 1972). Factors involved in the regulation of gene transcription such as the MLL2-WAR methyltransferase complex are localised in the nucleus (MIPS et al., 2008) as well as the CHD family members of ATP-dependent chromatin remodelling enzymes CHD7 and CHD8 (Marfella and Imbalzano, 2007). In fact, it was shown by ICC that CHD7, CHD8 and the members of the WAR complex are specifically expressed in the nuclei of HeLa cells (Fig. 6).

Direct Y2H experiments revealed no direct interaction for CHD7 and the WAR complex members (Fig. 8) (Schulz et al., 2014a). It is possible that the interaction region is located outside of the analysed CHD7 fragment (amino acids 1,591-2,181). Therefore, four overlapping fragments were generated spanning the whole CHD7 protein without interrupting any known functional domains (Fig. 9) (Schulz et al., 2014a). During writing this thesis, PhD student Luisa Freese performed direct Y2H

experiments with the four CHD7 fragments. CHD7-1pGBKT7 showed an auto activation of the yeast strain reporter genes and the other three CHD7 fragments revealed no direct interaction with the WAR complex members (Schulz et al., 2014a).

As shown by Yates et al. (2010) CHD8 interacts directly with WDR5, ASH2L and RBBP5. The direct Y2H experiments confirmed these interactions and narrowed down the responsible interaction side of CHD8 to the amino acids 1,789-2,302 (Fig. 8) (Schulz et al., 2014a). Furthermore, the recently shown direct interaction of the CHD7 fragment and the CHD8 fragment was observed (Fig. 8) (Batsukh et al., 2010; Schulz et al., 2014a). These data indicate that CHD7 is associated to the WAR complex most likely via the direct interaction with CHD8 (Schulz et al., 2014a). The association of CHD7 and KMT2D with the WAR complex connects these two genes to the same process of remodelling and modifying chromatin (Schulz et al., 2014a). Probably, CHD7 and KMT2D regulate the transcription of a subset of common genes (Schulz et al., 2014a). Therefore, it is likely that a mutation in either *CHD7* or *KMT2D* causes misregulation of common target genes, which could explain the phenotypic overlap of CHARGE syndrome and Kabuki syndrome (Schulz et al., 2014a).

4.4 CHD7 regulates genes required for proper NCC development

CHD7 is included within different complexes regulating time and tissue specific gene expression (Layman et al., 2010). Already in 1985, several years before mutations in *CHD7* were discovered to cause CHARGE syndrome, Siebert et al. (1985) postulated that a disturbance in NCC development is the pathogenic mechanism behind CHARGE syndrome. Recent studies demonstrated the involvement of Chd7 in NCC development (Bajpai et al., 2010). Bajpai et al. (2010) showed that Chd7 activates components, such as Slug, Sox9 and Twist which are critical for the formation of migratory NCCs. Furthermore, Bajpai et al. (2010) found that Chd7 binds to the PBAF complex and assumed that Chd7 cooperates with the PBAF complex to regulate gene expression during NCC formation in *Xenopus laevis*. In the mouse CHD7 is required in the pharyngeal ectoderm for normal pharyngeal arch artery development and it is likely that NCCs are the targets of

CHD7 based on alterations in NCC migration observed in *Chd7* heterozygous mouse embryos (Randall et al., 2009).

To analyse which genes are regulated by CHD7, a genome-wide microarray analysis was performed with embryos of the *Whirligig* mouse line (*Chd7*^{+/+}, *Chd7*^{Whi/+}, *Chd7*^{Whi/Whi}) at E9.5, a developmental stage during NCC migration (Schulz et al., 2014b). By using whole mouse embryos one important advantage is to identify genes involved in NCC development in different tissues although possible cancellation effects cannot be excluded (Schulz et al., 2014b). Differences in gene expression between females and males are present in several species, affecting not only sex chromosome linked genes, but also autosomal genes (Vawter et al., 2004; Yang et al., 2006; Zhang et al., 2009). To avoid gender specific effects on gene expression, the genome-wide microarray analysis was performed only with female mouse embryos. To confirm the data of the genome-wide microarray analysis by RT-qPCR, six genes were chosen which were identified to be differentially effected by CHD7. The expression of *Sema3a*, *Sema3d* and *Epha3* was found to be downregulated while the expression of *Sox10* and *Gfra2* was increased and the *Trp53bp2* expression was unaffected (appendix, Tab. 39) (Schulz et al., 2014b). The RNA of female mouse embryos which was also used for the microarray analysis was used for RT-qPCR. A similar expression of the selected genes was observed confirming the microarray data (Fig. 11) (Schulz et al., 2014b). Additionally, these genes were analysed by another RT-qPCR performed on male embryos. A gender specific affect for the analysed genes *Sema3a*, *Sema3d*, *Epha3*, *Sox10*, *Gfra2* and *Trp53bp2* was excluded (Fig. 12) (Schulz et al., 2014b). Since embryos from different breedings were obtained and used for the RT-qPCR experiments, slight differences in the developmental stage might occur, explaining the differences in expression of the same gene between the biological replicates.

The microarray data revealed 98 differentially expressed genes (appendix, Tab. 39); many of them are involved in NCC migration and NCC and axons guidance as well as in interaction between NCCs and other tissues (Schulz et al., 2014b). For instance, several cadherins were identified which play a role in cell adhesion (Takeichi, 1995). Changes in cell adhesion are important during EMT which enables NCC migration (Kuriyama and Mayor, 2008). Transcription factors such as *Sox10* and *Foxd3* were found to be differentially expressed (Schulz et al., 2014b). They are involved in early migration processes of NCCs (Kirby and Hutson, 2010). Furthermore, *Sox10* seems

to be important for the specification of NCCs (Gammill and Bronner-Fraser, 2003). In addition, secreted signalling molecules such as semaphorins, ephrins and slits were identified which act through protein kinase receptors to guide migrating NCCs (Perris, 1997; Gammill and Bronner-Fraser, 2003; Yazdani and Terman, 2006; Kuriyama and Mayor, 2008; Kirby and Hutson, 2010). Guidance molecules such as semaphorins and slits are expressed, for instance, in the surrounding epithelium of NCC localisation, guiding NCCs along specific pathways to their destination (Yazdani and Terman, 2006; Kuriyama and Mayor, 2008). Randall et al. (2009) observed that a rescue of CHD7 in murine NCCs alone did not rescue the phenotype of pharyngeal arch artery defects in CHD7 deficient mice whereas a rescue of CHD7 in NCCs and the pharyngeal ectoderm led to full rescue of pharyngeal arch artery alterations. Randall et al. (2009) assumed ephrins, Pdgfs (platelet-derived growth factors), semaphorins, slits and Vegfs (vascular endothelial growth factors) as downstream candidate genes of CHD7 involved in ectoderm-NCC interaction. The data from the microarray analysis (compare 3.4) revealed among others members of all signalling families postulated by Randall et al. (2009): *Epha3*, *Epha5*, *Epha7* (ephrins), *Pdgfc* (Pdgfs), *Sema3a*, *Sema3c*, *Sema3d* (semaphorins), *Slitrk6*, *Slitrk1* (slits) and *Vegfc* (Vegfs). It is likely that CHD7 regulates genes which expression is important in NCCs and the surrounding tissue to ensure proper NCC development (specification, migration and differentiation). Furthermore, the data of the microarray analysis indicate that disturbance of NCC development plays a role in the pathogenesis of CHARGE syndrome. It seems that additional pathogenic mechanisms exist behind CHARGE syndrome. Possibly, till now untested theories, are a disruption of the interaction of mesoderm and NCCs (Van Meter and Weaver, 1996) or the disturbance of mesenchymal-epithelial interaction (Williams, 2005).

4.5 Chd7 regulates *sema3a* expression and NCC induction and migration in *Xenopus laevis*

Chd7 is highly conserved across different species, for instance, human, mouse, zebrafish and *Xenopus laevis* (Bosman et al., 2005; Bajpai et al., 2010). Disruption of *Chd7* function in *Xenopus laevis* exposed defects comparable to symptoms seen in CHARGE syndrome (Bajpai et al., 2010). A downregulation of *Chd7* in *Xenopus laevis* embryos has an influence on the expression of the NCC marker *twist*

demonstrating alteration in NCC migration (Bajpai et al., 2010). Disruption of CHD7 function in mouse was found to result in a decreased expression of members of the semaphorin family, such as *Sema3a* and *Sema3d* (Schulz et al., 2014b).

To analyse whether there is a conserved regulatory mechanism across species, knockdown experiments on *Xenopus laevis* embryos were performed injecting MO in one blastomere of a two-cell stage. Analysis of *sema3a* expression after downregulation of Chd7 caused either decreased or complete depletion of *sema3a* expression (Fig. 16; Fig. 17) (Schulz et al., 2014b), exposing a conserved mechanism between mouse and *Xenopus laevis*.

4.6 SEMA3A and SEMA3D seem to play a role in the pathogenesis of CHARGE syndrome

To test whether disruption of Sema3a or Sema3d phenocopies the NCC defects observed after Chd7 loss of function, knockdown experiments of Chd7, Sema3a and Sema3d were performed with *Xenopus laevis* embryos and the expression pattern of the NCC marker *twist* was analysed by WMISH. While a Chd7 loss of function caused severe migration and induction defects of NCCs, knockdown of Sema3a or Sema3d revealed moderate migration defects of NCCs (Fig. 20; Fig. 21). The severe NCC alterations observed in *Xenopus laevis* after Chd7 downregulation are likely caused by the regulatory effect of Chd7 on several genes involved in NCC formation and migration (Schulz et al., 2014b). Nevertheless, the semaphorins Sema3a and Sema3d partially phenocopy the NCC defects observed during the Chd7 loss of function indicating a possible participation of these semaphorins in the pathogenesis of CHARGE syndrome.

Double knockdown of Chd7 and Sema3a or Sema3d was performed to analyse whether there is a synergistic effect. The percentage of embryos showing severe migration defects of NCCs was clearly increased but insufficient to determine a synergistic effect. In the mouse a significant decreased expression of different semaphorins were shown (appendix, Tab. 39) and in *Xenopus laevis* a Chd7 loss of function caused also a reduced *sema3a* expression (Fig. 16; Fig. 17) (Schulz et al., 2014b). A clear synergistic effect after the double knockdown of Chd7 and Sema3a or Chd7 and Sema3d was not observed (Fig. 22; Fig. 23). A possible explanation could be that the Chd7 knockdown itself has such a strong negative effect on the

expression of *sema3a* and *sema3d* that an additional knockdown of either *Sema3a* or *Sema3d* cannot cause a synergistic effect.

The *CHD7* expression pattern studied in different species (human, mouse, chick and others) correlates with the malformations observed in CHARGE syndrome (Bosman et al., 2005; Sanlaville et al., 2006; Aramaki et al., 2007; Hurd et al., 2007; Layman et al., 2009; Bergman et al., 2010; Kosaki, 2011; Janssen et al., 2012). *CHD7* is expressed, for instance, in the brain, heart, inner ear, olfactory epithelium and ganglia (Bosman et al., 2005; Lalani et al., 2006; Sanlaville et al., 2006; Aramaki et al., 2007; Hurd et al., 2007; Layman et al., 2009; Bergman et al., 2010). *SEMA3D* expression has been observed in bones and cartilage, heart, endothelial cells, fibroblasts, epidermis, glia and neurons (Luo et al., 1995; Halloran et al., 1999; Cohen et al., 2003; Serini et al., 2003; Lallier, 2004; Jin et al., 2006). In paraffin sections of mouse embryos (E12.5) *CHD7* and *SEMA3D* showed an overlapping expression pattern in the medulla oblongata, choroid plexus, cochlea, heart, cartilage primordium of body of vertebra and in different ganglia (Fig.19) indicating a possible role of *SEMA3D* in the pathogenesis of CHARGE syndrome, although further studies are needed to clarify this aspect.

4.7 Semaphorins might act as modifier in CHARGE syndrome

Semaphorins are conserved secreted and membrane-associated proteins which can be divided into eight classes according to domain architecture and phylogenetic tree analysis ("Unified nomenclature for the semaphorins/collapsins. Semaphorin Nomenclature Committee," 1999; Yazdani and Terman, 2006). Classes 3-7 are found only in vertebrates (Yazdani and Terman, 2006). Class 3 of semaphorins was identified to be required for NCC migration (Eickholt et al., 1999; Osborne et al., 2005; Yu and Moens, 2005).

The malformation disorder CHARGE syndrome was postulated to belong to the neurocristopathies (Siebert et al., 1985). Mutations in the *CHD7* gene were identified as the genetic cause in about two-thirds of CHARGE syndrome patients (Vissers et al., 2004; Sanlaville and Verloes, 2007). In 5-10 % of typical CHARGE patients and in 40-60 % of patients suspected of having CHARGE syndrome the cause remains unknown (Janssen et al., 2012). Several candidate genes, such as *PAX2* (*paired box 2*) and *PITX2* (*paired-like homeodomain 2*) were analysed but no mutations were

identified (Tellier et al., 2000; Martin et al., 2002). In a CHARGE syndrome patient originally described by Martin et al. (2001) with a de novo balanced translocation involving chromosomes 2 and 7, Lalani et al. (2004) mapped the translocation breakpoints and identified *SEMA3E* within 200 kb of the breakpoint on 7q21.11. By screening additional patients with CHARGE syndrome for mutations in the *SEMA3E* gene a de novo mutation was found (S703L) in an unrelated patient (Lalani et al., 2004). The S703L mutation was not found in the parents (Lalani et al., 2004). *CHD7* mutations were not detected in these two patients, but *CHD7* deletions could not be excluded (Lalani et al., 2006).

While the *Sema3e* expression was found to be unchanged in the genome-wide microarray analysis performed on *Whirligig* mouse embryos described in section 3.4, the expression of *Sema3a*, *Sema3c* and *Sema3d* were significantly reduced (Schulz et al., 2014b). Additional sequencing of the *SEMA3C* gene that is located 1.9 Mb centromeric from the translocation breakpoint in 24 patients revealed no mutation (Lalani et al., 2004). The *SEMA3D* gene lies with *SEMA3E* on 7q21.11, so it is possible that its function is disturbed by the translocation (Database, 2014a, b).

Sema3a knockout mice show altered olfactory bulb innervation and hypogonadism caused by abnormal development of Gonadotropin-releasing hormone (GnRH) neurons exhibiting a phenotype similar to Kallmann syndrome (Schwartz et al., 2000; Cariboni et al., 2011). Kallmann syndrome is a developmental disorder associated with idiopathic hypogonadotropic hypogonadism and congenitally absent or impaired sense of smell (anosmia) (Kallmann et al., 1944). Both features are also found in patients with CHARGE syndrome (Chalouhi et al., 2005; Pinto et al., 2005; Asakura et al., 2008; Blustajn et al., 2008). Additional abnormalities may occur in patients with Kallmann syndrome, such as cleft lip and palate, dental agenesis, unilateral renal agenesis, abnormal eye movements and neurological alterations (Santen and Alvin Paulsen, 1972; Wegenke et al., 1975; Lieblich et al., 1982; Schwankhaus et al., 1989; Hardelin et al., 1993a; Hardelin et al., 1993b; Kirk et al., 1994; de Zegher et al., 1995; Molsted et al., 1997; Soderlund et al., 2002; Dode et al., 2003; Kim et al., 2008a). Among others, mutations in *CHD7* were identified in some patients with Kallmann syndrome (Kim et al., 2008b; Jongmans et al., 2009). It was assumed that Kallmann syndrome represents the mild end of CHARGE syndrome (Kim et al., 2008b; Jongmans et al., 2009).

Young et al. (2012) reported a *SEMA3A* deletion in a family with Kallmann syndrome. A screen of 386 patients with Kallmann syndrome for mutations in *SEMA3A* revealed non-synonymous mutations in 24 patients (Hanchate et al., 2012). As described before, semaphorins seem to be involved in the pathogenesis of CHARGE syndrome. To analyse whether semaphorins contribute to the phenotype of CHARGE syndrome, 45 patients diagnosed with CHARGE but lacking a mutation in the *CHD7* gene were sequenced for the presence of mutations in the coding sequence of *SEMA3A* and *SEMA3D*.

Three non-synonymous mutations for *SEMA3A* in a heterozygous state, namely c.196 C>T (p.R66W), c.2002 A>G (p.I668V) and c.2062 A>G (p.T688A), were identified (Fig.14) (Schulz et al., 2014b). Interestingly, two of the identified missense mutations (p.R66W and p.T688A) were described in patients with Kallmann syndrome (Hanchate et al., 2012). Hanchate et al. (2012) exposed that the missense mutation p.R66W results in altered secretion of SEMA3A while p.T688A causes a reduced signalling activity of SEMA3A. Based on these findings a pathogenic effect in Kallmann syndrome was assumed (Hanchate et al., 2012). Further, it was postulated that a heterozygous mutation in *SEMA3A* alone is not sufficient to induce the phenotypic features of Kallmann syndrome, while in combination with mutations in other Kallmann syndrome causing genes it could contribute to it (Hanchate et al., 2012).

It was shown in this work that the non-synonymous mutation (p.R66W) identified in a CHARGE patient was inherited by the healthy father (Schulz et al., 2014b).

A mutation screen of the coding sequence of *SEMA3D* in 45 *CHD7* negative CHARGE patients revealed no disease causing nucleotide alteration nor a small deletion or insertion. Three non-synonymous mutations were identified in a heterozygous state, namely c.193 T>C (p.S65P), c.1272 C>A (p.H424Q) and c.2101 A>C (p.K701Q) (Fig. 15). The missense mutation p.His424Gln affects a conserved residue. While the common variant p.K701Q (allele frequency of 0.346 in the ESP cohort population) and the less common variant p.S65P (allele frequency of 0.017 in the ESP cohort population) are predicted to be benign (Polyphen and Polyphen2), the missense mutation p.H424Q with an allele frequency of 0.002 is predicted to be damaging (Polyphen, Polyphen2, Sift). Screening the parents of the patient carrying the p.H424Q variant revealed that the variation was inherited by the healthy father. These results indicate that heterogeneous mutations in *SEMA3A* or *SEMA3D* are not

sufficient to cause CHARGE syndrome but it is possible that these mutations contribute to the pathogenesis of CHARGE syndrome as suggested for *SEMA3A* mutations for Kallmann syndrome (Hanchate et al., 2012). CHARGE syndrome is a highly heterogeneous malformation disorder showing inter- and intra-familial heterogeneity (Aramaki et al., 2006; Jongmans et al., 2006; Lalani et al., 2006). Mutations in other genes like *SEMA3A* and *SEMA3D* might act as modifiers leading to a more severe phenotype explaining the heterogeneous appearance of patients with CHARGE syndrome (Schulz et al., 2014b).

4.8 Future perspective

Since CHD7 is associated with different complexes to regulate gene expression in a developmental stage and tissue specific manner, it would help to analyse the composition of CHD7 protein complexes. One method to analyse the structure and composition of especially heterogenic protein complexes is by chemical cross-linking combined with mass spectrometry (XL-MS) (Herzog et al., 2012). Furthermore, arrangement of proteins within complexes and the interplay of protein complexes in a signal transduction pathway can be investigated.

CHARGE syndrome is a phenotypic variable malformation syndrome and in the present work it is assumed that *SEMA3A* and *SEMA3D* might have modifying functions contributing to a more severe phenotype if they are mutated. Therefore, CHARGE patients carrying a *CHD7* mutation should be screened for additional mutations in *SEMA3A* and *SEMA3D*. Especially familial cases showing phenotypic variations would be of great value.

For the *Sema3a* and *Sema3d* knockdown experiments performed with *Xenopus laevis* embryos, rescue experiments have to be accomplished to prove that the observed phenotype is caused by the loss of *Sema3a* and *Sema3d* function.

The genome-wide microarray analysis revealed 98 differentially expressed genes. Several of these genes play a role in NCC development (specification, EMT, guidance of NCC migration and interaction of NCCs with other tissues). Functional analysis of other guidance factors, such as ephrins or slits can be performed which are also involved in axon guidance during neurogenesis (Kirby and Hutson, 2010). This is another important direction since neurologic disturbances exist in CHARGE

syndrome, for instance, cranial nerve palsy, arhinencephaly or abnormal olfactory bulbs and anosmia (Chalouhi et al., 2005; Sanlaville et al., 2005).

Further expression analysis by WMISH or immunohistochemistry in the mouse is recommendable. It would be interesting to analyse the expression pattern of SEMA3A, SEMA3D as well as CHD7 in embryos (wild-type (*Chd7*^{+/+}), heterozygous (*Chd7*^{Whi/+}) and homozygous (*Chd7*^{Whi/Whi})) of the *Whirligig* mouse line. Furthermore, NCC migration and development should be checked in these mice. Disturbances in NCC migration can be visualised by staining the expression pattern of the NCC marker *Twist* and the correct NCC differentiation can be checked, for instance, by observing the formation of dorsal root ganglia. Another possibility to analyse the process of NCC migration in vitro is to plate NCCs on a fibronectin layer (Rovasio et al., 1983). Fibronectin is one component of the extracellular matrix which migrating NCCs encounter (Tosney, 1978; Lofberg et al., 1980; D. Newgreen and Thiery, 1980; Duband and Thiery, 1982; D. F. Newgreen et al., 1982; Spieth and Keller, 1984; Brauer et al., 1985; Duband et al., 1986; Krotoski et al., 1986). It would be interesting to test the guidance potential of SEMA3A and SEMA3D on NCCs from wild-type (*Chd7*^{+/+}), heterozygous (*Chd7*^{Whi/+}) and homozygous (*Chd7*^{Whi/Whi}) mice by explanting NCCs on fibronectin containing matrices with alternating stripes of the semaphorin. Furthermore, the described non-synonymous mutations identified in the *SEMA3A* and *SEMA3D* screen in 45 *CHD7* negative CHARGE patients could be induced by site-directed mutagenesis into a wild-type semaphorin plasmid to generate a semaphorin with this defect and to test whether these mutations cause alterations in the guidance of migrating NCCs.

5 References

- Abcam. (n.d.). Immunocytochemistry (ICC) protocol. <http://docs.abcam.com/pdf/protocols/Immunocytochemistry-ICC-protocol.pdf> (Effective: 02/08/2014).
- AgilentTechnologies. (n.d.). PfuUltra High-Fidelity DNA Polymerase <https://www.chem.agilent.com/Library/usermanuals/Public/600380.pdf> (Effective: 01/08/2014).
- Ambion. (2012). mMESSAGE mACHINE® Kit. http://tools.lifetechnologies.com/content/sfs/manuals/cms_055516.pdf (Effective: 01/08/2014).
- Antipenko, A., Himanen, J.P., van Leyen, K., Nardi-Dei, V., Lesniak, J., Barton, W.A., Rajashankar, K.R., Lu, M., Hoemme, C., Puschel, A.W., and Nikolov, D.B. (2003). Structure of the semaphorin-3A receptor binding module. *Neuron* 39, 589-598.
- AppliedBiosystems. (n.d.). Allelic Discrimination Getting Started Guide http://tools.lifetechnologies.com/content/sfs/manuals/cms_042114.pdf (Effective: 01/08/2014).
- Aramaki, M., Kimura, T., Udaka, T., Kosaki, R., Mitsuhashi, T., Okada, Y., Takahashi, T., and Kosaki, K. (2007). Embryonic expression profile of chicken CHD7, the ortholog of the causative gene for CHARGE syndrome. *Birth defects research. Part A, Clinical and molecular teratology* 79, 50-57.
- Aramaki, M., Udaka, T., Kosaki, R., Makita, Y., Okamoto, N., Yoshihashi, H., Oki, H., Nanao, K., Moriyama, N., Oku, S., Hasegawa, T., Takahashi, T., Fukushima, Y., Kawame, H., and Kosaki, K. (2006). Phenotypic spectrum of CHARGE syndrome with CHD7 mutations. *The Journal of pediatrics* 148, 410-414.
- Arber, W., and Linn, S. (1969). DNA modification and restriction. *Annual review of biochemistry* 38, 467-500.
- Asakura, Y., Toyota, Y., Muroya, K., Kurosawa, K., Fujita, K., Aida, N., Kawame, H., Kosaki, K., and Adachi, M. (2008). Endocrine and radiological studies in patients with molecularly confirmed CHARGE syndrome. *The Journal of clinical endocrinology and metabolism* 93, 920-924.
- Atkinson, M.R., Deutscher, M.P., Kornberg, A., Russell, A.F., and Moffatt, J.G. (1969). Enzymatic synthesis of deoxyribonucleic acid. XXXIV. Termination of chain growth by a 2',3'-dideoxyribonucleotide. *Biochemistry* 8, 4897-4904.
- Bajpai, R., Chen, D.A., Rada-Iglesias, A., Zhang, J., Xiong, Y., Helms, J., Chang, C.P., Zhao, Y., Swigut, T., and Wysocka, J. (2010). CHD7 cooperates with PBAF to control multipotent neural crest formation. *Nature* 463, 958-962.
- Batsukh, T., Pieper, L., Koszucka, A.M., von Velsen, N., Hoyer-Fender, S., Elbracht, M., Bergman, J.E., Hoefsloot, L.H., and Pauli, S. (2010). CHD8 interacts with CHD7, a protein which is mutated in CHARGE syndrome. *Human molecular genetics* 19, 2858-2866.
- Batsukh, T., Schulz, Y., Wolf, S., Rabe, T.I., Oellerich, T., Urlaub, H., Schaefer, I.M., and Pauli, S. (2012). Identification and characterization of FAM124B as a novel component of a CHD7 and CHD8 containing complex. *PloS one* 7, e52640.
- Bergman, J.E., Bosman, E.A., van Ravenswaaij-Arts, C.M., and Steel, K.P. (2010). Study of smell and reproductive organs in a mouse model for CHARGE syndrome. *European journal of human genetics : EJHG* 18, 171-177.

References

- Bergman, J.E., Janssen, N., Hoefsloot, L.H., Jongmans, M.C., Hofstra, R.M., and van Ravenswaaij-Arts, C.M. (2011). CHD7 mutations and CHARGE syndrome: the clinical implications of an expanding phenotype. *Journal of medical genetics* 48, 334-342.
- BIO-RAD. (n.d.). Mini-Trans-Blot® Electrophoretic Transfer Cell <http://www.bio-rad.com/webroot/web/pdf/lsr/literature/M1703930.pdf> (Effective: 01/08/2014).
- Bioline. (n.d.). IMMOLASE™ DNA Polymerase http://www.bioline.com/downloads/dl/file/id/872/immolase_dna_polymerase_manual.pdf (Effective: 31/07/2014).
- Birnboim, H.C., and Doly, J. (1979). A rapid alkaline extraction procedure for screening recombinant plasmid DNA. *Nucleic acids research* 7, 1513-1523.
- Blake, K.D., Davenport, S.L., Hall, B.D., Hefner, M.A., Pagon, R.A., Williams, M.S., Lin, A.E., and Graham, J.M., Jr. (1998). CHARGE association: an update and review for the primary pediatrician. *Clin Pediatr (Phila)* 37, 159-173.
- Blustajn, J., Kirsch, C.F., Panigrahy, A., and Netchine, I. (2008). Olfactory anomalies in CHARGE syndrome: imaging findings of a potential major diagnostic criterion. *AJNR. American journal of neuroradiology* 29, 1266-1269.
- Bogershausen, N., and Wollnik, B. (2013). Unmasking Kabuki syndrome. *Clinical genetics* 83, 201-211.
- Bosman, E.A., Penn, A.C., Ambrose, J.C., Kettleborough, R., Stemple, D.L., and Steel, K.P. (2005). Multiple mutations in mouse Chd7 provide models for CHARGE syndrome. *Human molecular genetics* 14, 3463-3476.
- Bradford, M.M. (1976). A rapid and sensitive method for the quantitation of microgram quantities of protein utilizing the principle of protein-dye binding. *Analytical biochemistry* 72, 248-254.
- Brauer, P.R., Bolender, D.L., and Markwald, R.R. (1985). The distribution and spatial organization of the extracellular matrix encountered by mesencephalic neural crest cells. *The Anatomical record* 211, 57-68.
- Brown, C.B., Feiner, L., Lu, M.M., Li, J., Ma, X., Webber, A.L., Jia, L., Raper, J.A., and Epstein, J.A. (2001). PlexinA2 and semaphorin signaling during cardiac neural crest development. *Development* 128, 3071-3080.
- Bustin, S.A., Benes, V., Garson, J.A., Hellemans, J., Huggett, J., Kubista, M., Mueller, R., Nolan, T., Pfaffl, M.W., Shipley, G.L., Vandesompele, J., and Wittwer, C.T. (2009). The MIQE guidelines: minimum information for publication of quantitative real-time PCR experiments. *Clinical chemistry* 55, 611-622.
- Cariboni, A., Davidson, K., Rakic, S., Maggi, R., Parnavelas, J.G., and Ruhrberg, C. (2011). Defective gonadotropin-releasing hormone neuron migration in mice lacking SEMA3A signalling through NRP1 and NRP2: implications for the aetiology of hypogonadotropic hypogonadism. *Human molecular genetics* 20, 336-344.
- Chalouhi, C., Faulcon, P., Le Bihan, C., Hertz-Pannier, L., Bonfils, P., and Abadie, V. (2005). Olfactory evaluation in children: application to the CHARGE syndrome. *Pediatrics* 116, e81-88.
- Clontech_Laboratories. (2008). pGBKT7 Vector Information. http://www.google.de/url?sa=t&rct=j&q=&esrc=s&source=web&cd=1&ved=0CCIQFjAA&url=http%3A%2F%2Fwww.clontech.com%2Fxxclt_ibcGetA

- ttachment.jsp%3FcItemId%3D17639&ei=kQbzU7HfG-HIyAO70IG4Dg&usg=AFQjCNEEUsnDoR_EVk2vIAjpZat5uqUj4Q&bvm=bv.73231344,d.bGQ (Effective: 19/08/2014).
- Clontech_Laboratories. (2009a). Matchmaker® Gold Yeast Two-Hybrid System User Manual. http://www.google.de/url?sa=t&rct=j&q=&esrc=s&source=web&cd=3&ved=0CDQQFjAC&url=http%3A%2F%2Fwww.clontech.com%2Fxxclt_ibcGetAttachment.jsp%3FcItemId%3D17597&ei=Dg_zU9swpL3KA9DxgeAJ&usg=AFQjCNFpm8VCqNOXHa_3PgDVT0uDdNEj9g&bvm=bv.73231344,d.bGQ (Effective: 19/08/2014).
- Clontech_Laboratories. (2009b). Yeast Protocols Handbook http://www.google.de/url?sa=t&rct=j&q=&esrc=s&source=web&cd=1&ved=0CCcQFjAA&url=http%3A%2F%2Fwww.clontech.com%2Fxxclt_ibcGetAttachment.jsp%3FcItemId%3D17602&ei=dRXzU-ioIMfXyQPur4KQAQ&usg=AFQjCNFWn9PqpRF-CyAKX9dywFWOHBx2Q&bvm=bv.73231344,d.bGQ (Effective: 02/08/2014).
- Clontech_Laboratories. (2012). pGADT7 AD Vector Information. http://www.google.de/url?sa=t&rct=j&q=&esrc=s&source=web&cd=1&ved=0CCIQFjAA&url=http%3A%2F%2Fwww.clontech.com%2Fxxclt_ibcGetAttachment.jsp%3FcItemId%3D17640&ei=7gXzU66kAoLIyAPj_ICgDA&usg=AFQjCNHpmABnwjChso22m1kVV0Qq5XvcRQ&bvm=bv.73231344,d.bGQ (Effective: 19/08/2014).
- Cohen, R.I., Rottkamp, D.M., Maric, D., Barker, J.L., and Hudson, L.D. (2003). A role for semaphorins and neuropilins in oligodendrocyte guidance. *Journal of neurochemistry* 85, 1262-1278.
- Collazo, A., Bronner-Fraser, M., and Fraser, S.E. (1993). Vital dye labelling of *Xenopus laevis* trunk neural crest reveals multipotency and novel pathways of migration. *Development* 118, 363-376.
- Dalby, B., Cates, S., Harris, A., Ohki, E.C., Tilkins, M.L., Price, P.J., and Ciccarone, V.C. (2004). Advanced transfection with Lipofectamine 2000 reagent: primary neurons, siRNA, and high-throughput applications. *Methods* 33, 95-103.
- Database, T.G.H.G. (2014a). Complete information for SEMA3D gene (protein-coding), sema domain, immunoglobulin domain (Ig), short basic domain, secreted, (semaphorin) 3D, including: function, proteins, disorders, pathways, orthologs, and expression. GeneCards - The Human Gene Compendium. Crown Human Genome Center, Department of Molecular Genetics, the Weizmann Institute of Science
- Database, T.G.H.G. (2014b). SEMA3E, SEMA3E gene, SEM3E protein, SEM3E antibody, Sema Domain, Immunoglobulin Domain (Ig), Short Basic Domain, Secreted, (Semaphorin) 3E, SEMAH, KIAA0331, M-Sema H, M-SEMAH, M-SemaK, coll-5, semaphorin-3E, . Crown Human Genome Center, Department of Molecular Genetics, the Weizmann Institute of Science
- De Bellard, M.E., Rao, Y., and Bronner-Fraser, M. (2003). Dual function of Slit2 in repulsion and enhanced migration of trunk, but not vagal, neural crest cells. *The Journal of cell biology* 162, 269-279.
- de Zegher, F., Lagae, L., Declerck, D., and Vinckier, F. (1995). Kallmann syndrome and delayed puberty associated with agenesis of lateral maxillary incisors. *Journal of craniofacial genetics and developmental biology* 15, 87-89.

- den Dunnen, J.T., and Antonarakis, S.E. (2000). Mutation nomenclature extensions and suggestions to describe complex mutations: a discussion. *Human mutation* 15, 7-12.
- Dode, C., Levilliers, J., Dupont, J.M., De Paepe, A., Le Du, N., Soussi-Yanicostas, N., Coimbra, R.S., Delmaghani, S., Compain-Nouaille, S., Baverel, F., Pecheux, C., Le Tessier, D., Cruaud, C., Delpech, M., Speleman, F., Vermeulen, S., Amalfitano, A., Bachelot, Y., Bouchard, P., Cabrol, S., Carel, J.C., Delemarre-van de Waal, H., Goulet-Salmon, B., Kottler, M.L., Richard, O., Sanchez-Franco, F., Saura, R., Young, J., Petit, C., and Hardelin, J.P. (2003). Loss-of-function mutations in FGFR1 cause autosomal dominant Kallmann syndrome. *Nature genetics* 33, 463-465.
- Dou, Y., Milne, T.A., Ruthenburg, A.J., Lee, S., Lee, J.W., Verdine, G.L., Allis, C.D., and Roeder, R.G. (2006). Regulation of MLL1 H3K4 methyltransferase activity by its core components. *Nature structural & molecular biology* 13, 713-719.
- Duband, J.L., Rocher, S., Chen, W.T., Yamada, K.M., and Thiery, J.P. (1986). Cell adhesion and migration in the early vertebrate embryo: location and possible role of the putative fibronectin receptor complex. *The Journal of cell biology* 102, 160-178.
- Duband, J.L., and Thiery, J.P. (1982). Distribution of fibronectin in the early phase of avian cephalic neural crest cell migration. *Developmental biology* 93, 308-323.
- Egea, J., and Klein, R. (2007). Bidirectional Eph-ephrin signaling during axon guidance. *Trends in cell biology* 17, 230-238.
- Eickholt, B.J., Mackenzie, S.L., Graham, A., Walsh, F.S., and Doherty, P. (1999). Evidence for collapsin-1 functioning in the control of neural crest migration in both trunk and hindbrain regions. *Development* 126, 2181-2189.
- Ernst, P., and Vakoc, C.R. (2012). WRAD: enabler of the SET1-family of H3K4 methyltransferases. *Brief Funct Genomics* 11, 217-226.
- Fields, S., and Song, O. (1989). A novel genetic system to detect protein-protein interactions. *Nature* 340, 245-246.
- Fisher, M.P., and Dingman, C.W. (1971). Role of molecular conformation in determining the electrophoretic properties of polynucleotides in agarose-acrylamide composite gels. *Biochemistry* 10, 1895-1899.
- Flanagan, J.F., Blus, B.J., Kim, D., Clines, K.L., Rastinejad, F., and Khorasanizadeh, S. (2007). Molecular implications of evolutionary differences in CHD double chromodomains. *Journal of molecular biology* 369, 334-342.
- Flaus, A., Martin, D.M., Barton, G.J., and Owen-Hughes, T. (2006). Identification of multiple distinct Snf2 subfamilies with conserved structural motifs. *Nucleic acids research* 34, 2887-2905.
- Gammill, L.S., and Bronner-Fraser, M. (2003). Neural crest specification: migrating into genomics. *Nature reviews. Neuroscience* 4, 795-805.
- GeneTools. (n.d.). Home. <http://www.gene-tools.com/> (Effective: 16/07/2014).
- Georgiev, G.P. (1972). The structure of transcriptional units in eukaryotic cells. *Current topics in developmental biology* 7, 1-60.
- Gietz, D., St Jean, A., Woods, R.A., and Schiestl, R.H. (1992). Improved method for high efficiency transformation of intact yeast cells. *Nucleic acids research* 20, 1425.
- Gilbert, S.F. (2000). *Developmental Biology* (6th edn): Sinauer Associates.

- Gitler, A.D., Lu, M.M., and Epstein, J.A. (2004). PlexinD1 and semaphorin signaling are required in endothelial cells for cardiovascular development. *Developmental cell* 7, 107-116.
- Hall, B.D. (1979). Choanal atresia and associated multiple anomalies. *The Journal of pediatrics* 95, 395-398.
- Hall, J.A., and Georgel, P.T. (2007). CHD proteins: a diverse family with strong ties. *Biochemistry and cell biology = Biochimie et biologie cellulaire* 85, 463-476.
- Halloran, M.C., Severance, S.M., Yee, C.S., Gemza, D.L., Raper, J.A., and Kuwada, J.Y. (1999). Analysis of a Zebrafish semaphorin reveals potential functions in vivo. *Developmental dynamics : an official publication of the American Association of Anatomists* 214, 13-25.
- Hanahan, D. (1983). Studies on transformation of *Escherichia coli* with plasmids. *Journal of molecular biology* 166, 557-580.
- Hanchate, N.K., Giacobini, P., Lhuillier, P., Parkash, J., Espy, C., Fouveaut, C., Leroy, C., Baron, S., Campagne, C., Vanacker, C., Collier, F., Cruaud, C., Meyer, V., Garcia-Pinero, A., Dewailly, D., Cortet-Rudelli, C., Gersak, K., Metz, C., Chabrier, G., Pugeat, M., Young, J., Hardelin, J.P., Prevot, V., and Dode, C. (2012). SEMA3A, a gene involved in axonal pathfinding, is mutated in patients with Kallmann syndrome. *PLoS genetics* 8, e1002896.
- Hardcastle, Z., Chalmers, A.D., and Papalopulu, N. (2000). FGF-8 stimulates neuronal differentiation through FGFR-4a and interferes with mesoderm induction in *Xenopus* embryos. *Current biology : CB* 10, 1511-1514.
- Hardelin, J.P., Levilliers, J., Blanchard, S., Carel, J.C., Leutenegger, M., Pinard-Bertelatto, J.P., Bouloux, P., and Petit, C. (1993a). Heterogeneity in the mutations responsible for X chromosome-linked Kallmann syndrome. *Human molecular genetics* 2, 373-377.
- Hardelin, J.P., Levilliers, J., Young, J., Pholsena, M., Legouis, R., Kirk, J., Bouloux, P., Petit, C., and Schaison, G. (1993b). Xp22.3 deletions in isolated familial Kallmann's syndrome. *The Journal of clinical endocrinology and metabolism* 76, 827-831.
- Hardouin, S.N., and Nagy, A. (2000). Mouse models for human disease. *Clinical genetics* 57, 237-244.
- Harland, R.M. (1991). In situ hybridization: an improved whole-mount method for *Xenopus* embryos. *Methods in cell biology* 36, 685-695.
- Hawker, K., Fuchs, H., Angelis, M.H., and Steel, K.P. (2005). Two new mouse mutants with vestibular defects that map to the highly mutable locus on chromosome 4. *International journal of audiology* 44, 171-177.
- Hedderich, M.C. (2012). Molecular characterization of Ptf1a activity during *Xenopus* embryogenesis. *Developmental Biochemistry*. Goettingen: Georg-August-University.
- Helling, R.B., Goodman, H.M., and Boyer, H.W. (1974). Analysis of endonuclease R-EcoRI fragments of DNA from lambdoid bacteriophages and other viruses by agarose-gel electrophoresis. *Journal of virology* 14, 1235-1244.
- Herzog, F., Kahraman, A., Boehringer, D., Mak, R., Bracher, A., Walzthoeni, T., Leitner, A., Beck, M., Hartl, F.U., Ban, N., Malmstrom, L., and Aebersold, R. (2012). Structural probing of a protein phosphatase 2A network by chemical cross-linking and mass spectrometry. *Science* 337, 1348-1352.
- HGVS. (2013). Description of sequence changes: examples protein-level <http://www.hgvs.org/mutnomen/examplesAA.html#sub> (Effective: 21/07/2014).

- Hill, J., Donald, K.A., and Griffiths, D.E. (1991). DMSO-enhanced whole cell yeast transformation. *Nucleic acids research* 19, 5791.
- Hittner, H.M., Hirsch, N.J., Kreh, G.M., and Rudolph, A.J. (1979). Colobomatous microphthalmia, heart disease, hearing loss, and mental retardation--a syndrome. *Journal of pediatric ophthalmology and strabismus* 16, 122-128.
- Ho, L., Jothi, R., Ronan, J.L., Cui, K., Zhao, K., and Crabtree, G.R. (2009a). An embryonic stem cell chromatin remodeling complex, esBAF, is an essential component of the core pluripotency transcriptional network. *Proceedings of the National Academy of Sciences of the United States of America* 106, 5187-5191.
- Ho, L., Ronan, J.L., Wu, J., Staahl, B.T., Chen, L., Kuo, A., Lessard, J., Nesvizhskii, A.I., Ranish, J., and Crabtree, G.R. (2009b). An embryonic stem cell chromatin remodeling complex, esBAF, is essential for embryonic stem cell self-renewal and pluripotency. *Proceedings of the National Academy of Sciences of the United States of America* 106, 5181-5186.
- Hrabe de Angelis, M.H., Flaswinkel, H., Fuchs, H., Rathkolb, B., Soewarto, D., Marschall, S., Heffner, S., Pargent, W., Wuensch, K., Jung, M., Reis, A., Richter, T., Alessandrini, F., Jakob, T., Fuchs, E., Kolb, H., Kremmer, E., Schaeble, K., Rollinski, B., Roscher, A., Peters, C., Meitinger, T., Strom, T., Steckler, T., Holsboer, F., Klopstock, T., Gekeler, F., Schindewolf, C., Jung, T., Avraham, K., Behrendt, H., Ring, J., Zimmer, A., Schughart, K., Pfeffer, K., Wolf, E., and Balling, R. (2000). Genome-wide, large-scale production of mutant mice by ENU mutagenesis. *Nature genetics* 25, 444-447.
- Huang da, W., Sherman, B.T., and Lempicki, R.A. (2009a). Bioinformatics enrichment tools: paths toward the comprehensive functional analysis of large gene lists. *Nucleic acids research* 37, 1-13.
- Huang da, W., Sherman, B.T., and Lempicki, R.A. (2009b). Systematic and integrative analysis of large gene lists using DAVID bioinformatics resources. *Nature protocols* 4, 44-57.
- Hubrecht-Laboratorium (Embryologisch Instituut), Nieuwkoop, P.D., and Faber, J. (1967). Normal table of *Xenopus laevis* (Daudin). A systematical and chronological survey of the development from the fertilized egg till the end of metamorphosis (2. edn). Amsterdam,: North-Holland Pub. Co.
- Hurd, E.A., Capers, P.L., Blauwkamp, M.N., Adams, M.E., Raphael, Y., Poucher, H.K., and Martin, D.M. (2007). Loss of Chd7 function in gene-trapped reporter mice is embryonic lethal and associated with severe defects in multiple developing tissues. *Mammalian genome : official journal of the International Mammalian Genome Society* 18, 94-104.
- Illumina. (2011). Using Passive Reference Dyes for Normalization and Troubleshooting in qPCR. http://res.illumina.com/documents/products/technotes/technote_qpcr_using_rox_normalization.pdf (Effective: 19/08/2014).
- Invitrogen. (2010). Platinum®Taq DNA Polymerase <http://www.lifetechnologies.com/content/dam/LifeTech/migration/files/pcr/pdfs.par.26652.file.dat/platinumtaq-pps.pdf> (Effective: 01/08/2014).
- Ito, H., Fukuda, Y., Murata, K., and Kimura, A. (1983). Transformation of intact yeast cells treated with alkali cations. *Journal of bacteriology* 153, 163-168.
- Janssen, N., Bergman, J.E., Swertz, M.A., Tranebjaerg, L., Lodahl, M., Schoots, J., Hofstra, R.M., van Ravenswaaij-Arts, C.M., and Hoefsloot, L.H. (2012).

- Mutation update on the CHD7 gene involved in CHARGE syndrome. *Human mutation* 33, 1149-1160.
- Jin, Z., Chau, M.D., and Bao, Z.Z. (2006). Sema3D, Sema3F, and Sema5A are expressed in overlapping and distinct patterns in chick embryonic heart. *Developmental dynamics : an official publication of the American Association of Anatomists* 235, 163-169.
- Jongmans, M.C., Admiraal, R.J., van der Donk, K.P., Vissers, L.E., Baas, A.F., Kapusta, L., van Hagen, J.M., Donnai, D., de Ravel, T.J., Veltman, J.A., Geurts van Kessel, A., De Vries, B.B., Brunner, H.G., Hoefsloot, L.H., and van Ravenswaaij, C.M. (2006). CHARGE syndrome: the phenotypic spectrum of mutations in the CHD7 gene. *Journal of medical genetics* 43, 306-314.
- Jongmans, M.C., van Ravenswaaij-Arts, C.M., Pitteloud, N., Ogata, T., Sato, N., Claahsen-van der Grinten, H.L., van der Donk, K., Seminara, S., Bergman, J.E., Brunner, H.G., Crowley, W.F., Jr., and Hoefsloot, L.H. (2009). CHD7 mutations in patients initially diagnosed with Kallmann syndrome--the clinical overlap with CHARGE syndrome. *Clinical genetics* 75, 65-71.
- Kallmann, F.J., Schoenfeld, W.A., and Barrera, S.E. (1944). The genetic aspects of primary eunuchoidism. *American journal of mental deficiency*, 203-236.
- Kim, H.G., Bhagavath, B., and Layman, L.C. (2008a). Clinical manifestations of impaired GnRH neuron development and function. *Neuro-Signals* 16, 165-182.
- Kim, H.G., Kurth, I., Lan, F., Meliciani, I., Wenzel, W., Eom, S.H., Kang, G.B., Rosenberger, G., Tekin, M., Ozata, M., Bick, D.P., Sherins, R.J., Walker, S.L., Shi, Y., Gusella, J.F., and Layman, L.C. (2008b). Mutations in CHD7, encoding a chromatin-remodeling protein, cause idiopathic hypogonadotropic hypogonadism and Kallmann syndrome. *American journal of human genetics* 83, 511-519.
- Kirby, M.L., and Hutson, M.R. (2010). Factors controlling cardiac neural crest cell migration. *Cell adhesion & migration* 4, 609-621.
- Kirk, J.M., Grant, D.B., Besser, G.M., Shalet, S., Quinton, R., Smith, C.S., White, M., Edwards, O., and Bouloux, P.M. (1994). Unilateral renal aplasia in X-linked Kallmann's syndrome. *Clinical genetics* 46, 260-262.
- Kleppe, K., Ohtsuka, E., Kleppe, R., Molineux, I., and Khorana, H.G. (1971). Studies on polynucleotides. XCVI. Repair replications of short synthetic DNA's as catalyzed by DNA polymerases. *Journal of molecular biology* 56, 341-361.
- Knecht, A.K., and Bronner-Fraser, M. (2002). Induction of the neural crest: a multigene process. *Nature reviews. Genetics* 3, 453-461.
- Kontges, G., and Lumsden, A. (1996). Rhombencephalic neural crest segmentation is preserved throughout craniofacial ontogeny. *Development* 122, 3229-3242.
- Korbie, D.J., and Mattick, J.S. (2008). Touchdown PCR for increased specificity and sensitivity in PCR amplification. *Nature protocols* 3, 1452-1456.
- Kosaki, K. (2011). Role of rare cases in deciphering the mechanisms of congenital anomalies: CHARGE syndrome research. *Congenital anomalies* 51, 12-15.
- Krotoski, D.M., Domingo, C., and Bronner-Fraser, M. (1986). Distribution of a putative cell surface receptor for fibronectin and laminin in the avian embryo. *The Journal of cell biology* 103, 1061-1071.

- Kuriyama, S., and Mayor, R. (2008). Molecular analysis of neural crest migration. *Philosophical transactions of the Royal Society of London. Series B, Biological sciences* 363, 1349-1362.
- Laemmli, U.K. (1970). Cleavage of structural proteins during the assembly of the head of bacteriophage T4. *Nature* 227, 680-685.
- Lalani, S.R., Safiullah, A.M., Fernbach, S.D., Harutyunyan, K.G., Thaller, C., Peterson, L.E., McPherson, J.D., Gibbs, R.A., White, L.D., Hefner, M., Davenport, S.L., Graham, J.M., Bacino, C.A., Glass, N.L., Towbin, J.A., Craigen, W.J., Neish, S.R., Lin, A.E., and Belmont, J.W. (2006). Spectrum of CHD7 mutations in 110 individuals with CHARGE syndrome and genotype-phenotype correlation. *American journal of human genetics* 78, 303-314.
- Lalani, S.R., Safiullah, A.M., Molinari, L.M., Fernbach, S.D., Martin, D.M., and Belmont, J.W. (2004). SEMA3E mutation in a patient with CHARGE syndrome. *Journal of medical genetics* 41, e94.
- Lallier, T.E. (2004). Semaphorin profiling of periodontal fibroblasts and osteoblasts. *Journal of dental research* 83, 677-682.
- Lampe, P.D., and Lau, A.F. (2000). Regulation of gap junctions by phosphorylation of connexins. *Archives of biochemistry and biophysics* 384, 205-215.
- Layman, W.S., Hurd, E.A., and Martin, D.M. (2010). Chromodomain proteins in development: lessons from CHARGE syndrome. *Clinical genetics* 78, 11-20.
- Layman, W.S., McEwen, D.P., Beyer, L.A., Lalani, S.R., Fernbach, S.D., Oh, E., Swaroop, A., Hegg, C.C., Raphael, Y., Martens, J.R., and Martin, D.M. (2009). Defects in neural stem cell proliferation and olfaction in Chd7 deficient mice indicate a mechanism for hyposmia in human CHARGE syndrome. *Human molecular genetics* 18, 1909-1923.
- Lee, P.Y., Costumbrado, J., Hsu, C.Y., and Kim, Y.H. (2012). Agarose gel electrophoresis for the separation of DNA fragments. *Journal of visualized experiments : JoVE*.
- Lepore, J.J., Mericko, P.A., Cheng, L., Lu, M.M., Morrissey, E.E., and Parmacek, M.S. (2006). GATA-6 regulates semaphorin 3C and is required in cardiac neural crest for cardiovascular morphogenesis. *The Journal of clinical investigation* 116, 929-939.
- Li, Y., Bogershausen, N., Alanay, Y., Simsek Kiper, P.O., Plume, N., Keupp, K., Pohl, E., Pawlik, B., Rachwalski, M., Milz, E., Thoenes, M., Albrecht, B., Prott, E.C., Lehmkuhler, M., Demuth, S., Utine, G.E., Boduroglu, K., Frankenbusch, K., Borck, G., Gillissen-Kaesbach, G., Yigit, G., Wieczorek, D., and Wollnik, B. (2011). A mutation screen in patients with Kabuki syndrome. *Human genetics* 130, 715-724.
- Liebllich, J.M., Rogol, A.D., White, B.J., and Rosen, S.W. (1982). Syndrome of anosmia with hypogonadotropic hypogonadism (Kallmann syndrome): clinical and laboratory studies in 23 cases. *The American journal of medicine* 73, 506-519.
- Lofberg, J., Ahlfors, K., and Fallstrom, C. (1980). Neural crest cell migration in relation to extracellular matrix organization in the embryonic axolotl trunk. *Developmental biology* 75, 148-167.
- Luo, Y., Shepherd, I., Li, J., Renzi, M.J., Chang, S., and Raper, J.A. (1995). A family of molecules related to collapsin in the embryonic chick nervous system. *Neuron* 14, 1131-1140.
- Luxan, G., Casanova, J.C., Martinez-Poveda, B., Prados, B., D'Amato, G., MacGrogan, D., Gonzalez-Rajal, A., Dobarro, D., Torroja, C., Martinez, F.,

- Izquierdo-Garcia, J.L., Fernandez-Friera, L., Sabater-Molina, M., Kong, Y.Y., Pizarro, G., Ibanez, B., Medrano, C., Garcia-Pavia, P., Gimeno, J.R., Monserrat, L., Jimenez-Borreguero, L.J., and de la Pompa, J.L. (2013). Mutations in the NOTCH pathway regulator MIB1 cause left ventricular noncompaction cardiomyopathy. *Nature medicine* 19, 193-201.
- Marfella, C.G., and Imbalzano, A.N. (2007). The Chd family of chromatin remodelers. *Mutation research* 618, 30-40.
- Martin, D.M., Probst, F.J., Fox, S.E., Schimmenti, L.A., Semina, E.V., Hefner, M.A., Belmont, J.W., and Camper, S.A. (2002). Exclusion of PITX2 mutations as a major cause of CHARGE association. *American journal of medical genetics* 111, 27-30.
- Martin, D.M., Sheldon, S., and Gorski, J.L. (2001). CHARGE association with choanal atresia and inner ear hypoplasia in a child with a de novo chromosome translocation t(2;7)(p14;q21.11). *American journal of medical genetics* 99, 115-119.
- MGI. (2011). Guidelines for Nomenclature of Genes, Genetic Markers, Alleles, and Mutations in Mouse and Rat <http://www.informatics.jax.org/mgihome/nomen/gene.shtml> (Effective: 21/07/2014).
- Miller, T., Krogan, N.J., Dover, J., Erdjument-Bromage, H., Tempst, P., Johnston, M., Greenblatt, J.F., and Shilatifard, A. (2001). COMPASS: a complex of proteins associated with a trithorax-related SET domain protein. *Proceedings of the National Academy of Sciences of the United States of America* 98, 12902-12907.
- MIPS, GenRE, and GSF. (2008). Navigation: » Corum » Intro <http://mips.helmholtz-muenchen.de/genre/proj/corum/complexdetails.html?id=1399> (Effective: 01/08/2014).
- Mohrmann, L., and Verrijzer, C.P. (2005). Composition and functional specificity of SWI2/SNF2 class chromatin remodeling complexes. *Biochimica et biophysica acta* 1681, 59-73.
- Molsted, K., Kjaer, I., Giwercman, A., Vesterhauge, S., and Skakkebaek, N.E. (1997). Craniofacial morphology in patients with Kallmann's syndrome with and without cleft lip and palate. *The Cleft palate-craniofacial journal : official publication of the American Cleft Palate-Craniofacial Association* 34, 417-424.
- Morin-Kensicki, E.M., and Eisen, J.S. (1997). Sclerotome development and peripheral nervous system segmentation in embryonic zebrafish. *Development* 124, 159-167.
- Mullis, K., Faloona, F., Scharf, S., Saiki, R., Horn, G., and Erlich, H. (1986). Specific enzymatic amplification of DNA in vitro: the polymerase chain reaction. *Cold Spring Harbor symposia on quantitative biology* 51 Pt 1, 263-273.
- Newgreen, D., and Thiery, J.P. (1980). Fibronectin in early avian embryos: synthesis and distribution along the migration pathways of neural crest cells. *Cell and tissue research* 211, 269-291.
- Newgreen, D.F., Gibbins, I.L., Sauter, J., Wallenfels, B., and Wutz, R. (1982). Ultrastructural and tissue-culture studies on the role of fibronectin, collagen and glycosaminoglycans in the migration of neural crest cells in the fowl embryo. *Cell and tissue research* 221, 521-549.

- Ng, S.B., Bigham, A.W., Buckingham, K.J., Hannibal, M.C., McMillin, M.J., Gildersleeve, H.I., Beck, A.E., Tabor, H.K., Cooper, G.M., Mefford, H.C., Lee, C., Turner, E.H., Smith, J.D., Rieder, M.J., Yoshiura, K., Matsumoto, N., Ohta, T., Niikawa, N., Nickerson, D.A., Bamshad, M.J., and Shendure, J. (2010). Exome sequencing identifies MLL2 mutations as a cause of Kabuki syndrome. *Nature genetics* 42, 790-793.
- Nolte, J. (2008). Pluripotency of Spermatogonial stem cell lines. Institute of Human Genetics. Goettingen: Georg-August-University.
- OlinkBiosciences. (2010). Doulink II Fluorescence User manual. <http://www.eurogentec.com/EGT/files/Olink/Duolink-II-Fluorescence-User-Manual.pdf> (Effective: 14/07/2014).
- Opitz, L., Salinas-Riester, G., Grade, M., Jung, K., Jo, P., Emons, G., Ghadimi, B.M., Beissbarth, T., and Gaedcke, J. (2010). Impact of RNA degradation on gene expression profiling. *BMC medical genomics* 3, 36.
- Osborne, N.J., Begbie, J., Chilton, J.K., Schmidt, H., and Eickholt, B.J. (2005). Semaphorin/neuropilin signaling influences the positioning of migratory neural crest cells within the hindbrain region of the chick. *Developmental dynamics : an official publication of the American Association of Anatomists* 232, 939-949.
- Pagon, R.A., Graham, J.M., Jr., Zonana, J., and Yong, S.L. (1981). Coloboma, congenital heart disease, and choanal atresia with multiple anomalies: CHARGE association. *The Journal of pediatrics* 99, 223-227.
- Parisis, N. (2012). *Xenopus laevis as a Model System*. Labome.
- Peqlab. (n.d.). *peqGOLD Pwo-DNA-Polymerase** http://www.peqlab.de/wcms/de/pdf/01-5020_m.pdf (Effective: 31/07/2014).
- Perris, R. (1997). The extracellular matrix in neural crest-cell migration. *Trends in neurosciences* 20, 23-31.
- Pingoud, A., Alves, J., and Geiger, R. (1993). Restriction enzymes. *Methods Mol Biol* 16, 107-200.
- Pingoud, A., and Jeltsch, A. (2001). Structure and function of type II restriction endonucleases. *Nucleic acids research* 29, 3705-3727.
- Pinto, G., Abadie, V., Mesnage, R., Blustajn, J., Cabrol, S., Amiel, J., Hertz-Pannier, L., Bertrand, A.M., Lyonnet, S., Rappaport, R., and Netchine, I. (2005). CHARGE syndrome includes hypogonadotropic hypogonadism and abnormal olfactory bulb development. *The Journal of clinical endocrinology and metabolism* 90, 5621-5626.
- Randall, V., McCue, K., Roberts, C., Kyriakopoulou, V., Beddow, S., Barrett, A.N., Vitelli, F., Prescott, K., Shaw-Smith, C., Devriendt, K., Bosman, E., Steffes, G., Steel, K.P., Simrick, S., Basson, M.A., Illingworth, E., and Scambler, P.J. (2009). Great vessel development requires biallelic expression of Chd7 and Tbx1 in pharyngeal ectoderm in mice. *The Journal of clinical investigation* 119, 3301-3310.
- Rickmann, M., Fawcett, J.W., and Keynes, R.J. (1985). The migration of neural crest cells and the growth of motor axons through the rostral half of the chick somite. *Journal of embryology and experimental morphology* 90, 437-455.
- Ringrose, L., and Paro, R. (2004). Epigenetic regulation of cellular memory by the Polycomb and Trithorax group proteins. *Annual review of genetics* 38, 413-443.

- Rohani, N., Canty, L., Luu, O., Fagotto, F., and Winklbauer, R. (2011). EphrinB/EphB signaling controls embryonic germ layer separation by contact-induced cell detachment. *PLoS biology* 9, e1000597.
- Rovasio, R.A., Delouree, A., Yamada, K.M., Timpl, R., and Thiery, J.P. (1983). Neural crest cell migration: requirements for exogenous fibronectin and high cell density. *The Journal of cell biology* 96, 462-473.
- Sanger, F., and Coulson, A.R. (1975). A rapid method for determining sequences in DNA by primed synthesis with DNA polymerase. *Journal of molecular biology* 94, 441-448.
- Sanlaville, D., Etchevers, H.C., Gonzales, M., Martinovic, J., Clement-Ziza, M., Delezoide, A.L., Aubry, M.C., Pelet, A., Chemouny, S., Cruaud, C., Audollent, S., Esculpavit, C., Goudefroye, G., Ozilou, C., Fredouille, C., Joye, N., Morichon-Delvallez, N., Dumez, Y., Weissenbach, J., Munnich, A., Amiel, J., Encha-Razavi, F., Lyonnet, S., Vekemans, M., and Attie-Bitach, T. (2006). Phenotypic spectrum of CHARGE syndrome in fetuses with CHD7 truncating mutations correlates with expression during human development. *Journal of medical genetics* 43, 211-217.
- Sanlaville, D., Genevieve, D., Bernardin, C., Amiel, J., Baumann, C., de Blois, M.C., Cormier-Daire, V., Gerard, B., Gerard, M., Le Merrer, M., Parent, P., Prieur, F., Prieur, M., Raoul, O., Toutain, A., Verloes, A., Viot, G., Romana, S., Munnich, A., Lyonnet, S., Vekemans, M., and Turleau, C. (2005). Failure to detect an 8p22-8p23.1 duplication in patients with Kabuki (Niikawa-Kuroki) syndrome. *European journal of human genetics : EJHG* 13, 690-693.
- Sanlaville, D., and Verloes, A. (2007). CHARGE syndrome: an update. *European journal of human genetics : EJHG* 15, 389-399.
- Santen, R.J., and Alvin Paulsen, C. (1972). Hypogonadotropic Eunuchoidism. I. Clinical Study of the Mode of Inheritance. *The Journal of Clinical Endocrinology & Metabolism* 36, 1-47.
- Sato, M., Tsai, H.J., and Yost, H.J. (2006). Semaphorin3D regulates invasion of cardiac neural crest cells into the primary heart field. *Developmental biology* 298, 12-21.
- Schena, M., Shalon, D., Davis, R.W., and Brown, P.O. (1995). Quantitative monitoring of gene expression patterns with a complementary DNA microarray. *Science* 270, 467-470.
- Scherer, W.F., Syverton, J.T., and Gey, G.O. (1953). Studies on the propagation in vitro of poliomyelitis viruses. IV. Viral multiplication in a stable strain of human malignant epithelial cells (strain HeLa) derived from an epidermoid carcinoma of the cervix. *The Journal of experimental medicine* 97, 695-710.
- Schiestl, R.H., and Gietz, R.D. (1989). High efficiency transformation of intact yeast cells using single stranded nucleic acids as a carrier. *Current genetics* 16, 339-346.
- Schnetz, M.P., Handoko, L., Akhtar-Zaidi, B., Bartels, C.F., Pereira, C.F., Fisher, A.G., Adams, D.J., Flicek, P., Crawford, G.E., Laframboise, T., Tesar, P., Wei, C.L., and Scacheri, P.C. (2010). CHD7 targets active gene enhancer elements to modulate ES cell-specific gene expression. *PLoS genetics* 6, e1001023.
- Schulz, Y., Freese, L., Manz, J., Zoll, B., Volter, C., Brockmann, K., Bogershausen, N., Becker, J., Wollnik, B., and Pauli, S. (2014a). CHARGE and Kabuki syndromes: a phenotypic and molecular link. *Human molecular genetics*.

- Schulz, Y., Wehner, P., Opitz, L., Salinas-Riester, G., Bongers, E.M., van Ravenswaaij-Arts, C.M., Wincent, J., Schoumans, J., Kohlhase, J., Borchers, A., and Pauli, S. (2014b). CHD7, the gene mutated in CHARGE syndrome, regulates genes involved in neural crest cell guidance. *Human genetics*.
- Schwankhaus, J.D., Currie, J., Jaffe, M.J., Rose, S.R., and Sherins, R.J. (1989). Neurologic findings in men with isolated hypogonadotropic hypogonadism. *Neurology* 39, 223-226.
- Schwarting, G.A., Kostek, C., Ahmad, N., Dibble, C., Pays, L., and Puschel, A.W. (2000). Semaphorin 3A is required for guidance of olfactory axons in mice. *The Journal of neuroscience : the official journal of the Society for Neuroscience* 20, 7691-7697.
- Serini, G., Valdembrì, D., Zanivan, S., Morterra, G., Burkhardt, C., Caccavari, F., Zammataro, L., Primo, L., Tamagnone, L., Logan, M., Tessier-Lavigne, M., Taniguchi, M., Puschel, A.W., and Bussolino, F. (2003). Class 3 semaphorins control vascular morphogenesis by inhibiting integrin function. *Nature* 424, 391-397.
- Shapiro, A.L., Vinuela, E., and Maizel, J.V., Jr. (1967). Molecular weight estimation of polypeptide chains by electrophoresis in SDS-polyacrylamide gels. *Biochemical and biophysical research communications* 28, 815-820.
- Sharp, P.A., Sugden, B., and Sambrook, J. (1973). Detection of two restriction endonuclease activities in *Haemophilus parainfluenzae* using analytical agarose-ethidium bromide electrophoresis. *Biochemistry* 12, 3055-3063.
- Shoval, I., Ludwig, A., and Kalcheim, C. (2007). Antagonistic roles of full-length N-cadherin and its soluble BMP cleavage product in neural crest delamination. *Development* 134, 491-501.
- Siebert, J.R., Graham, J.M., Jr., and MacDonald, C. (1985). Pathologic features of the CHARGE association: support for involvement of the neural crest. *Teratology* 31, 331-336.
- Smith, A., Robinson, V., Patel, K., and Wilkinson, D.G. (1997). The EphA4 and EphB1 receptor tyrosine kinases and ephrin-B2 ligand regulate targeted migration of branchial neural crest cells. *Current biology : CB* 7, 561-570.
- Smith, W.C., and Harland, R.M. (1991). Injected Xwnt-8 RNA acts early in *Xenopus* embryos to promote formation of a vegetal dorsalizing center. *Cell* 67, 753-765.
- SNPdev. (n.d.). dbSNP Short Genetic Variations. http://www.ncbi.nlm.nih.gov/projects/SNP/snp_ref.cgi?rs=147821428 (Effective: 14/08/2014).
- Soderlund, D., Canto, P., and Mendez, J.P. (2002). Identification of three novel mutations in the KAL1 gene in patients with Kallmann syndrome. *The Journal of clinical endocrinology and metabolism* 87, 2589-2592.
- Song JJ, K.R. (2008). WDR5 interacts with mixed lineage leukemia (MLL) protein via the histone H3-binding pocket. *J Biol Chem*.
- Spieth, J., and Keller, R.E. (1984). Neural crest cell behavior in white and dark larvae of *Ambystoma mexicanum*: differences in cell morphology, arrangement, and extracellular matrix as related to migration. *The Journal of experimental zoology* 229, 91-107.
- Steward, M.M., Lee, J.S., O'Donovan, A., Wyatt, M., Bernstein, B.E., and Shilatifard, A. (2006). Molecular regulation of H3K4 trimethylation by ASH2L, a shared subunit of MLL complexes. *Nature structural & molecular biology* 13, 852-854.

- Takada, I., Mihara, M., Suzawa, M., Ohtake, F., Kobayashi, S., Igarashi, M., Youn, M.Y., Takeyama, K., Nakamura, T., Mezaki, Y., Takezawa, S., Yogiashi, Y., Kitagawa, H., Yamada, G., Takada, S., Minami, Y., Shibuya, H., Matsumoto, K., and Kato, S. (2007). A histone lysine methyltransferase activated by non-canonical Wnt signalling suppresses PPAR-gamma transactivation. *Nature cell biology* 9, 1273-1285.
- Takeichi, M. (1995). Morphogenetic roles of classic cadherins. *Current opinion in cell biology* 7, 619-627.
- Tellier, A.L., Amiel, J., Delezoide, A.L., Audollent, S., Auge, J., Esnault, D., Encha-Razavi, F., Munnich, A., Lyonnet, S., Vekemans, M., and Attie-Bitach, T. (2000). Expression of the PAX2 gene in human embryos and exclusion in the CHARGE syndrome. *American journal of medical genetics* 93, 85-88.
- Thompson, B.A., Tremblay, V., Lin, G., and Bochar, D.A. (2008). CHD8 is an ATP-dependent chromatin remodeling factor that regulates beta-catenin target genes. *Molecular and cellular biology* 28, 3894-3904.
- Thompson BA, T.V., Lin G, Bochar DA. (2008). CHD8 is an ATP-dependent chromatin remodeling factor that regulates beta-catenin target genes. *Mol Cell Biol.* .
- Tosney, K.W. (1978). The early migration of neural crest cells in the trunk region of the avian embryo: an electron microscopic study. *Developmental biology* 62, 317-333.
- Towbin, H., and Gordon, J. (1984). Immunoblotting and dot immunobinding--current status and outlook. *Journal of immunological methods* 72, 313-340.
- Towbin, H., Staehelin, T., and Gordon, J. (1979). Electrophoretic transfer of proteins from polyacrylamide gels to nitrocellulose sheets: procedure and some applications. *Proceedings of the National Academy of Sciences of the United States of America* 76, 4350-4354.
- Towbin, H., Staehelin, T., and Gordon, J. (1992). Electrophoretic transfer of proteins from polyacrylamide gels to nitrocellulose sheets: procedure and some applications. 1979. *Biotechnology* 24, 145-149.
- Trotter, K.W., and Archer, T.K. (2008). The BRG1 transcriptional coregulator. *Nuclear receptor signaling* 6, e004.
- Unified nomenclature for the semaphorins/collapsins. Semaphorin Nomenclature Committee. (1999). *Cell* 97, 551-552.
- Van Meter, T.D., and Weaver, D.D. (1996). Oculo-auriculo-vertebral spectrum and the CHARGE association: clinical evidence for a common pathogenetic mechanism. *Clinical dysmorphology* 5, 187-196.
- Vawter, M.P., Evans, S., Choudary, P., Tomita, H., Meador-Woodruff, J., Molnar, M., Li, J., Lopez, J.F., Myers, R., Cox, D., Watson, S.J., Akil, H., Jones, E.G., and Bunney, W.E. (2004). Gender-specific gene expression in post-mortem human brain: localization to sex chromosomes. *Neuropsychopharmacology : official publication of the American College of Neuropsychopharmacology* 29, 373-384.
- Verloes, A. (2005). Updated diagnostic criteria for CHARGE syndrome: a proposal. *American journal of medical genetics. Part A* 133A, 306-308.
- Vissers, L.E., van Ravenswaaij, C.M., Admiraal, R., Hurst, J.A., de Vries, B.B., Janssen, I.M., van der Vliet, W.A., Huys, E.H., de Jong, P.J., Hamel, B.C., Schoenmakers, E.F., Brunner, H.G., Veltman, J.A., and van Kessel, A.G. (2004). Mutations in a new member of the chromodomain gene family cause CHARGE syndrome. *Nature genetics* 36, 955-957.

- Wain, H.M., Bruford, E.A., Lovering, R.C., Lush, M.J., Wright, M.W., and Povey, S. (2002). Guidelines for human gene nomenclature. *Genomics* 79, 464-470.
- Waterston, R.H., Lindblad-Toh, K., Birney, E., Rogers, J., Abril, J.F., Agarwal, P., Agarwala, R., Ainscough, R., Alexandersson, M., An, P., Antonarakis, S.E., Attwood, J., Baertsch, R., Bailey, J., Barlow, K., Beck, S., Berry, E., Birren, B., Bloom, T., Bork, P., Botcherby, M., Bray, N., Brent, M.R., Brown, D.G., Brown, S.D., Bult, C., Burton, J., Butler, J., Campbell, R.D., Carninci, P., Cawley, S., Chiaromonte, F., Chinwalla, A.T., Church, D.M., Clamp, M., Clee, C., Collins, F.S., Cook, L.L., Copley, R.R., Coulson, A., Couronne, O., Cuff, J., Curwen, V., Cutts, T., Daly, M., David, R., Davies, J., Delehaunty, K.D., Deri, J., Dermitzakis, E.T., Dewey, C., Dickens, N.J., Diekhans, M., Dodge, S., Dubchak, I., Dunn, D.M., Eddy, S.R., Elnitski, L., Emes, R.D., Eswara, P., Eyas, E., Felsenfeld, A., Fewell, G.A., Flicek, P., Foley, K., Frankel, W.N., Fulton, L.A., Fulton, R.S., Furey, T.S., Gage, D., Gibbs, R.A., Glusman, G., Gnerre, S., Goldman, N., Goodstadt, L., Grafham, D., Graves, T.A., Green, E.D., Gregory, S., Guigo, R., Guyer, M., Hardison, R.C., Haussler, D., Hayashizaki, Y., Hillier, L.W., Hinrichs, A., Hlavina, W., Holzer, T., Hsu, F., Hua, A., Hubbard, T., Hunt, A., Jackson, I., Jaffe, D.B., Johnson, L.S., Jones, M., Jones, T.A., Joy, A., Kamal, M., Karlsson, E.K., Karolchik, D., Kasprzyk, A., Kawai, J., Keibler, E., Kells, C., Kent, W.J., Kirby, A., Kolbe, D.L., Korf, I., Kucherlapati, R.S., Kulbokas, E.J., Kulp, D., Landers, T., Leger, J.P., Leonard, S., Letunic, I., Levine, R., Li, J., Li, M., Lloyd, C., Lucas, S., Ma, B., Maglott, D.R., Mardis, E.R., Matthews, L., Mauceli, E., Mayer, J.H., McCarthy, M., McCombie, W.R., McLaren, S., McLay, K., McPherson, J.D., Meldrim, J., Meredith, B., Mesirov, J.P., Miller, W., Miner, T.L., Mongin, E., Montgomery, K.T., Morgan, M., Mott, R., Mullikin, J.C., Muzny, D.M., Nash, W.E., Nelson, J.O., Nhan, M.N., Nicol, R., Ning, Z., Nusbaum, C., O'Connor, M.J., Okazaki, Y., Oliver, K., Overton-Larty, E., Pachter, L., Parra, G., Pepin, K.H., Peterson, J., Pevzner, P., Plumb, R., Pohl, C.S., Poliakov, A., Ponce, T.C., Ponting, C.P., Potter, S., Quail, M., Reymond, A., Roe, B.A., Roskin, K.M., Rubin, E.M., Rust, A.G., Santos, R., Sapojnikov, V., Schultz, B., Schultz, J., Schwartz, M.S., Schwartz, S., Scott, C., Seaman, S., Searle, S., Sharpe, T., Sheridan, A., Shownkeen, R., Sims, S., Singer, J.B., Slater, G., Smit, A., Smith, D.R., Spencer, B., Stabenau, A., Stange-Thomann, N., Sugnet, C., Suyama, M., Tesler, G., Thompson, J., Torrents, D., Trevaskis, E., Tromp, J., Ucla, C., Ureta-Vidal, A., Vinson, J.P., Von Niederhausern, A.C., Wade, C.M., Wall, M., Weber, R.J., Weiss, R.B., Wendl, M.C., West, A.P., Wetterstrand, K., Wheeler, R., Whelan, S., Wierzbowski, J., Willey, D., Williams, S., Wilson, R.K., Winter, E., Worley, K.C., Wyman, D., Yang, S., Yang, S.P., Zdobnov, E.M., Zody, M.C., and Lander, E.S. (2002). Initial sequencing and comparative analysis of the mouse genome. *Nature* 420, 520-562.
- Wegenke, J.D., Uehling, D.T., Wear, J.B., Jr., Gordon, E.S., Bargman, J.G., Deacon, J.S., Herrmann, J.P., and Opitz, J.M. (1975). Familial Kallmann syndrome with unilateral renal aplasia. *Clinical genetics* 7, 368-381.
- Wehner, P. (2012). Analyzing PTK7/RACK1 interaction in neural morphogenesis. *Developmental Biochemistry*. Goettingen: Georg-August-University.
- Wieczerek, K. (2012). Analysis of coiled coil domain containing 33 protein (CCDC33) and determination of infertility causes in mutant mouse line with

- the deletion of six germ cell-specific genes. Institute of Human Genetics. Goettingen: Georg-August-University.
- Williams, M.S. (2005). Speculations on the pathogenesis of CHARGE syndrome. *American journal of medical genetics. Part A* 133A, 318-325.
- Witt, D. (2013). Analyse zur Rolle von pflanzlichen Wirkstoffen und Histondeacetylase-Inhibitoren auf Wachstumsfaktoren und deren Signalwege in Prostatakarzinomzellen. Institute of Human Genetics. Goettingen: Georg-August-University.
- Woodage, T., Basrai, M.A., Baxevanis, A.D., Hieter, P., and Collins, F.S. (1997). Characterization of the CHD family of proteins. *Proceedings of the National Academy of Sciences of the United States of America* 94, 11472-11477.
- Wright, C.G., Brown, O.E., Meyerhoff, W.L., and Rutledge, J.C. (1986). Auditory and temporal bone abnormalities in CHARGE association. *The Annals of otology, rhinology, and laryngology* 95, 480-486.
- Wysocka, J., Swigut, T., Milne, T.A., Dou, Y., Zhang, X., Burlingame, A.L., Roeder, R.G., Brivanlou, A.H., and Allis, C.D. (2005). WDR5 associates with histone H3 methylated at K4 and is essential for H3 K4 methylation and vertebrate development. *Cell* 121, 859-872.
- Xenbase. (2013). Gene Nomenclature Guidelines
<http://www.xenbase.org/gene/static/geneNomenclature.jsp> (Effective: 21/07/2014).
- Xenbase. (n.d.). Introduction to Xenopus, the frog model
<http://www.xenbase.org/anatomy/intro.do> (Effective: 17/07/2014).
- Yang, X., Schadt, E.E., Wang, S., Wang, H., Arnold, A.P., Ingram-Drake, L., Drake, T.A., and Lusk, A.J. (2006). Tissue-specific expression and regulation of sexually dimorphic genes in mice. *Genome research* 16, 995-1004.
- Yates, J.A., Menon, T., Thompson, B.A., and Bochar, D.A. (2010). Regulation of HOXA2 gene expression by the ATP-dependent chromatin remodeling enzyme CHD8. *FEBS Lett* 584, 689-693.
- Yazdani, U., and Terman, J.R. (2006). The semaphorins. *Genome biology* 7, 211.
- Yokoyama, A., Wang, Z., Wysocka, J., Sanyal, M., Aufiero, D.J., Kitabayashi, I., Herr, W., and Cleary, M.L. (2004). Leukemia proto-oncoprotein MLL forms a SET1-like histone methyltransferase complex with menin to regulate Hox gene expression. *Molecular and cellular biology* 24, 5639-5649.
- Young, J., Metay, C., Bouligand, J., Tou, B., Francou, B., Maione, L., Tosca, L., Sarfati, J., Brioude, F., Esteve, B., Briand-Suleau, A., Brisset, S., Goossens, M., Tachdjian, G., and Guiochon-Mantel, A. (2012). SEMA3A deletion in a family with Kallmann syndrome validates the role of semaphorin 3A in human puberty and olfactory system development. *Hum Reprod* 27, 1460-1465.
- Yu, H.H., and Kolodkin, A.L. (1999). Semaphorin signaling: a little less per-plexin. *Neuron* 22, 11-14.
- Yu, H.H., and Moens, C.B. (2005). Semaphorin signaling guides cranial neural crest cell migration in zebrafish. *Developmental biology* 280, 373-385.
- Zhang, W., Huang, R.S., Duan, S., and Dolan, M.E. (2009). Gene set enrichment analyses revealed differences in gene expression patterns between males and females. *In silico biology* 9, 55-63.
- Zipper, H., Brunner, H., Bernhagen, J., and Vitzthum, F. (2004). Investigations on DNA intercalation and surface binding by SYBR Green I, its structure

References

determination and methodological implications. Nucleic acids research 32, e103.

6 Appendix

Table 39: Microarray gene expression analysis

No.	Gene symbol	Gene name	Wild-type vs. <i>Chd7^{Whi/Whi}</i>			Gene Ontology category and function in neural crest development*
			log2 FC	P-Value	FDR	
Upregulated genes						
1	Casp12	caspase 12	1.69	3.48E-04	4.253	
2	Rasl10a	RAS-like, family 10, member A	1.65	2.56E-07	0.086	
3	Mt1	metallothionein 1	1.50	1.36E-04	2.653	ion homeostasis
4	Acsbg1	acyl-CoA synthetase bubblegum family member 1	1.53	5.53E-06	0.363	
5	Pkp1	plakophilin 1	1.41	3.83E-04	4.513	Cell adhesion
6	Foxd3	forkhead box D3	1.30	1.51E-04	2.768	Neural crest cell migration embryonic organ development positive regulation of gene expression chordate embryonic development
7	Vstm21	V-set and transmembrane domain containing 2-like	1.26	2.74E-04	3.774	
8	Cdh22	cadherin 22	1.21	3.06E-04	3.896	Cell adhesion
9	Sox10	SRY-box containing gene 10	1.16	7.26E-05	1.952	Neural crest cell migration positive regulation of gene expression chordate embryonic development
10	Igfbp6	insulin-like growth factor binding protein 6	1.16	1.20E-04	2.481	
11	Pcsk9	proprotein convertase subtilisin/kexin type 9	1.15	2.88E-04	3.847	neuron differentiation
12	Jph4	junctophilin 4	1.13	4.47E-04	4.77	
13	Mt2	metallothionein 2	1.13	2.19E-04	3.424	ion homeostasis
14	Gfra2	glial cell line derived neurotrophic factor family receptor alpha 2	1.13	5.25E-06	0.363	transmembrane receptor protein tyrosine kinase signaling pathway
15	Grik3	glutamate receptor, ionotropic, kainate 3	1.13	1.25E-05	0.62	ion homeostasis
16	Cdh13	cadherin 13	1.12	1.49E-04	2.754	Cell adhesion
17	Flrt1	fibronectin leucine rich transmembrane protein 1	1.11	8.65E05	2.097	
18	Lmo1	LIM domain only 1	1.06	4.25E-04	4.642	
19	Phf15	PHD finger protein 15	1.06	5.28E-06	0.363	
20	2200002K05Rik	RIKEN cDNA 2200002K05 gene	1.04	4.13E-04	4.583	
21	Fam162b	family with sequence similarity 162, member B	1.01	3.04E-06	0.290	
Downregulated genes						
22	Pcdh19	protocadherin 19	-1.00	1.06E-04	2.271	Cell adhesion
23	Vegfc	vascular endothelial growth factor C	-1.00	2.00E-06	0.245	Neural crest cell guidance transmembrane receptor protein tyrosine kinase signaling pathway vasculature development

Table 1 (Continued)

No.	Gene symbol	Gene name	Wild-type vs. <i>Chd7</i> ^{Whi/Whi}			Gene Ontology category and function in neural crest development*
			log2 FC	P-Value	FDR	
24	Tmeff2	transmembrane protein with EGF-like and two follistatin-like domains 2	-1.02	1.57E-04	2.814	
25	Gm2496	predicted gene 2496	-1.02	1.04E-04	2.262	
26	Gpm6a	glycoprotein m6a	-1.03	2.75E-04	3.774	
27	Pdgfc	platelet-derived growth factor, C polypeptide	-1.04	1.55E-05	0.68	Neural crest cell migration transmembrane receptor protein tyrosine kinase signaling pathway
28	Txlnb	taxilin beta	-1.05	4.13E-04	4.583	
29	Sema3c	semaphorin 3C	-1.05	1.46E-05	0.666	Neural crest cell guidance vasculature development cellular component movement
30	D030007L05Rik	RIKEN cDNA D030007L05 gene	-1.06	2.22E-05	0.853	
31	Clec1b	C-type lectin domain family 1, member b	-1.06	6.23E-05	1.752	
32	Flrt2	fibronectin leucine rich transmembrane protein 2	-1.06	7.21E-05	1.952	Neural crest cell migration
33	Slc35d3	solute carrier family 35, member D3	-1.07	1.28E-04	2.554	
34	Clec9a	C-type lectin domain family 9, member a	-1.08	2.77E-05	1.007	
35	Lin7a	lin-7 homolog A (C. elegans)	-1.08	5.59E-05	1.671	regulation of neurotransmitter levels
36	6720420G18Rik	RIKEN cDNA 6720420G18 gene	-1.08	6.03E-05	1.744	
37	Lhx9	LIM homeobox protein 9	-1.09	1.39E-04	2.676	
38	Bdnf	brain derived neurotrophic factor	-1.11	2.55E-06	0.284	Axonogenesis, inner ear development neuron differentiation
39	A930038C07Rik	RIKEN cDNA A930038C07 gene	-1.11	1.52E-05	0.68	Extracellular matrix organization
40	Gad2	glutamic acid decarboxylase 2	-1.17	3.21E-05	1.21	regulation of neurotransmitter levels
41	Saa2	serum amyloid A 2	-1.18	4.15E-06	0.34	
42	Pcdh17	protocadherin 17	-1.19	2.12E-04	3.374	Cell adhesion
43	St8sia4	ST8 alpha-N-acetyl-neuraminide alpha-2,8-sialyl-transferase 4	-1.19	8.98E-05	2.104	
44	D030024E09Rik	RIKEN cDNA D030024E09 gene	-1.20	6.49E-05	1.789	
45	Pcdhac2	protocadherin alpha subfamily C, 2	-1.24	1.85E-04	3.108	Cell adhesion
46	Tnfaip6	tumor necrosis factor alpha induced protein 6	-1.25	1.68E-04	2.936	Cell adhesion
47	Inpp4b	inositol polyphosphate-4-phosphatase, type II	-1.25	4.47E-05	1.51	
48	Asb4	ankyrin repeat and SOCS box-containing 4	-1.26	2.60E-05	0.96	
49	Sema3a	semaphorin 3A	-1.26	2.21E-06	0.26	Neural crest cell guidance, Axonogenesis neuron differentiation cellular component movement
50	Hnmt	histamine N-methyltransferase	-1.27	1.68E-04	2.936	regulation of neurotransmitter levels
51	Aldh1a7	aldehyde dehydrogenase family 1, subfamily A7	-1.27	1.57E-04	2.814	

Table 1 (Continued)

No.	Gene symbol	Gene name	Wild-type vs. <i>Chd7</i> ^{Whi/Whi}			Gene Ontology category and function in neural crest development*
			log2 FC	P-Value	FDR	
52	Zic1	zinc finger protein of the cerebellum 1	-1.30	4.36E-04	4.708	Neural crest induction inner ear development embryonic organ development
53	Dmrta2	doublesex and mab-3 related transcription factor like family A2	-1.32	2.57E-04	3.658	
54	Pou3f2	POU domain, class 3, transcription factor 2	-1.34	4.25E-04	4.642	neuron differentiation positive regulation of gene expression cellular component movement ion homeostasis
55	Slitrk1	SLIT and NTRK-like family, member 1	-1.37	1.90E-07	0.07	Neural crest cell guidance, Axonogenesis neuron differentiation
56	Epha7	Eph receptor A7	-1.38	5.58E-06	0.363	Neural crest cell guidance, Axonogenesis, neuron differentiation, transmembrane receptor protein tyrosine kinase signaling pathway, cellular component movement
57	Abca9	ATP-binding cassette, sub-family A, member 9	-1.39	1.02E-06	0.196	
58	Gm7325	predicted gene 7325	-1.40	1.78E-04	3.035	
59	Zfhx4	zinc finger homeodomain 4	-1.42	4.81E-05	1.553	
60	1700042O10Rik	RIKEN cDNA 1700042O10 gene	-1.43	2.62E-04	3.668	
61	Clvs1	clavesin 1	-1.44	1.75E-04	3.015	
62	Cdh10	cadherin 10	-1.44	4.50E-05	1.51	Cell adhesion
63	Col3a1	collagen, type III, alpha 1	-1.51	1.86E-05	0.794	Extracellular matrix organization vasculature development
64	Meox2	mesenchyme homeobox 2	-1.51	3.15E-05	1.114	Palate development, limb development muscle tissue development chordate embryonic development vasculature development
65	Mmrn1	multimerin 1	-1.52	1.01E-04	2.229	
66	Dach1	dachshund 1 (Drosophila)	-1.59	1.42E-06	0.202	
67	Anxa1	annexin A1	-1.60	5.76E-06	0.363	
68	Tnfsf18	tumor necrosis factor (ligand) superfamily, member 18	-1.60	1.10E-04	2.348	
69	Chd7	chromodomain helicase DNA binding protein 7	-1.60	1.56E-07	0.07	inner ear development, limb development embryonic organ development chordate embryonic development vasculature development
70	Gm715	predicted pseudogene 715	-1.61	4.84E-07	0.145	
71	Myf6	myogenic factor 6	-1.64	9.57E-07	0.196	positive regulation of gene expression muscle tissue development chordate embryonic development
72	Scn3a	sodium channel, voltage-gated, type III, alpha	-1.66	5.20E-06	0.363	
73	Foxp2	forkhead box P2	-1.74	1.26E-04	2.552	muscle tissue development
74	Rspo2	R-spondin 2 homolog (Xenopus laevis)	-1.74	4.05E-04	4.583	
75	Olig3	oligodendrocyte transcription factor 3	-1.79	1.29E-05	0.62	
76	Armc4	armadillo repeat containing 4	-1.85	8.26E-07	0.196	
77	Tnnc2	troponin C2, fast	-1.85	5.45E-06	0.363	
78	Sema3d	semaphorin 3D	-1.87	1.36E-06	0.20	Neural crest cell guidance
79	Pcdh10	protocadherin 10	-1.96	1.33E-06	0.20	Cell adhesion
80	LOC552873	hypothetical LOC552873	-2.01	1.22E-05	0.62	

Table 1 (Continued)

No.	Gene symbol	Gene name	Wild-type vs. <i>Chd7</i> ^{Whi/Whi}			Gene Ontology category and function in neural crest development*
			log2 FC	P-Value	FDR	
81	Lrrn3	leucine rich repeat protein 3, neuronal	-2.07	9.13E-06	0.50	
82	Zic4	zinc finger protein of the cerebellum 4	-2.09	3.80E-04	4.513	Neural crest induction
83	Vit	vitrin	-2.14	5.04E-08	0.036	Extracellular matrix organization
84	Alx1	ALX homeobox 1	-2.15	7.09E-07	0.191	Palate development inner ear development limb development embryonic organ development positive regulation of gene expression chordate embryonic development
85	Nts	neurotensin	-2.15	5.37E-08	0.036	
86	9530003O04Rik	RIKEN cDNA 9530003O04 gene	-2.16	1.17E-04	2.464	
87	Dach2	dachshund 2 (Drosophila)	-2.16	3.74E-04	4.469	
88	Slitrk6	SLIT and NTRK-like family, member 6	-2.23	1.53E-07	0.07	Neural crest cell guidance, Axonogenesis neuron differentiation
89	Pln	phospholamban	-2.43	3.07E-04	3.896	
90	Epha3	Eph receptor A3	-2.42	4.47E-05	1.51	Neural crest cell guidance transmembrane receptor protein tyrosine kinase signaling pathway
91	Epha5	Eph receptor A5	-2.48	1.29E-05	0.62	Neural crest cell guidance transmembrane receptor protein tyrosine kinase signaling pathway
92	Gm5127	predicted gene 5127	-2.50	1.35E-04	2.639	
93	Myh3	myosin, heavy polypeptide 3, skeletal muscle, embryonic	-2.52	3.24E-04	4.088	
94	Chl1	cell adhesion molecule with homology to L1CAM	-2.56	4.79E-06	0.363	Cell adhesion, Axonogenesis neuron differentiation cellular component movement
95	Tecrl	trans-2,3-enoyl-CoA reductase-like	-2.61	8.55E-05	2.097	
96	Csn3	casein kappa	-2.68	4.99E-10	0.001	
97	D030025E07Rik	RIKEN cDNA D030025E07	-2.72	4.13E-08	0.036	
98	Myog	myogenin	-3.50	5.52E-06	0.363	positive regulation of gene expression muscle tissue development

Differentially expressed genes with a log2 fold-change (FC) ≤ -1 or ≥ 1 and a false discovery rate (FDR) $< 5\%$. Genes are listed in the order of the most upregulated to the most downregulated gene. Selected gene ontology categories are shown

(GO:0060021: palate development, GO:0007155 cell adhesion, GO:0007409 axonogenesis, GO:0048839 inner ear development, GO:0060173 limb development, GO:0030182 neuron differentiation, GO:0048568 embryonic organ development, GO:0010628 positive regulation of gene expression, GO:0060537 muscle tissue development, GO:0007169 transmembrane receptor protein tyrosine kinase signaling pathway, GO:0001944 vasculature development, GO:0043009 chordate embryonic development, GO:0006928 cellular component movement, GO:0001505 regulation of neurotransmitter levels. GO:0050801 ion homeostasis, GO:0030198 extracellular matrix organization).

* Kirby and Hutson (2010)

Table modified after Schulz et al. (2014b).

7 Curriculum vitae

Personal

Name: Schulz
 Surname: Yvonne
 Date of birth: 10/20/1983
 Place of birth: Hamburg, Germany
 Nationality: german
 Address: Schulweg 10, 37083 Goettingen
 E-Mail: yschulz83@googlemail.com

Work experience

- Since 03/2011 **Institute of Human Genetics, Goettingen**
- PhD thesis**
- participation of diverse GGNB Short Method Courses:
 - Mouse histology & in situ expression analyses
 - Basic statistics for graduate students in the life sciences
 - Chromatin Immunoprecipitation (ChIP)
 - participation of GGNB Professional Skills Course:
 - Effective scientific communication: journal papers, seminar or conference presentations, and posters
 - Seminar on Good Scientific Practice
 - Speaking in public
 - Tailor-Made Job Applications: How to Apply for a Job and be Hired
 - Poster presentations at conferences
 - European Human Genetics Conference 2012, June 23-26, 2012, Nuremberg, Germany
 - European Human Genetics Conference 2013, June 8-11, 2013, Paris, France
 - supervision of a bachelor student and students in practical trainings
- 05/2009 - 10/2009 research assistant in the Johann-Friedrich-Blumenbach-Institute for Zoology and Anthropology, Georg-August-University, Goettingen

Study

- 10/2005 – 01/2011 **Diploma Biology study, Georg-August-University, Goettingen**
- Major field of study: Human Genetic, Developmental Biology, Pytomedicine
 - Subsidiary subjects during studies were mathematic, chemistry, botanic, zoology, microbiology, biochemistry, and genetic
 - Diploma in the Institute of Human Genetics: Functional studies of CHARGE syndrome, Final grade: A

Publications

CHD7, the gene mutated in CHARGE syndrome, regulates genes involved in neural crest cell guidance. **Schulz Y.**, Wehner P., Opitz L., Salinas-Riester G., Bongers E.M.H.F, van Ravenswaaij-Arts C.M.A., Wincent J., Schoumans J., Kohlhase J., Borchers A., Pauli S.; Human Genetics, 2014

CHARGE and Kabuki syndromes: A phenotypic and molecular link. **Schulz Y.**, Freese L., Mänz J., Zoll B., Völter C., Brockmann K., Bögershausen N., Becker J., Wollnik B., Pauli S.; Human Molecular Genetics, 2014

Identification and characterization of FAM124B as a novel component of a CHD7 and CHD8 containing complex. Batsukh T., **Schulz Y.**, Wolf S., Rabe T.I., Oellerich T., Urlaub H., Schaefer I.M., Pauli S.; PLoS One, 2012

Ccdc33, a predominantly testis-expressed gene, encodes a putative peroxisomal protein. Kaczmarek K., Niedzialkowska E., Studencka M., **Schulz Y.**, Grzmil P.; Cytogenetic Genome Research, 2009

Advanced trainings / Practical trainings

- 02/2004 – 03/2005 AuPair in New Jersey, USA
- 04/2005 – 08/2005 Practical training at the Nature and Biodiversity Conservation Union, Bremervoerde
- 03/2008 – 04/2008 6-week practical training in the rainforest station for reafforestation Bilsa, Ecuador